



Universität für Bodenkultur Wien

Department of Forest and Soil Sciences
Institute of Silviculture
Supervisor: Univ. Prof. Dipl.–Ing. Dr. Hubert Hasenauer

IMPACTS OF EXTANT CLIMATE CHANGE ON FOREST GROWTH AND FOREST FIRE HAZARD IN AUSTRIA

Chris S. Eastaugh

Dissertation to obtain a doctoral degree (Dr. nat. techn.) at the University of
Natural Resources and Life Sciences (BOKU), Vienna

Vienna, May 2012

DEDICATION

This dissertation is dedicated to those who – for better or worse – made me who I am. To my mother Lorraine, for bedtime stories, an appreciation of the written word, and unquestioning love and support. To my late father David, for an introduction to technical literature, adventures in the bush, and a burning need to know what is out there and how it works. And to my brother Alex, for dinnertable physics tutorials and the realisation that mathematics is the key to understanding. I guess that for a long while you all thought that your efforts had been wasted, but some lessons are never truly forgotten.

Chris Eastaugh

PREFACE

This work was conducted as a ‘cumulative dissertation’, consisting of seven individual journal articles and a ‘framework paper’ that demonstrates the overall theme of the study and how the individual components fit together. The framework consists of chapters 1 through 9 of this book, and the seven papers are listed on the following page and reproduced in the appendix. Formatting and citation styles vary between the papers in the appendix in line with the requirements of the various journals in which they have been published or are currently in review with.

To avoid unnecessary repetition the framework assumes an expert’s familiarity with the topics in question and is not intended to serve as a standalone document. The framework briefly summarises the rationale for each journal paper and the main results, but its primary purpose is to provide structure for the entirety of the work (chapters 1 to 3) and draw conclusions that were beyond the scope of the individual papers (chapter 7). Readers with a desire for a deeper understanding of chapters 4 to 6 should study the appropriate papers in the appendix.

Citations to this work should refer to: Eastaugh CS (2012) Impacts of extant climate change on forest growth and forest fire hazard in Austria, Dr. nat. techn. dissertation at the University of Natural Resources and Life Sciences (BOKU), Vienna, or, by preference, to the individual journal articles.

LIST of PAPERS

I) Eastaugh CS and Hasenauer H (2012a) Biases in volume increment estimates derived from successive angle-count sampling. *Forest Science*. (in press 28/09/2011) <http://dx.doi.org/10.5849/forsci.11-007>. [SCI]

II) Hasenauer H and Eastaugh CS (2012) Assessing forest production using terrestrial monitoring data. *International Journal of Forestry Research*. Article ID 961576, 8pp.

III) Eastaugh CS, Petritsch R and Hasenauer H (2010) Climate characteristics across the Austrian forest estate from 1960 to 2008. *Austrian Journal of Forest Science* 127:133-146. [SCIE]

IV) Eastaugh CS and Vacik H (2012) Fire size/frequency distributions as a means of assessing wildfire database reliability. [Manuscript]

V) Eastaugh CS, Arpacı A and Vacik H (2012) A cautionary note regarding comparisons of fire danger indices. *Natural Hazards and Earth System Sciences* 12:927-934. [SCIE]

VI) Eastaugh CS, Pötzelsberger E and Hasenauer H (2011) Assessing the impacts of climate change and nitrogen deposition on Norway spruce (*Picea abies* L. Karst) growth in Austria with BIOME-BGC. *Tree Physiology* 31(3):262-274. [SCI]

VII) Eastaugh CS and Hasenauer H (2012b) Biogeochemical process modeling of forest fire ignition hazard. [Manuscript]

ABSTRACT

Significant climate change has been observed in Austria over the past half century, with a national rising trend in average temperatures of 1.5°C in 50 years. While studies into the prospective effects of future climate change are not uncommon, there are relatively few that examine the impacts of the significant change that has already occurred. The purpose of this work was to examine correlations between changing climates and forest growth and fire hazard in Austria, and gain a better understanding of the impacts that have occurred. This was done through the application of a biogeochemical forest growth model, using three major national-scale data products pertaining to daily climate interpolations, national forest inventory and a collation of national wildfire reports.

As is common in science, the value of this study lies at least as much in its data analysis and methodological development as in its final results. As necessary interim steps in the overall work I have developed an improved procedure for comparing forest fire hazard indices and means of assessing the reliability of both large-scale forest inventories based on Bitterlich's angle count method and databases of wildfire records. The application of physiological modelling to wildfire hazard analyses has highlighted the importance of biophysical factors in forest fire ignition.

The overall study results show that at the national scale the direct impact of climate change on forest increment rates have been small, due in part to opposing effects at the regional level. Even at the regional scale however the impact of changed temperatures and precipitation levels is small compared to the positive impact of increased atmospheric nitrogen deposition. The magnitude of the climatically-driven changes in forest increments is sufficiently low that this is unlikely to have a bearing on management practices or policy setting at the current level. The risk of extreme wildfire conditions however has risen sharply, and if warming and drying regional climatic trends continue then this will demand a policy response.

CONTENTS

PREFACE.....	i
LIST of PAPERS	ii
ABSTRACT.....	iii
1. INTRODUCTION	1
2. OBJECTIVES	3
3. WORKFLOW	4
4. DATA	5
4.1 Climate.....	5
4.2 Inventories.....	5
4.3 Wildfire.....	6
5. DATASET ANALYSES	7
5.1 Climate.....	7
5.2 Inventories.....	8
5.3 Wildfire.....	9
6. INTEGRATION / RESULTS	11
6.1 Forest growth	11
6.2 Forest fire hazard	12
7. DISCUSSION and CONCLUSIONS	14
8. ACKNOWLEDGEMENTS.....	16
9. REFERENCES	17
10. APPENDICES	23

1. INTRODUCTION

In recent decades there has been intense speculation about the prospective changes to forest growth and disturbance regimes in response to climate change. These changes are likely to have serious environmental, social and economic consequences (Eastaugh 2008), and prudence demands that we understand the issues well enough to mitigate or adapt to the changes that are likely to occur. Much of the research work on these matters has relied on predictive modeling under assumed future scenarios rather than on the formal testing of hypotheses against observed data. Although such work is not without value from the perspective of understanding models' responses to particular stimuli, such predictions lack the advantage of being refutable in a Popperian sense. What is missing is a broad scale long term study of how climate change is already impacting forests, supported by both observed data and an understanding of the physical and physiological drivers of the effects.

It is often considered that a future 2°C rise in global average temperature will have substantial impacts on terrestrial ecosystems (e.g. Hughes 2003; Leemans and Eickout 2004). Given that over the past 50 years average temperatures in some regions have already risen by more than this amount, it is reasonable to expect that ecosystem changes should already be noticeable. Soja et al. (2007) reviewed evidence of climate change impacts on boreal ecosystems and concluded that some response is already apparent in some areas. That review however was a collation of site-specific evidence rather than a systematic piece of original research. Boisvenue and Running (2006) reviewed global forest productivity over the past 55 years and concluded that a net positive trend was apparent, but that "At finer spatial scales, a trend is difficult to decipher". The European growing season has lengthened by almost 11 days since 1960 (Menzel 2000), perhaps as much as 20 days in some areas (Linderholm, 2006; Walther and Linderholm, 2006). Specifically in Austria, Hasenauer et al. (1999) found an 11 day increase from 1961 to 1990, and Petritsch and Hasenauer (2009) found that since 1960 Austria has had a statistically significant trend to increasing growing season lengths of 0.34 days per year. This positive effect of climate change may however in some areas be offset by an increase in climate-related disturbance events such as windthrow (Peltola et al. 1999; Klaus et al. 2011), insect infestations (Seidl et al. 2008; Bentz et al. 2010) or wildfire. Wildfire in particular is commonly held to be one of the principle increasing risk factors for forests under a warming climate (Williams et al. 2001; Brown et al. 2004; Flannigan et al. 2005; Gossow et al. 2008; Pausas and Fernández-Muñoz 2012).

The effects of environmental change are likely to differ widely between regions, depending on the degree of change, the susceptibility of the ecosystem and a host of other factors. To examine the issue properly then needs a study over both a sufficiently wide geographical scale and at a fine enough level of detail to enable internal contrasts to be found. Unfortunately, suitable long-term datasets with this range and scale of detail are not common. The understanding of climate impacts is further complicated by the fact that climate is not the only environmental change that forests are currently experiencing; chemical depositions from the atmosphere and changing management regimes may also

have great impact (Spieker 1999; de Vries et al. 2006; Solberg et al. 2009). Austria provided an ideal situation to study these issues, due to having had a well-respected permanent plot National Forest inventory since the early 1980s, a recently developed quality controlled national wildfire database, a dense network of long-term climate monitoring stations and the availability of a validated climate interpolation tool and biogeochemical forest growth model. Also advantageous is Austria's diversity of terrain and climate, allowing comparisons and contrasts to be made between regions.

2. OBJECTIVES

The overall objective of this work was to determine the impacts of climate changes over the past half-century on forest growth rates and wildfire hazard in Austrian forests. This was to be achieved with the aid of National Forest Inventory (NFI) data, a collation of national wildfire records, a previously validated climate interpolation and a biogeochemical forest growth model. The purpose of the model in this study is not to extrapolate changes into the future, but to provide a diagnostic tool for interpreting physiological explanations from observed changes.

Several interim steps were required to achieve this objective, and each step produced results that were not only necessary inputs or background for the overall study but also important outcomes in themselves. These relate to:

- a) An analysis of climate trends over the Austrian forest estate,
- b) The delineation of regions where climate change has been particularly or less pronounced,
- c) An examination of different methods of deriving forest increment from angle-count based inventories, and the determination of which method was most suited to this study,
- d) A study of the likely changes in the comprehensiveness of the wildfire database, and
- e) The development of a robust method of comparing forest fire hazard indices.

With these pieces in place, it was then possible to directly address the main objectives of the study. This is done in two separate works, which besides answering the main research questions,

- f) Separate the impacts of changing climate from that of changing Nitrogen deposition on the growth rates of Norway spruce (*Picea abies* L. Karst), and
- g) Develop fire hazard indices which take into account the biophysical impact of forest conditions on wildfire ignition hazard.

3. WORKFLOW

For each of the three data themes (inventory, climate and fire records) I conducted an initial exploration of how the choice of analysis method may affect results and conclusions, or an examination of what limitations may be inherent in the dataset (referred to below as ‘Analysis and limitations’). This was followed by a study of how this data could be applied to the research question, and what methodological issues may be of concern (‘Application methodology’). In the third phase, the Austrian adaptation of the BIOME-BGC model (Pietsch et al. 2005) is used to integrate different datasets and draw conclusions relevant to the overall objective. Figure 1 outlines the progression from raw data through to the final results.

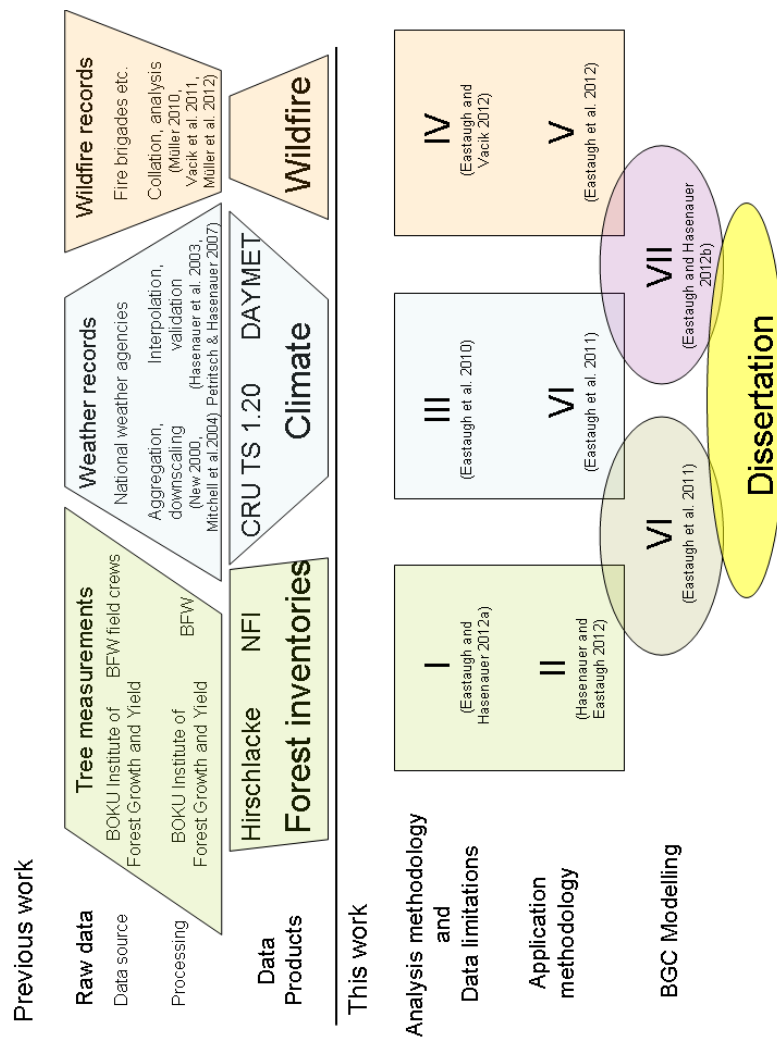


Figure 1 Workflow diagram.

Each paper in this series is self contained, with its own data, methods and results. In the context of the broader study however papers [III] and [IV] could be viewed as the ‘data’ section, [I], [II] and [V] as ‘methods’ and [VI] and [VII] as ‘results’.

4. DATA

For the most part, completely raw data was not used for this study. To varying extents, each dataset had previously been collated, cleaned, analysed or processed. Five data products were applied in the study, pertaining to forest inventories, climate and wildfire records. The origins of these datasets will be briefly described here. Further details are given in the published papers where the datasets are used, but it should be understood that credit for these datasets lies with their originators; their collection and collation was not part of my study. My own work begins further below, under the heading ‘Dataset analyses’.

4.1 Climate

The CRU TS1.20 European climate dataset (Mitchell et al. 2004) is publicly available on request from the Climatic Research Unit of the University of East Anglia. It is a gridded dataset with a resolution of 10', formed by the updating and downscaling of the global 0.5° grid of New et al. (2000). Austria contains 350 of these 10' grid cells.

The DAYMET climate interpolation routine was developed by Thornton et al. (1997), and adapted and validated for Austrian conditions by Hasenauer et al. (2003). DAYMET interpolates maximum and minimum daily temperatures and precipitation, and with information regarding latitude, elevation, and horizon angle calculates vapour pressure deficit, solar radiation and daylength. The interpolation was originally developed to supply daily information over a regular grid, but this was adapted by Petritsch (2002) in order that daily climate could be interpolated to any given set of coordinates. DAYMET uses daily climate data from several hundred weather stations in Austria and surrounding countries and takes into account the orographic effects of elevation.

4.2 Inventories

BOKU's Institute for Forest Growth and Yield maintains a large set of permanent plot forest growth monitoring sites across Austria. One of these is the 3.47ha Hirschlacke plot in northern Austria, near the Czech and German borders. First established in 1977, the plot has been remeasured each five years since. Records are kept of diameters, heights and precise Cartesian locations for all trees of over 5.0cm dbh. The site represents a plot where the management style has changed from almost pure 110 year old Norway spruce in 1977 to a regime targeting an equilibrium dbh distribution (Sterba and Zingg 2001). The site was chosen for its size and diversity, as the intention was to use this as a test case for theoretical work involving the estimation of forest increment from simulated angle count samples (Hradetzky 1995).

The Austrian National Forest Inventory in its current form (Gabler and Schadauer 2006) dates from the early 1980s, with remeasurement intervals of between five and eight years. Tracts are located on square grid of 3.89km sides, with each tract comprising four points in a square of 200m sides. At each point an angle count sample (Bitterlich 1948) is made of trees over 10.4cm, and a fixed-area plot of 2.6m radius installed to measure all trees of over 5.0cm. Locations are recorded as azimuth and distance from the plot centre. A 300m² circular plot is also established, and an estimate made of what percentage of this 300m² should be classified as 'forest'. The grid of 5582 tracts covers the whole of Austria, and roughly 11 000 plots are forested. For this study, data was made available for one plot on each tract that was forested in the first modern inventory in the early 1980s, which gave 2224 plots. Inventories are conducted with staggered timing, where only one third to one fifth of plots are measured in any particular year. Inventory measurements covered the periods 1981–85, 1986–90, 1992–96 and 2000–02. On any plot, the intervening increment periods are 5 years for the first inter-measurement period, 6 years for the second and variously 6, 7 or 8 years for the third.

4.3 Wildfire

The Austrian wildfire dataset (Müller 2010; Vacik et al. 2011; Müller et al. 2012) was collated in the BOKU Institute of Silviculture as part of the AFFRI and ALP FFIRS projects (Valese et al. 2010; Vacik and Gossow 2011). Records were collated from public online fire news platforms 'www.wax.at' and 'www.feuerwehr-news.at', from regional fire brigade records and through direct contact with various Austrian municipalities and Federal government departments. The raw collated data as of April 2011 consisted of 2660 records. After removing repeated observations of the same fire event 2455 records remain, 1870 of which pertain to forest fires, the earliest being in the year 1874. Geographic coordinates were determined for all fires, and 1012 have a value recorded for area burnt. These areas range from 1m² to 200ha.

5. DATASET ANALYSES

5.1 Climate

Analysis and limitations

In paper [III] I applied the DAYMET interpolation routine to generate daily series of temperature and precipitation for 2224 point of the Austrian National Forest Inventory. These were aggregated into monthly mean temperature and total precipitation for each point, to enable comparison with the publicly available CRU TS 1.20 dataset. Monthly data was also collated for 28 ‘high value’ meteorological stations (those with data for at least 2/3 of the days in every month from 1960 to 2005). A comparison of the nationally aggregated results showed that both DAYMET and CRU TS 1.20 closely followed trends in the station series, but were both consistently 1.0° degrees warmer. This was because station locations are on average lower in altitude than the forest inventory sites or the national average.

337 CRU TS 1.20 cells contained at least one NFI tract, with an average of 6.64 tracts per cell. This enabled a comparison at the cell level of both the mean and range of the DAYMET data. Within-cell variation was found to be very high, with often several degrees of difference in mean temperature and hundreds of millimeters of precipitation. It was concluded from this that the downscaled climate data may be accurate across wide geographic areas, but is likely be insufficiently precise for use as a model driver in highly heterogeneous terrain. The decision was made to use DAYMET for subsequent work.

Application methodology

In paper [III] I also calculated the linear trend of temperature and precipitation on each NFI point. This showed marked regional variation, with some geographic areas being well outside one standard deviation of the national trend. This work was extended in paper [VI], where I used a Gaussian kernel smoothing (Baddeley and Turner 2005) to delineate those areas. This was done on the assumption that any signal in forest growth rates or wildfire frequency trends was likely to be more easily determined in regions that have experienced the greatest climate changes. Andreassen et al. (2006) have pointed out the need for sub-national scale studies of forest responses to climate change, as different effects may be apparent in different areas. Figure 2 shows the climate change regions that form the basis of the comparisons of changes in forest growth and wildfire hazard in papers [VI] and [VII].

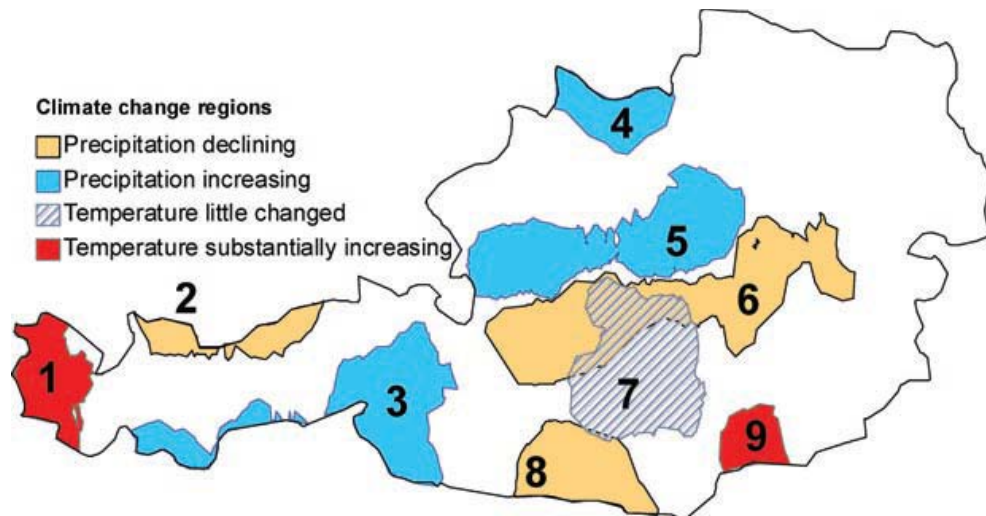


Figure 2 Austrian climate change regions (Eastaugh et al. 2011)

5.2 Inventories

Analysis and limitations

Three common methods exist for estimating forest increment from inventories based on angle count sampling. Schieler (1997) termed these the ‘Difference method’, the ‘Starting value method’ and the ‘End value method’. Thomas and Roesch (1990) interpreted a statewide inventory in Alabama with each method and found differences in increment results of up to 50% , which they attributed to fieldwork error. In paper [I] I reviewed the mathematical background of volume and volume increment estimation from angle count samples, and examine the effect of fieldwork errors on the results of each. The paper explains the observational results of Thomas and Roesch (1990) and provides the theoretical background for estimation difference in the presence of error. I then demonstrated this using the Hirschlacke dataset as a basis for 12 000 simulated angle count samples at 5 yearly intervals. Hirschlacke was ideal for this purpose as every tree is measured and locations precisely recorded, so it was possible to estimate increment with each method under a range of simulated error conditions and compare with the ‘no error’ case. Two varieties of errors were examined: ‘measurement error’ being mistakes in the recorded diameter of sampled trees and ‘summation error’ being cases where trees were incorrectly counted either inside or outside the sample.

The Difference method is resistant to measurement error, as the mis-measurement of a tree’s basal area is precisely compensated for by an equal and opposite misestimate of the number of represented trees per hectare. This is not the case for the other methods, and measurement error will result in bias. Over single increment periods (between two measurements) summation errors can have a far greater impact on the Difference method estimates than on the Starting or End Value methods. At Hirschlacke estimates of over 44% of increment arose from errors that caused only a 4.6% misestimation of standing volume. In most cases however this bias will be reversed in the Difference method when

a subsequent (correct) inventory is made, thus over several periods the method can be unbiased even in the presence of summation error. When using the other methods this 'self-correcting' behaviour is absent, and some bias will remain.

Application methodology

Although each increment estimation method can be proven to be mathematically unbiased (Van Deusen et al. 1986), they give different results due to statistical variation even in the absence of error; the increment results are an estimate, not a measurement. The results are equally valid, but precision may be poor if relatively few plots are sampled. In such cases, it may be difficult to determine which estimated value should be accepted, and which (if any) of the estimators may be error affected. If inventory data is to be used as a baseline to compare against modeled estimates of forest characteristics (as in paper [VI]), then it is important to first ensure the integrity of the inventory estimate. In principle this can be done by applying more than one estimation method, and ensuring that the final results are within a pre-determined range of each other. In paper [II] I used the Hirschlacke site to simulate an NFI without error, and determined that to reliably separate the effects of possible error from the random variation in angle-count increment estimates would require far greater number of NFI observations than were available for this study. This does not of course imply that significant errors are present, merely that I was unable to clearly prove an absence of error. For this reason, the Difference method was chosen for the estimation of long-term trends in inventory data in paper [VI], as this reduces the chance of methodological artifacts being present in the results.

5.3 Wildfire

Analysis and limitations

Long time series of historical events are often hampered by changing data quality or completeness over time, making trend analysis difficult. I addressed this issue in paper [IV] by examining the relationship between the size of fires in particular time periods and their frequency of occurrence. Prior authors (Ricotta et al. 1999; Malamud et al. 2005) have suggested that this relationship follows a power law distribution, but this was shown not to be the case in Austria, in line with other work by Reed and McKelvey (2002) and Clauset et al. (2009). Graphical and non-parametric Komolgorov Smirnov distribution tests showed that periods prior to 1995 in particular showed considerably different size/frequency relationships to subsequent periods. As there is no clear physical reason why this should be so, so doubt must fall on the quality of the earlier periods in the database. As the comprehensiveness and reliability of records prior to 1995 cannot be guaranteed, I decided it would be unwise to use the dataset itself for an analysis of temporal trends in wildfire hazard from 1960 onwards, which is one of the objectives of this work. The period from 1995 on however is suitable for use as a hazard model validation dataset.

Application methodology

Forest fire hazard is normally assessed through the use of meteorological indices, which are various combinations of temperature, humidity and precipitation data. A great many of these indices have been formulated, and it is often not certain which index is most suitable for a particular area. Various means of judging the precision of these indices have been proposed (i.e. Viegas et al. 1999; Andrews et al. 2003; Verbesselt et al. 2006), but many ignore the fact that different indices will have different distributions of values. Comparators that rely on parametric testing may therefore detect the difference in index distributions, rather than the difference in index performance. This was explored with an abstract example in paper [V], where I formulated a simple sinusoidal index and three mathematical transformations of that index, and demonstrated that previously published parametric comparison methods suggested different degrees of precision between them. I then developed a graphical representation of index performance, whereby the percentile of each index value is calculated for each day in the period of interest, and the percentiles on days when a fire occurs are plotted in rank order. This provides a cumulative probability curve of index percentiles on fire days. The main characteristics of the curve of points can be described by the intercept and slope of a robust regression line. A hypothetically 'perfect' fire index would have its highest values only on days when a fire truly occurs, and thus would plot as a line with an intercept of 100 and a slope of 0, whereas an index of random numbers would approach an intercept of zero and a slope of 100 divided by the total number of fires. This 'ranked percentile' method showed that the mathematically transformed indices were of equal value in predicting fire hazard.

6. INTEGRATION / RESULTS

The work described above allowed the combination of the data products in order to directly address the study objectives. This was achieved with the aid of the BIOME-BGC ecosystem model (Thornton et al. 2002; Pietsch et al. 2005). BIOME-BGC is a fully mechanistic biogeochemical process model that tracks the pools and fluxes of water, carbon and nitrogen through an ecosystem on a daily timestep. Inputs for the model include daily climate data derived from the DAYMET interpolation of paper [I], site variables from the Austrian NFI, nitrogen deposition data of Schneider (1998) and Placer and Schneider (2001), soil data interpolations of Petritsch and Hasenauer (2007) and the species-specific ecophysiological parameters of Pietsch et al. (2005). A fuller description of the model, its inputs and assumptions is given in paper [VI].

6.1 Forest growth

In paper [VI] I applied BIOME-BGC to the 1188 NFI plots that were predominantly Norway spruce in the first modern inventory period (1981-1985) in order to study differences in increment changes between the regions shown in figure 2. The modeled trends were shown to be consistent with trends observed in the NFI data from the early 1980s to the early 2000s. At the national scale, a statistically significant increasing trend in increment is present, loosely tracking the increase in national average temperatures from 1960 to 2008. Increments of aboveground woody biomass calculated from NFI data show an increase from 5600kg/ha/yr in the first period to 6790kg/ha/yr in the third (2000-2002). This trend is also apparent in the various sub-regions, with a greater increase in the ‘warming’ and ‘wetting’ areas.

To separate the impact of climate change from other effects, I then re-ran the model keeping the climatic input data constant (repeating the annual course of 1960 in each year from 1960 to 2008), and found the increasing trend in increment was still present. A comparison of the ‘constant climate’ results and the ‘true climate’ results allowed the separation of the climate signal in each climate change region (figure 3).

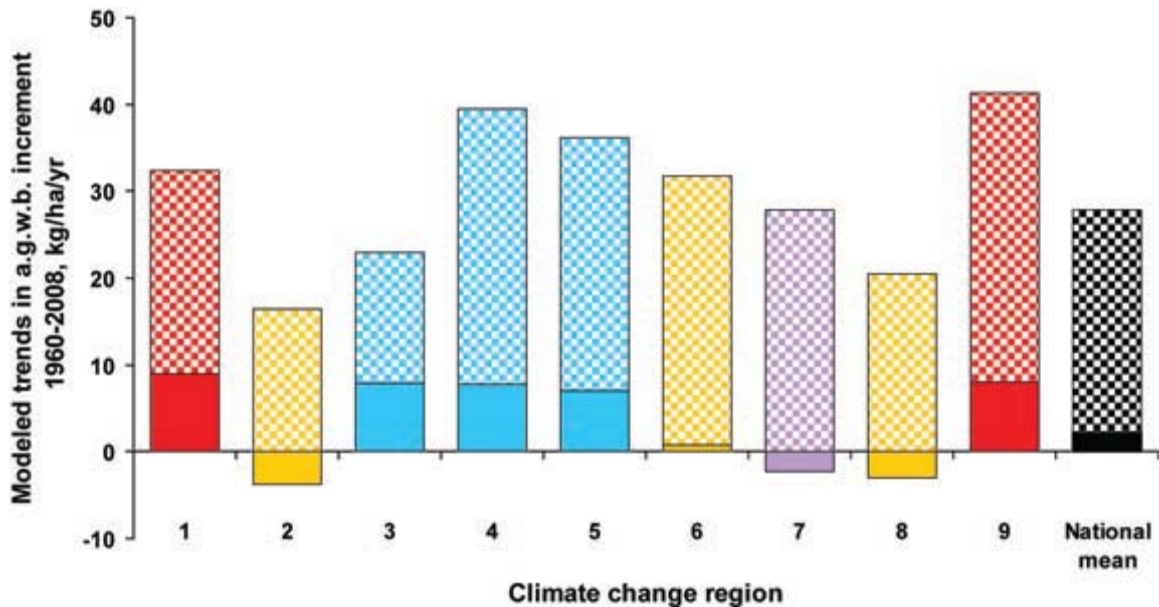


Figure 3 (Eastaugh et al. 2011) Separation of modelled climatic and non-climatic influences. The upper extents of the columns represent the mean annual increases in aboveground woody biomass (a.g.w.b.) increment rate per year from 1960 to 2008. The total height of each column is the modelled increase in increment rates under observed climate conditions. The solid portions of each column represent the influence of climate (the difference between the simulation results with or without climate change), while the checked portions of each column are the increases in increment rates that are common to both simulations and are thus driven by other impactors. Colours and numbering are consistent with Figure 2.

At the national scale, the impact of climate change on forest growth (solid portions of the columns in figure 3) is less than 8% of the total increase. In part, this is due to opposing effects at the regional scale, with a negative impact in regions 2, 7 and 8, negligible impact in region 6 and positive impact in the others. The greatest positive impact is in region 1, where a warming trend of $0.045^{\circ}\text{C}/\text{yr}$ is responsible for a $9.0\text{kg}/\text{ha}/\text{yr}^2$ increase in increment rates over the past half century. The greatest negative impact is in the drying region 2, where a declining precipitation trend of $-5.2\text{mm}/\text{yr}$ reduces increment rates by $3.8\text{kg}/\text{ha}/\text{yr}^2$. In all regions however the impact of climate change is small compared to the impact of non-climatic factors. A regression of the non climatic growth acceleration in figure 3 against the mean increase in nitrogen deposition rates in each region shows that this implies a response of 21.6kg of added aboveground woody biomass per kilogram of extra nitrogen. This result compares well with estimates derived through other methods (i.e. de Vries et al. 2006; de Vries et al. 2008; Solberg et al. 2009; Laubhann et al. 2009; Wamelink et al. 2009).

6.2 Forest fire hazard

Forest fire ignition hazard indices usually rely solely on meteorological variables, although it is known that fuel conditions also play an important role (i.e. Tanskanen and

Venäläinen 2008; Pausas and Fernández-Muñoz 2012). BIOME-BGC tracks variables that may be of relevance in assessing forest fire ignition hazard, so in paper [VII] I tested the hypothesis that simulated values of soil moisture content and labile litter carbon may be better indicators of forest fire hazard than other common indices that rely solely on meteorological data. The index comparison method developed in paper [V] showed that the model-derived indices that included feedbacks from the biophysical environment were an improvement over the purely meteorological indices when tested against Austrian wildfire database from 1995 – 2008.

Forest fires in Austria may occur in the summer or spring seasons. Spring fires are associated with a high mass of labile carbon in the forest litter, as this collects over the winter but does not break down until snow melts and soils warm. This may be used as a proxy for the amount of highly flammable terpenes in forest litter. In Alpine regions particularly in spring there sometimes occurs short periods of very dry air, which rapidly dries surface fuels. The BGC-LV fire hazard index I developed in paper [V] proved to be the most precise indicator of fire ignition hazard at the national scale. Dividing the index values into hazard classes then allowed the tracking of hazard from 1960 to 2008. Of most note is a reducing trend in days of ‘no fire hazard’ in both seasons and a reduction in days of ‘low fire hazard’ in summer in all Austrian regions.

In extreme summer conditions, fire hazard is more closely associated with long-term dry periods, which reduce the moisture content of heavier fuels. This may be tracked with BIOME-BGC’s ‘soil water’ variable. Examining the average number of days per year with extreme soil dryness in the period 1991 to 2008 against a 1960 – 1990 baseline shows a marked increase in fire hazard, most clearly in the warming and drying regions (fig 4). The national risk of extreme fire hazard has more than tripled in the modern period, and is much as 600% higher in regions 2 and 9. Wetting regions 4 and 5 also show an increase (but of less than the national average), while only in region 3 has the occurrence of extreme summer fire hazard fallen.

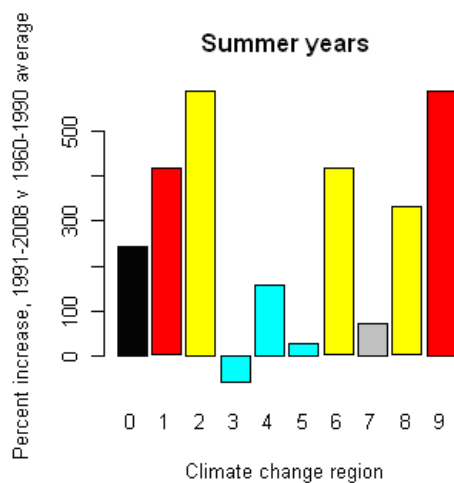


Figure 4 Increasing summer fire hazard is most notable in drying and warming regions (Eastaugh and Hasenauer 2012b). Columns represent the regions in figure 2, with heights corresponding to the increased probability of extreme fire weather in the period 1991-2008 over a 1960-1990 baseline.

7. DISCUSSION and CONCLUSIONS

The analysis of climatic datasets in this work confirms a general warming trend in Austria of around 1.5°C over the past 50 years, but highlights strong regional variation in this trend. Most of the western province of Vorarlberg and part of the southeast of the country exhibit substantially more warming. Precipitation change patterns show a decreasing trend in the southeast and in the northern parts of Tyrol, and increasing trends in other areas. It is beyond the scope of this work to explain the reasons for these patterns, but it is interesting to note that Austria receives its weather from both the north and the south, with the Alps acting as somewhat of a barrier. Alpine regions receive precipitation originating in the western Mediterranean, while southern and eastern Austria also have some input from the Adriatic (Schicker et al. 2010). Seibert et al. (2007) identified seven distinct synoptic patterns that can be responsible for heavy precipitation events in Austria, many of which originate in the northwest. It is plausible to speculate that global warming has an effect on the relative frequency of the various synoptic patterns that dominate different regions of Austria at different times, and thereby impacts differently on regional precipitation. Regardless of the causal agents, the climatic analyses in this work clearly support the need for adaptation efforts to be considered at a sub-national scale.

Inventories were designed as static measures of timber volume and there is no indication in this work that the Austrian NFI does not admirably fulfill this role. The detection of change is substantially more demanding (Scott and Alegria 1990). The studies into theoretical aspects of angle-count sampling in this thesis point out the high statistical variance in estimates of increment and the difficulties in detecting possible bias. Thomas and Roesch (1990) first showed the effect of field errors on the different increment estimators, but my work in paper [I] is the first to provide a mathematical explanation of their observation. Inventory practitioners often quite rightly bewail the somewhat otherworldly approach of academics with a statistical focus (e.g. Iles 2009, Leech 2012). They are quite right to do so, inventories are designed to provide cost-effective practical guides for management activities and public policy, not indisputable scientific facts. If such inventory data is to be used for scientific purposes however it should be examined critically, and any potential errors and biases accounted for and fully understood. Scientific work demands an extraordinary level of rigour; the common level of 95% significance is a high mark that is often well in excess of what can economically be obtained in the 'real world'. This certainly does not mean that datasets such as NFI's can not be used in scientific work, quite the contrary, they are seriously underutilized goldmines of information. Nevertheless, scientific users of inventory data should have an understanding of the potential for their interpretations of that data to give misleading results. With a sufficiently large body of data the procedures developed in papers [I] and [II] could easily be applied to assess the potential impact of field error in angle count based NFIs, although the subset of the Austrian NFI supplied for this study proved to be too small for this test.

The procedure I developed for testing the wildfire database is similarly novel, and could be easily applied to other regional collections of wildfire data to avoid spurious trend detection in time series due to the changing quality of record keeping over time, a problem previously noted by Camia et al. (2011) and not unique to wildfires (Kron et al. 2012). The determination of which time periods contain data with consistent size/frequency relationships allows for a more rigorous validation of fire hazard models or indices. The graphical 'ranked percentile' method of index comparison I developed proved to be of great use in exploring the physical reasons behind the seasonality of Austrian wildfires in paper [VII], as the strengths and weaknesses of each index could be clearly seen. Other non-parametric comparators such as the 'c' index or the area under a receiver operating characteristic curve (Verbesselt et al. 2006; Padilla and Viegas-Garcia 2011) could be used, but give less information than the comparator that I developed. My ranked percentile method is currently being applied by Arpaci et al. (in prep) and will form the basis of recommendations to the Austrian Central Institute for Meteorology and Geodynamics (ZAMG) regarding the updating of their official fire hazard warning system..

The direct impact of climate change on forest growth at the national scale over the past half century was found to be small; changes in nitrogen deposition are far more influential. As atmospheric nitrogen deposition rates in Austria appear to have stabilized recently (Anderl et al. 2009) it seems likely that observed rapid increases in forest growth in the latter part of the 20th century may not continue, or will at least slow considerably. At the regional scale the positive impact of warming temperatures and the negative impact of declining precipitation amounts to changes in annual Norway spruce productivity of roughly +1.0 and -0.4 m³/ha respectively, over the past 50 years (based on biomass equations of Pietsch et al. 2005). Although this will affect the accuracy of traditional yield tables it is not likely in itself to warrant changing management practices or policy settings. If climate changes continue however consideration may have to be given to whether current stocking densities can be maintained in regions of reducing precipitation.

Of more concern than direct climate impact is the clear increase in days of extreme summer fire ignition hazard, particularly in warming and drying regions. This is due mostly to the direct climatological impact, but is also influenced by changing forest conditions. Denser, faster growing forests produce more highly flammable litter and extract more moisture from the soil, and including these effects via the BIOME-BGC model provided a more precise tracking of fire hazard than relying simply on meteorological factors. The magnitude of the increase in fire hazard is such that some policy response is necessary, particularly in more fire-prone areas such as Carinthia and parts of Lower Austria. If recent trends continue then the occurrence of life-threatening forest fires in Austria will become a certainty, particularly as infrastructure, public perception, dwelling construction and community plans are not designed for life in a fire-prone area.

8. ACKNOWLEDGEMENTS

No research programme can be conducted in a vacuum, and the list of people who have provided support and assistance over the past three years is long. The technical help of Richard Petritsch on DAYMET and Stephan Pietsch on BIOME-BGC is greatly appreciated, as is access to the Austrian wildfire database compiled by Mortimer Müller, Natalie Arndt and Harald Vacik. Colleagues Christopher Thurnher, Elisabeth Pötzelsberger and Alexander Arpaci often provided sympathetic and knowledgeable sounding boards for ideas both valuable and stupid. Outside of BOKU the encouragement and advice of participants in COST Actions FP0601, FP0603 and FP0903 was always of great value, and I extend thanks to the organizers of COST for the opportunities they provided me for international collaborations and friendships.

The projects that made up this study were variously funded by the Energy Fund of the Federal State of Austria (managed by Kommunalkredit Public Consulting GmbH), the European Regional Development fund of the Alpine Space Program and the Austrian Science Fund. I am also grateful to the Austrian Federal Research and Training Centre for Forests, Natural Hazards and Landscape (BFW) for provision of the National forest inventory data, to the BOKU Institute of Forest Growth and Yield for the Hirschlacke dataset, and to the Climatic Research Unit of the University of East Anglia for making their dataset publically available.

Thanks must also go to my Doctoral supervisor, Univ. Prof. Dipl.–Ing. Dr. Hubert Hasenauer. It cannot have been easy for a distinguished Viennese university professor to tolerate a pushy Australian farmboy for three years, but somehow he managed it and this dissertation is the tangible result. The intangible results will be with me for a long time to come, and will stand me in good stead in further academic pursuits.

Finally, this thesis represents – if not the high point, then at least a significant waypoint in my academic career. It is appropriate then that I take this opportunity to thank those who set my feet on the path, smoothed some of the bumps and kept my eyes on the prize: John Worden of USQ, Peter Hairsine of CSIRO and Curly Humphries ex of ANU.

9. REFERENCES

Anderl M, Köther T, Muik B, Pazdernik K, Poupa S and Schodl B (2009) *Austria's annual air emission inventory 1990–2008*. Umweltbundesamt GmbH, Vienna, 39 p.

Andreassen K, Solberg S, Tveito OE and Lystad SF (2006) Regional differences in climatic responses of Norway spruce (*Picea abies* L. Karst) growth in Norway. *Forest Ecology and Management* 222:211–221.

Andrews PL, Loftsgaarden DO and Bradshaw LS (2003) Evaluation of fire danger rating indexes using logistic regression and percentile analysis. *International Journal of Wildland Fire* 12:213-226.

Arpaci A, Eastaugh CS and Vacik H (2012, in prep) Selecting the best performing Fire Weather Indices for Austrian Ecozones.

Baddeley A and Turner R (2005) Spatstat: an R package for analyzing spatial point patterns. *Journal of Statistical Software* 12:1–42.

Bentz BJ, Régnière J, Fettig CJ, Hansen EM, Hayes JL, Hicke JA, Kelsey RG, Negrón JF and Seybold SJ (2010) Climate change and bark beetles of the western United States and Canada: Direct and indirect effects. *BioScience* 60(8):602-613.

Bitterlich W (1948) Die Winkelzählprobe. *Allgemeine Forst- und Holzwirtschaftliche Zeitung* 59(1-2):4-5.

Boisvenue C and Running SW (2006) Impacts of climate change on natural forest productivity – evidence since the middle of the 20th century. *Global Change Biology* 12:1-21.

Brown TJ, Hall BL and Westerling AL (2004) The impact of twenty-first century climate change on wildland fire danger in the western United States: An applications perspective. *Climatic Change* 62:365-388.

Camia A, San-Miguel-Ayanz J, Vilar del Hoyo L and Houston Durrant T (2011) Spatial and temporal patterns of large forest fires in Europe. *Geophysical Research Abstracts* Vol. 13, EGU2011-13996.

Clauset A, Shalizi CR, Newman MEJ (2009) Power Law distributions in empirical data. *SIAM Review* 51(4): 661-703.

de Vries W, Reinds GJ, Gundersen P and Sterba H (2006) The impact of nitrogen deposition on carbon sequestration in European forests and forest soils. *Global Change Biology* 12:1151–1173.

de Vries, W, Solberg S, Dobbertin M, Sterba H, Laubhann D, Reinds GJ, G.J. Nabuurs, Gundersen P and Sutton MA (2008) Ecologically implausible carbon response? *Nature* 451:E1–E3.

Eastaugh C (2008) Adaptations of forests to climate change: a multidisciplinary review. *IUFRO Occasional Paper* 21, International Union of Forest Research Organizations, Vienna. Online via <http://www.iufro.org/publications/series/occasional-papers> 89 p.

Flannigan MD, Amiro BD, Logan KA, Stocks BJ and Wotton BM (2005) Forest fires and climate change in the 21st century. *Mitigation and Adaptation Strategies for Global Change* 11:847-859.

Gabler K and Schadauer K 2006. Methoden der Österreichischen Waldinventur 2000/02. BFW Berichte vol. 135, *Bundeszentrums- und Ausbildungszentrum für Wald, Naturgefahren und Landschaft*, Vienna, 132 pp.

Gossow H, Hafellner R, Arndt N (2008) More forest fires in the Austrian Alps – a real coming danger? pp 356-362 in: Borsdorf, A., Stötter, J., Veuillet, E., Managing Alpine Future - Proceedings of the Innsbruck Conference, October 2007, Verlag der Österr. Akademie der Wissenschaften, 446 p.

Hasenauer, H., Nemani RR, Schadauer K and Running SW. 1999. Forest growth response to changing climate between 1961 and 1990 in Austria. *Forest Ecology and Management* 122:209–219.

Hasenauer H, Merganicova K, Petritsch R, Pietsch S and Thornton P (2003) Validating daily climate interpolation over complex terrain in Austria. *Agricultural and Forest Meteorology* 119:87–107.

Hradetzky J (1995) Concerning the precision of growth estimation using permanent horizontal point samples. *Forest Ecology and Management* 71:203-210.

Hughes L (2003) Climate Change and Australia: Trends, Projections and Impacts. *Austral Ecology* 28:423-443.

Iles K (2009) The Compassman, the Nun, and the Steakhouse Statistician. 259 p. <http://www.island.net/~kiles/>

Klaus M, Holsten A, Hostert P and Kropp JP (2011) Integrated methodology to assess windthrow impacts on forest stands under climate change. *Forest Ecology and Management* 261(11):1799-1810.

Kron W, Steuer M, Löw P and Wirtz A (2012) How to deal properly with a natural catastrophe database – analysis of flood losses. *Natural Hazards and Earth System Sciences* 12: 535-550.

Laubhann D, Sterba H, Reinds GJ and de Vries W (2009) The impact of atmospheric deposition and climate on forest growth in European monitoring plots: an individual tree growth model. *Forest Ecology and Management* 258:1751–1761.

Leech J (2012) Lessons not learned at University #6: Pushing statistics too far? *The Forester* 55(1):29-30.

Leemans R and Eickhout B (2004) Another reason for concern: regional and global impacts on ecosystems for different levels of climate change. *Global Environmental Change* 14:219-228.

Linderholm HW (2006) Growing season changes in the last century, *Agricultural and Forest Meteorology* 137:1-14.

Malamud BD, Millington JDA and Perry GLW (2005) Characterizing wildfire regimes in the USA. *Proceedings of the National Academy of Sciences* 102(13):4694-4699.

Menzel A (2000) Trends in phenological phases in Europe between 1951 and 1996, *International Journal of Biometeorology* 44:76-81.

Mitchell T, Carter T, Jones P, Hulme M and New M (2004) A comprehensive set of high-resolution grids for Europe and the globe: the observed record (1901-2000) and 16 scenarios (2001-2100). Working Paper 55, Tyndall Centre for Climate Change Research, Norwich, 25 pp.

Müller MM (2010) Analyse der durch Blitzschlag ausgelösten Waldbrände in Österreich. Master thesis, University of Natural Resources and Life Sciences (BOKU), Vienna.

Müller M, Vacik H, Diendorfer G, Arpacı A, Formayer H and Gossow H (2012) Analysis of lightning induced forest fires in Austria. *Theoretical and Applied Climatology* (accepted).

New M, Hulme M and Jones PD (2000) Representing twentieth century space-time climate variability. Part 2: development of 1901–96 monthly grids of terrestrial surface climate. *Journal of Climate* 13:2217-2238.

Padilla M and Vega-García C (2011) On the comparative importance of fire danger rating indices and their integration with spatial and temporal variables for predicting daily human-caused fire occurrences in Spain. *International Journal of Wildland Fire* 20:46-58.

Pausas JG and Fernández-Muñoz S (2012) Fire regime changes in the Western Mediterranean basin: from fuel limited to drought-driven fire regime. *Climatic Change* 110:215-226.

Peltola H, Kellomäki S and Väisänen H (1999) Model computations of the impact of climatic change on the windthrow risk of trees. *Climatic Change* 41(1):17-36.

Petritsch R (2002) *Anwendung und Validierung des Klimainterpolationsmodells DAYMET in Österreich*. Master's thesis, University of Natural Resources and Life Sciences, Vienna, 95p.

Petritsch R and Hasenauer H (2007) Interpolating input parameters for large scale ecosystem models. *Austrian Journal of Forest Science* 124:135–151.

Petritsch R and Hasenauer H (2009) Tägliche Wetterdaten im 1 km Raster von 1960 bis 2008 über Österreich. *Austrian Journal of Forest Science* 126:215–225.

Pietsch SA, Hasenauer H and Thornton PE (2005) BGC-model parameters for tree species growing in central European forests. *Forest Ecology and Management* 211:264–295.

Placer K and Schneider J (2001) *Arbeit zur Kartierung der trockenen Deposition in Österreich*. Federal Environment Agency, Austria.

Reed WJ and McKelvey KS (2002) Power-law behaviour and parametric models for the size-distribution of forest fires. *Ecological Modelling* 150: 239-254.

Ricotta C, Avena G and Marchetti M (1999) The flaming sandpile: self-organised criticality and wildfires. *Ecological Modelling* 119: 73-77.

Schicker I, Radanovics S and Seibert P (2010) Origin and transport of Mediterranean moisture and air. *Atmospheric Chemistry and Physics* 10:5089-5105.

Schieler K (1997) *Methode der Zuwachsberechnung der Österreichischen Waldinventur*. PhD Thesis, University of Natural Resources and Applied Life Sciences, Institute of Forest Growth, Vienna, Austria.

Schneider J (1998) *Kartierung der nassen Deposition in Österreich*. Austrian Federal Environment Agency, Vienna, 40 pp.

Scott CT and Alegria J (1990) Fixed- versus variable-radius plots for change estimation. P. 126-132 in V.J. LaBau, and T. Cunia (eds) Workshop Proceedings, Symposium on State of the Art Methodology of Forest Inventory, July 30 - August 5, 1989; Syracuse, NY. Gen. Tech. Rpt. PNW-GTR-263. Portland, OR: USDA, Forest Service, Pacific Northwest Research Station.

Seibert P, Frank A and Formayer H (2007) Synoptic and regional patterns of heavy precipitation in Austria. *Theoretical and Applied Climatology* 87:139-153.

Seidl R, Rammer W, Jäger D and Lexer MJ (2008) Impact of bark beetle (*Ips typographus* L.) disturbance on timber production and carbon sequestration in different management strategies under climate change. *Forest Ecology and Management* 256:209-220.

Soja AJ, Tchebakova NM, French NHF, Flannigan MD, Shugart HH, Stocks BJ, Sukhinin AI, Parfenova EI, Chapin FS III and Stackhouse PW Jr (2007) Climate- induced boreal forest change: Predictions versus current observations, *Global and Planetary Change* 56:274-296.

Solberg S, Dobbertin M, Reinds GJ, Lange H, Andreassen K, Fernandez PG, Hildingsson A and deVries W (2009) Analyses of the impact of changes in atmospheric deposition and climate on forest growth in European monitoring plots: a stand growth approach. *Forest Ecology and Management* 258:1735–1750.

Spiecker H (1999) Overview of recent growth trends in European forests. *Water, Air and Soil Pollution* 116:33–46.

Sterba H and Zingg A (2001) Target diameter harvesting – a strategy to convert even-aged forests. *Forest Ecology and Management* 151(1-3):95-105.

Tanskanen H and Venäläinen A (2008) The relationship between fire activity and fire weather indices at different stages of the growing season in Finland. *Boreal Environmental Research* 13:285-302.

Thornton PE, Law BE, Gholz HL, Clark KL, Falge E, Ellsworth DS, Goldstein AH, Monson RK, Hollinger D, Falk M, Chen J and Sparks JP (2002) Modeling and measuring the effects of disturbance history and climate on carbon and water budgets in evergreen needleleaf forests. *Agricultural and Forest Meteorology* 113:185-222.

Vacik H, Arndt N, Arpacı A, Koch V, Müller M and Gossow H (2011) Characterisation of forest fires in Austria. *Austrian Journal of Forest Science* 128(1):1-32

Vacik H and Gossow H (2011) Forest Fire Research and Management Options in Austria: Lessons Learned from the AFFRI and the ALPFFIRS Networks. In: Borsdorf A, Stötter J, Veulliet E, editors. Managing Alpine Future II conference, 21-23 November 2011, Innsbruck, Verlag der Österreichischen Akademie der Wissenschaften. pp 203-211.

Valese E, Beck A, Comini B, Conedera M, Cvenkel H, Di Narda N, Ghiringhelli A, Japelj A, Lemessi A, Mangiavillano A, Pelfini F, Pelosini R, Ryser D, Vacik H and Wastl C (2010) The Alpine Forest Fire Warning System (ALP FFIRS) project. In: Viegas DX, editor. VI International Conference on Forest Fire Research. p. 9. Online at http://www.alpffirs.eu/index.php?option=com_docman&task=doc_download&gid=239&Item id

Van Deusen P, Dell TR and Thomas CE (1986) Volume growth estimation from permanent horizontal plots. *Forest Science* 32(2):415-432.

Verbesselt J, Jönsson P, Lhermitte S, van Aardt J and Coppin P (2006) Evaluating satellite and climate data-driven indices as fire risk indicators in savanna ecosystems, *IEEE Transactions on Geoscience and Remote Sensing* 44:1622-1632, 2006.

Viegas DX, Bovio G, Ferreira A, Nosenzo A and Sol B (1999) Comparative study of various methods of fire danger evaluation in southern Europe. *International Journal of Wildland Fire* 9:235-246.

Walther A and Linderholm HW (2006) A comparison of growing season indices for the Greater Baltic Area, *International Journal of Biometeorology* 51(2): 107-118.

Wamelink GWW, van Dobben HF, Mol-Dijkstra JP, Schouwenberg EPAG, Kros J, de Vries W and Berendse F (2009) Effect of nitrogen deposition reduction on biodiversity and carbon sequestration. *Forest Ecology and Management* 258:1774–1779.

Williams AAJ, Karoly DJ and Tapper N (2001) The sensitivity of Australian fire danger to climate change, *Climatic Change* 49:171-191

10. APPENDICES

I) Eastaugh CS and Hasenauer H (2012a) Biases in volume increment estimates derived from successive angle-count sampling. *Forest Science*. (in press 28/09/2011) <http://dx.doi.org/10.5849/forsci.11-007>. [SCI] **Page A.1**

II) Hasenauer H and Eastaugh CS (2012) Assessing forest production using terrestrial monitoring data. *International Journal of Forestry Research*. Article ID 961576, 8pp. **Page A.15**

III) Eastaugh CS, Petritsch R and Hasenauer H (2010) Climate characteristics across the Austrian forest estate from 1960 to 2008. *Austrian Journal of Forest Science* 127:133-146. [SCIE] **Page A.29**

IV) Eastaugh CS and Vacik H (2012, *in review 05/04/2012*) Fire size/frequency distributions as a means of assessing wildfire database reliability. *PLoS ONE*. [SCIE] **Page A.37**

V) Eastaugh CS, Arpaci A and Vacik H (2012) A cautionary note regarding comparisons of fire danger indices. *Natural Hazards and Earth System Sciences* 12:927-934. [SCIE] **Page A.53**

VI) Eastaugh CS, Pötzelsberger E and Hasenauer H (2011) Assessing the impacts of climate change and nitrogen deposition on Norway spruce (*Picea abies* L. Karst) growth in Austria with BIOME-BGC. *Tree Physiology* 31(3):262-274. [SCI] **Page A.61**

VII) Eastaugh CS and Hasenauer H (2012b, *in review 11/05/2012*) Biogeochemical process modeling of forest fire ignition hazard. *Climatic Change*. [SCI] **Page A.74**

Climate Characteristics across the Austrian Forest Estate from 1960 to 2008

Chris S. Eastaugh^{*}, Richard Petritsch and Hubert Hasenauer

*Institute of Silviculture
University of Natural Resources and Life Sciences (BOKU)
Vienna*

Summary

Process modelling of forest growth for any purpose requires precise climatic data. This data is rarely available for the exact site being studied, so climate parameters are often taken from a nearby weather station or downscaled from broad-scale gridded datasets. This paper presents a third option, based on a detailed climate interpolation developed at the University of Natural Resources and Applied Sciences (BOKU) in Vienna. DAYMET gives precise daily climate data for 2224 forest inventory sites in Austria. The interpolation compares well with other datasets at the National scale, and provides more precise information at any specific site. Marked regional differences are apparent within Austria for both temperature and precipitation trends. Modelling applications often require precise climate inputs, and downscaled data from broad grids or the use of data from the nearest climate station may not be adequate. Interpolated datasets such as DAYMET can provide both an accurate representation of broad-scale averages and precise point data for model inputs.

Key words: Regional climate, Weather data, Interpolation, Forest Inventory, DAYMET

^{*} Corresponding author.

Email addresses: `chris.eastaugh@boku.ac.at` (Chris S. Eastaugh),
`richard.petritsch@boku.ac.at` (Richard Petritsch),
`hubert.hasenauer@boku.ac.at` (Hubert Hasenauer).

Article published in Austrian Journal of Forestry 127 (2010) 133–146

Zusammenfassung

Stoffkreislaufmodelle zur Beschreibung von Waldökosystemen erfordern detaillierte Klimadaten. Meist sind diese Daten jedoch nicht für die Bestände, die untersucht werden sollen, vorhanden. Aus diesem Grund werden üblicherweise Daten der nächstgelegenen Meßstation oder aus überregionalen Datensätzen herangezogen. Die vorliegende Arbeit stellt eine weitere Möglichkeit vor: das Klimainterpolationstool DAYMET, das am Institut für Waldbau der Universität für Bodenkultur Wien (BOKU) entwickelt wurde. Mit diesem wurden tägliche Wetterdaten zwischen 1960 und 2008 für 2224 Inventurpunkte berechnet. Vergleichbar mit anderen Datensätzen nationaler Ebene, liefert die Interpolation detaillierte Informationen für jeden beliebigen Punkt. Regionale Unterschiede in den Trends für Temperatur und Niederschlag sind bei der Verwendung von Klimadaten der nächstliegenden Meßstation oder aus einem überregionalen Datensatz oft nicht sichtbar. Interpolierte Daten, wie DAYMET sie liefert, stellen jedoch eine Alternative dar, die großräumige Mittelwerte ebenso wie genaue Punktdaten liefern kann. In dieser Studie werden regionale Unterschiede in den klimatischen Trends an den Punkten der Österreichischen Waldinventur aufgezeigt, wie sie aus DAYMET aber nicht aus einem überregionalen Datensatz abgeleitet werden können.

1 Introduction

Forests comprise a major part of the natural environment in many Central European countries, and in Austria cover 47% of the total land surface. Forests have a wide ranging influence on other systems such as the water cycle (Chang, 2006), wildlife habitat (Patton, 2010), avalanche protection (Teich and Bebi, 2009), the climate system (Pielke et al., 2002) and social and economic systems (Davidson et al., 2003). Similarly, forest growth is influenced by a wide range of biotic and abiotic considerations, both natural and manmade (Pretzsch, 2009). The complexities of these interactions make modeling an essential tool for understanding processes and drawing conclusions about the likely effects of environmental change on forests and inter-related systems.

Many processes relevant to forest growth operate in a non-linear fashion (Zeide, 1993). This presents some difficulties in upscaling results from limited field tri-

als to a national level useful for policy guidance. Developing an accurate representation of diverse forest growth at a national scale requires a high number of study sites, each with measured or accurately estimated input data. Forest growth information is commonly available from forest inventory studies, but it is rare to find accurate data for some other model inputs (particularly meteorological records) at these precise sites.

Biogeochemical models (process or mechanistic models) seek to mimic the major drivers of natural processes and thus give a greater understanding of the influence and interrelations of key variables. In climate impact studies this approach has an advantage over purely statistical models, in that the effects of changing climate parameters can be validly extrapolated beyond historical ranges, if the impact of changes to various model inputs are supported by an understanding of physiology and the overall model operation is supported by observation. A major restriction of process modeling however is the need for precise input data, particularly for comprehensive models such as BIOME-BGC (Thornton, 1998) or CABALA (Battaglia et al., 2004) which require accurate measures of daily precipitation, maximum and minimum temperatures, vapour pressure deficit and solar radiation.

Precise climatic data is rarely available for the exact site being studied, so climate parameters are often estimated from nearby weather station records or downscaled from broad-scale gridded datasets. These approximations can lead to significant errors in process model results (Mummery and Battaglia, 2004). This paper presents a third option, based on a detailed climate interpolation developed at the University of Natural Resources and Applied Sciences (BOKU) in Vienna. DAYMET (Thornton et al., 1997, Hasenauer et al., 2003) can give precise daily climate data for all forest inventory sites in Austria.

Interpretation of data or model outputs often requires aggregation, particularly if some input data (i.e. past site management history) are uncertain and must be statistically estimated, or if random factors have a substantial impact on results. Aggregation can increase the signal to noise ratio in model outputs, but at the risk of losing potentially important differentiation within aggregations.

The purpose of this paper is to determine local climatology and regional trends across the Austrian forest estate, and to compare site-specific climate data for forest inventory sites with data obtained through downscaling from a Europe-wide dataset. Specifically, we validate the national trends of the DAYMET in-

terpolation against two independent datasets and examine the added detail gained from an increase in spatial precision from a smaller scale interpolation. A methodology for defining sub-national 'forest climate change regions' is developed, which will be useful in future work in determining the effects of extant climate change on Austrian forests, and to make informed speculations about the possible effects of future change.

2 Data and Interpolation

The Austrian National Forest Inventory (Gabler and Schadauer, 2006) contains a total of about 11000 forested points, organized into tracts each of 4 points on a 200m square. 5600 tracts are arranged in a square grid pattern across the country, including over areas that are not currently forested. Using one point from each forested tract, a total of 2224 points is obtained. These points are therefore maximally representative of Austrian forests, and encompass all combinations of species, topographical arrangements and prior and current management regimes. The inventory contains information on individual tree locations, species, growth stage, age class, basal area, top and crown height and tree health status. Other necessary model input data such as soil information (Petritsch and Hasenauer, 2007), atmospheric CO₂ and nitrogen levels (Schneider, 1998; Placer and Schneider, 2001) may also be estimated for these sites.

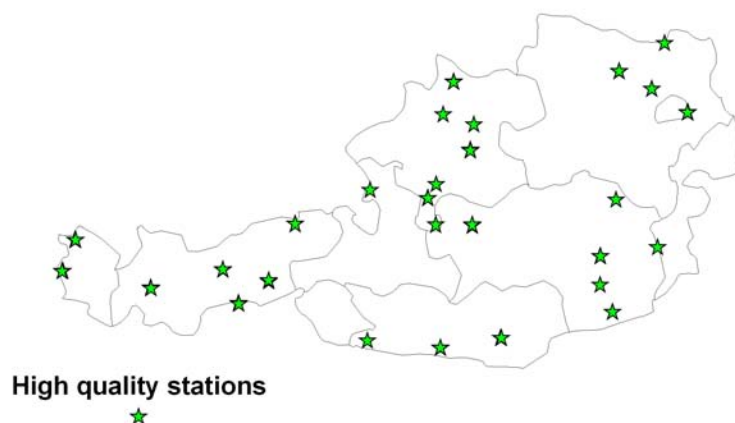


Figure 1. High quality, long record stations.

Data is available from the Austrian Meteorological Service for several hundred locations. Many stations however cover only short periods, or have significant gaps, and so cannot be used to calculate national averages or trends. In many cases stations at the same physical location have separate records for different time periods. A 'high quality' subset of the station data was extracted here through the following procedure: Incomplete time series records were merged geographically so that any stations within 1000 metres horizontally and 50 metres of elevation were considered to be in the same location. Any calendar month at any station with records for less than $2/3$ of the days was discarded, as was any year without a full series of months. This procedure left 28 stations with records from 1960-2005 (fig. 1). Although raw data was used the possible advantages of homogenization are expected to be small, with Auer et al. (2001) finding a required homogenization adjustment in the Austrian mean within the time period of our study of only around 0.3 degrees for temperature and about 2% for precipitation.

Interpolated inventory site climate dataset

Climate data from the full range of Austrian stations was used to create an interpolation covering all 2224 points of the Austrian forest inventory (Petritsch, 2002). The DAYMET interpolation used here is a version of the DAYMET climate interpolation developed in the USA (Thornton et al., 1997), optimized for the mountainous terrain of Austria and expanded to enable interpolation to given geographical points, rather than simply to a grid. DAYMET's interpolation algorithms were validated by Hasenauer et al. (2003). Cross-validation of the interpolation process showed a mean absolute error nation wide of 1.17 degrees for minimum temperature, 1.01 degrees for maximum temperature and 3.0 mm for precipitation. Respective mean errors however were only 0.00 degrees, -0.01 degrees and 0.1 mm, suggesting that subsequent upscaling of interpolated data can reduce errors to practically negligible levels.

DAYMET produces three direct interpolations: precipitation and maximum and minimum temperatures. From this it is possible to produce calculated or estimated values for mean daily temperature, growing season length, vapour pressure deficit, solar radiation and drought index. As all of these secondary factors are derived from the primary DAYMET outputs (Thornton et al., 2000), this paper will concentrate solely on precipitation and average temperature values.

Downscaled climate grids

Previously published downscaled climate interpolations (i.e. Böhm et al., 2001; Mitchell et al., 2004; Haylock et al., 2008) are based on a selection of 'high value' meteorological station records, with largely uninterrupted records over long time periods. One commonly used variant is the CRU TS 1.20 dataset for Europe from the Climatic Research Unit of the University of East Anglia (Mitchell et al., 2004), which provides monthly climate averages at a resolution of 10', downscaled from a 0.5° global grid.

Table 1
Summary of input datasets.

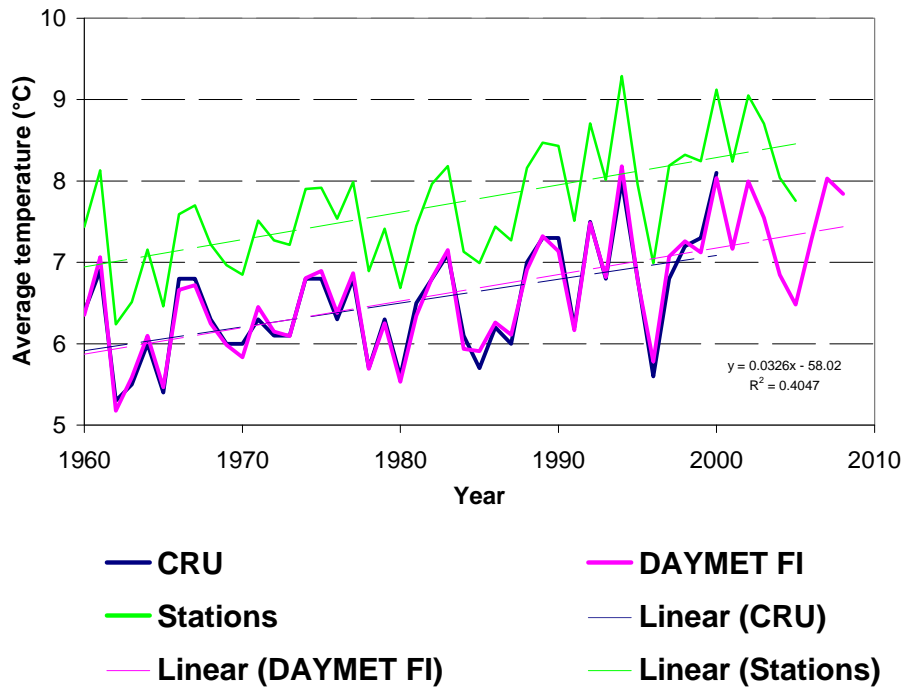
Dataset	Output data points in Austria	Mean Elevation (m asl)	Record period	Temperature (°C)			Precipitation (mm)		
				National annual mean	S.D.	Mean national trend (°C/yr)	National annual mean	S.D.	Mean national trend (mm/yr)
High-value Stations	28	658	1960–2005	7.70	0.71	+0.0336	1062	117.7	+0.75
Forest Inventory sites	2224	917	1960–2008	6.65	1.86	+0.0326	1109	300.0	-0.33
CRU downscaling	360	951	1960–2000	6.33	2.74	+0.0292	1097	316.7	-0.08

3 Results

A comparison of interpolated climatic trends over the Austrian forest estate against station data and the CRU TS 1.20 dataset shows agreement at the national scale (fig. 2). Trends are similar in each case, and the higher values for station-based mean national temperature may be explained by the difference in mean elevation of the data points. At a national scale, there is clear correlation between the temperature data sourced through the three different methodologies. Agreement among the precipitation data is less perfect, but clear signal years at both high and low extremes are present.

The density of high-value stations as defined in this study is 1 per 2990 km². The mean distance of the inventory sites to the nearest climate station is 30.10 km, with a standard deviation of 15.18 km and a maximum of 80.15 km.

Average Austrian temperature 1960-2008



Average Austrian precipitation 1960-2008

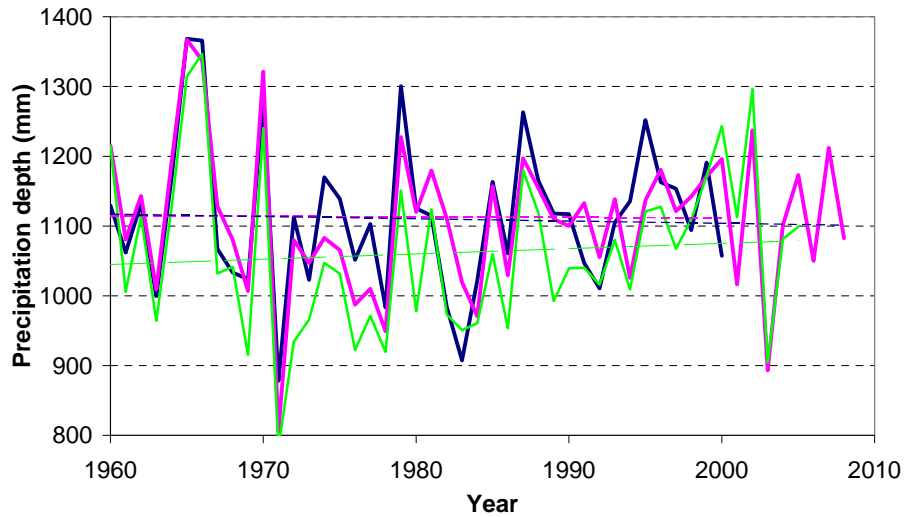


Figure 2. Temperature and precipitation trends, national scale.

Inventory site interpolation

Substantial regional and seasonal differences are apparent in both temperature and precipitation trends across the Austrian forest estate. The data points in

figures 3 and 4 represent the linear climate trends at each of the 2224 Forest Inventory sites. Temperatures are mostly warming, although this is less pronounced in the Seetaler Alps of Steiermark and Kärnten, particularly in the autumn months where cooling is apparent. Precipitation is more variable, but shows clear trends to decreasing rainfall in the southeast of the country and in the northern parts of Tyrol in the west, and increasing trends in other areas.

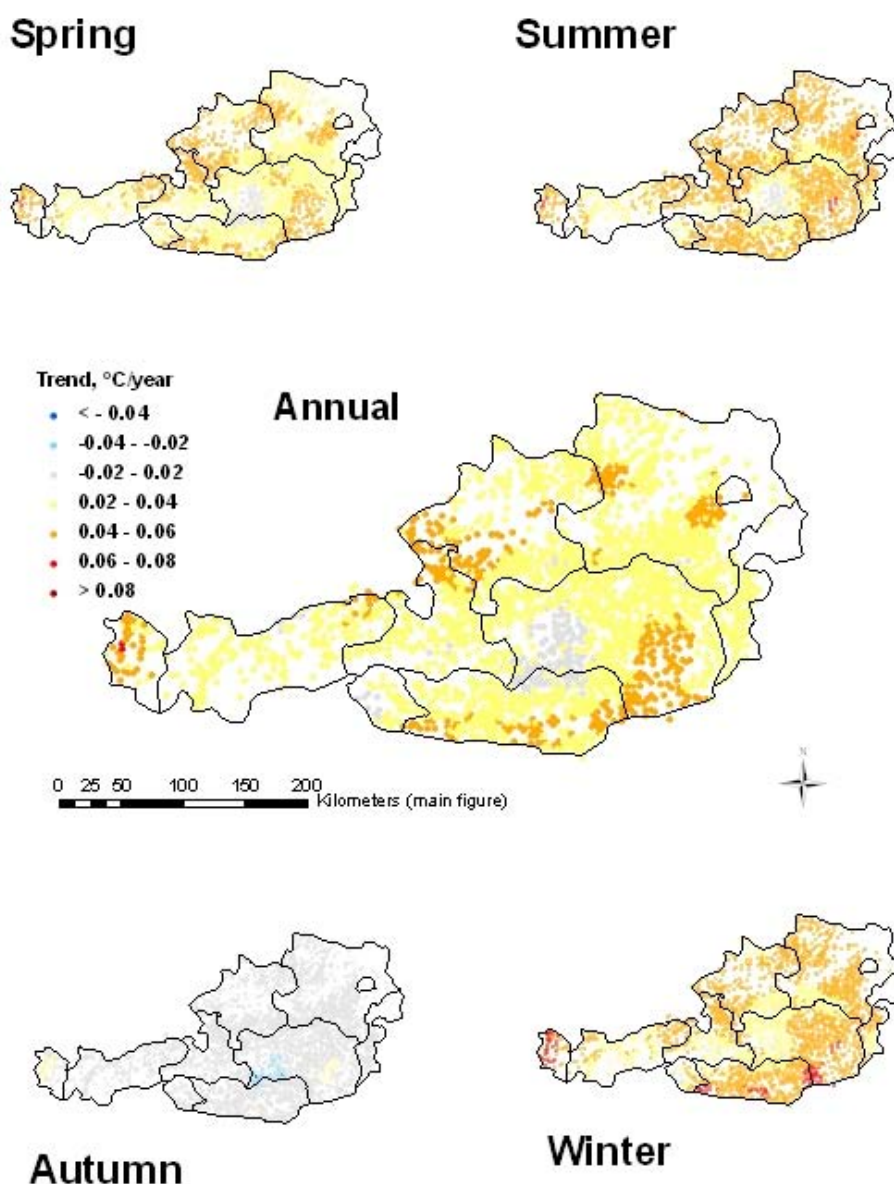


Figure 3. Temperature trends on Austrian Forest Inventory sites, 1960 - 2008.

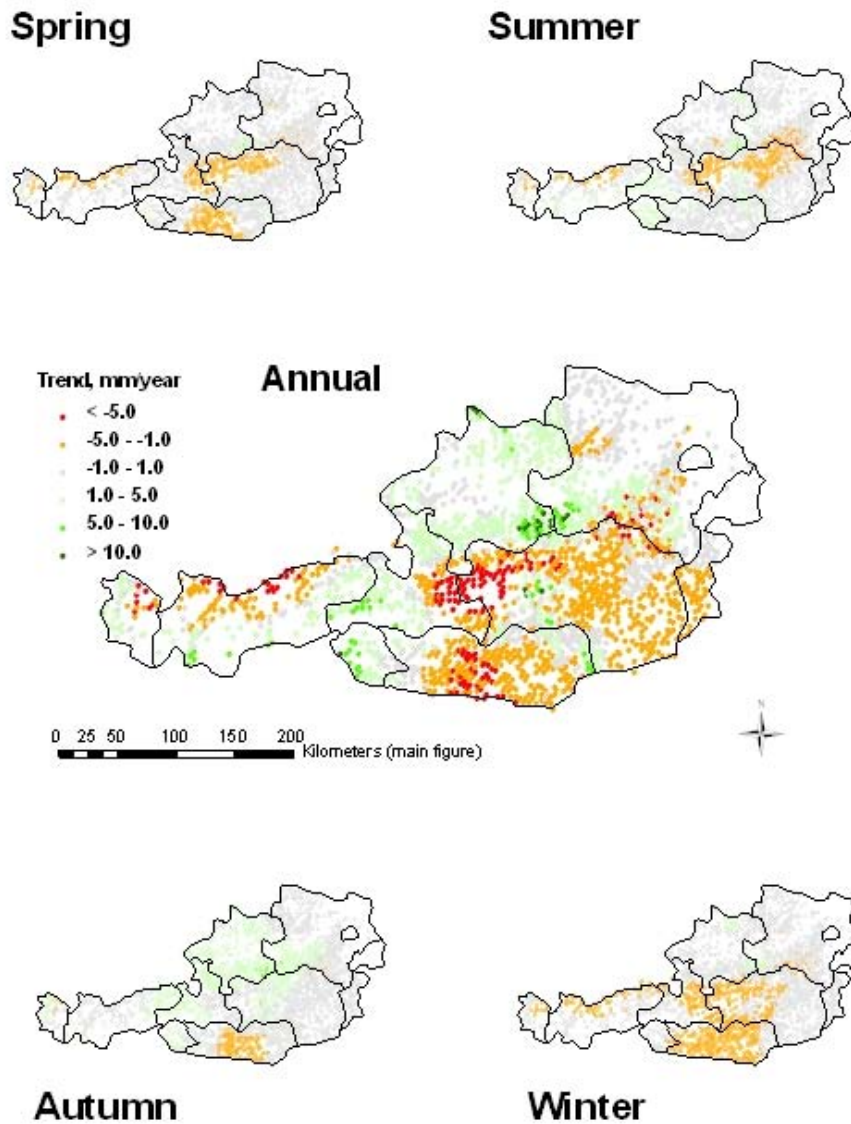


Figure 4. Precipitation trends on Austrian Forest Inventory sites, 1960 - 2008.

Downscaled climate grids

The CRU TS 1.20 dataset is a Europe-wide $10'$ grid downscaled from a 0.5° global grid. As shown in figure 5 the downscaling does reflect some regional differences in temperature and precipitation trends across Austria. The warming trend in the southeast and far west of the country is noticeable, but other trends apparent in the DAYMET interpolation are not readily seen in the CRU data. This agrees with (Schöner et al., 2000), who pointed out that an earlier version of the 0.5° CRU data was not useful for describing regional climate variability.

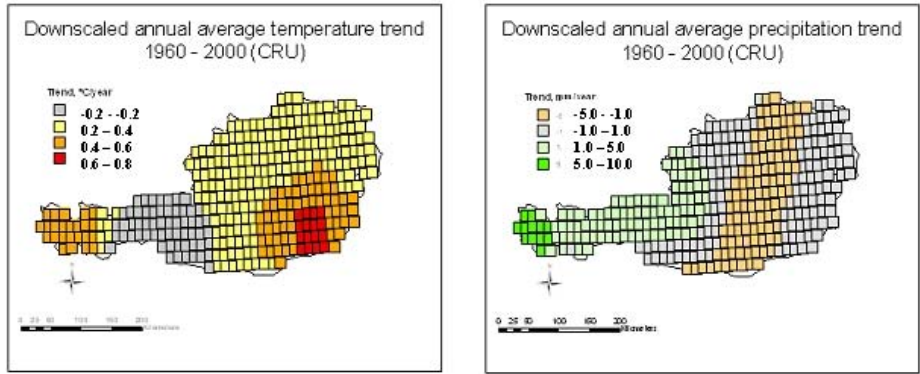


Figure 5. CRU TS 1.20 downscaled climate grids.

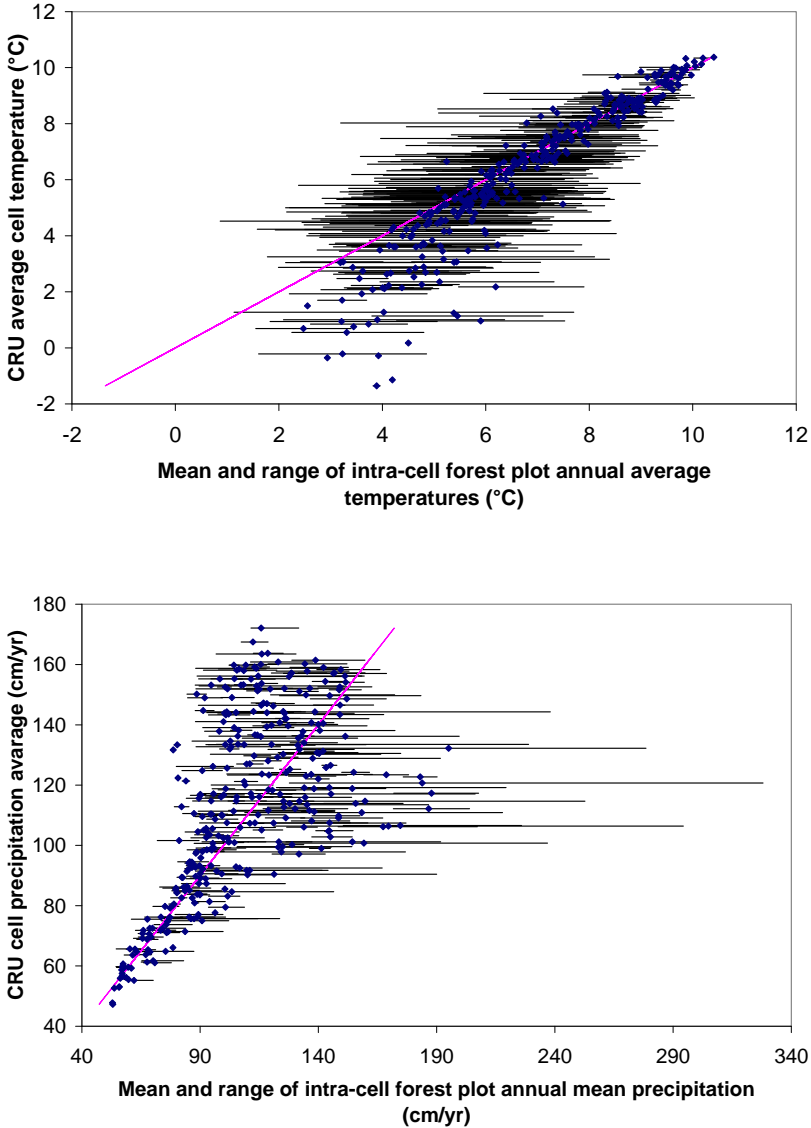


Figure 6. Comparison of downscaled CRU data with means and ranges of in-cell forest plot data.

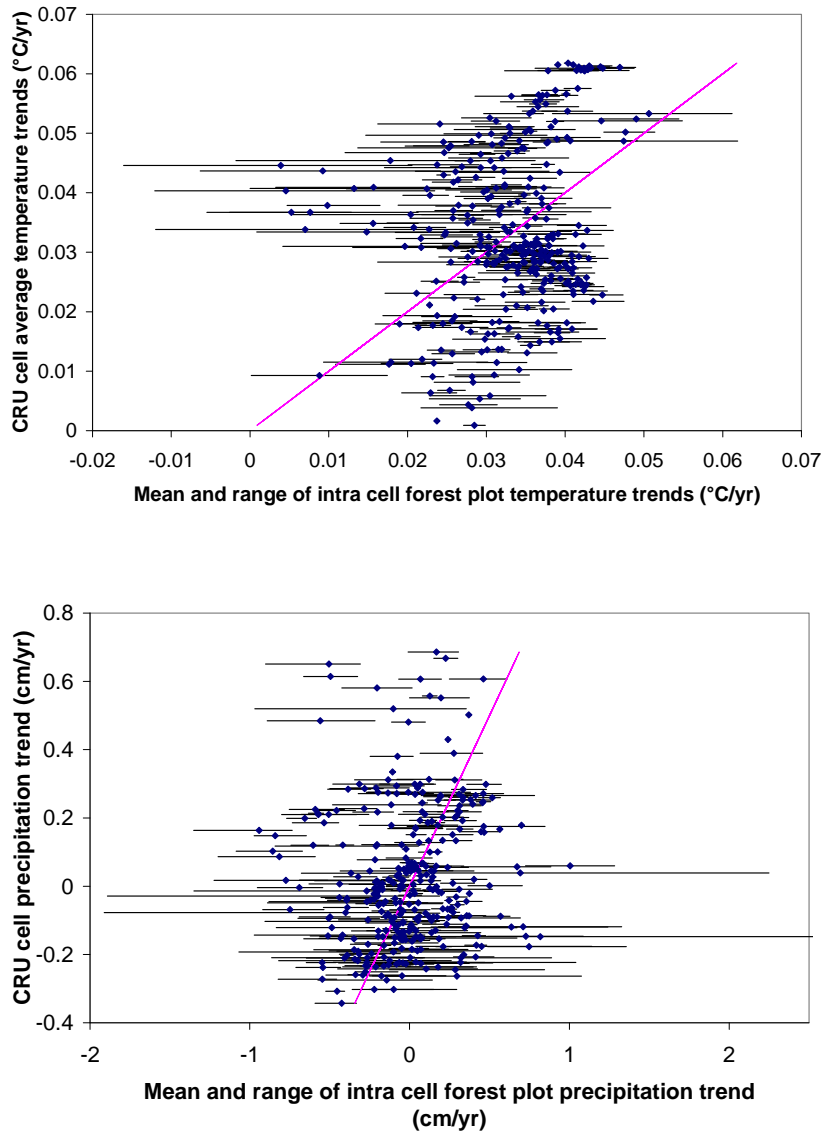


Figure 7. Comparison of trends in downscaled CRU data with means and ranges of in-cell forest plot data.

Site-specific differences

Of the 350 10' CRU grid cells across Austria, 337 contain at least one forest inventory site, with an average of 6.64 sites per cell. Average annual temperature and precipitation of each forested cell was compared with the mean and range of the forest plots within that cell (Figure 6). Trends in both variables were examined in the same way (Figure 7).

4 Discussion and Conclusion

Modelling applications often require precise climate inputs. Downscaled data from broad grids or the use of data from the nearest climate station may not be adequate, and the use of such approximations may in some cases invalidate model outputs. Interpolated datasets such as DAYMET can provide both an accurate representation of broad-scale averages and precise point data for model inputs.

Estimating site climate history from the nearest high-value climate station has a high potential for error, given the low density of such stations even in relatively advanced countries such as Austria. Aggregating such high-value data across complex terrain may provide useful information at a national scale, but the regional variability is not reflected in the results. The high degree of variability in both means and trends of forest sites within relatively small areas (10' square) demonstrates the potential risks of using averaged results across sites even quite small distances apart. In some cases even the means of forest sites within such a 10' grid cell showed marked variation from the CRU interpolation, particularly for cells with high average elevations, where forest sites are likely to be in the lower, warmer, dryer parts of the cell. At the national scale, temperature averages determined simply from the high value climate stations tend to be higher than those from interpolations for a similar reason, because such climate stations are more likely to be located in populated, warmer, low elevation regions.

Although this study used the monthly means of DAYMET outputs (due to the difficulty of sourcing other daily climate interpolations for comparison), the issues raised here are likely to be further accentuated at a daily scale. Models whose output may vary according to daily climate patterns must use precise input data, and the poor precision of estimated or downscaled data may have a serious effect on model accuracy.

References

Auer, I., Böhm, R., Schöner, W., 2001. Austrian long-term climate 1767-2000: multiple instrumental climate time series from Central Europe. Österreichis-

- che Beiträge zu Meteorologie und Geophysik, vol.25, Zentralanstalt für Meteorologie und Geodynamik, Vienna, 146 pp.
- Battaglia, M., Sands, P., White, D., Mummery, D., 2004. CABALA: a linked carbon, water and nitrogen model of forest growth for silvicultural decision support. *Forest Ecology and Management* 193, 251–282.
- Böhm, R., Auer, I., Brunetti, M., Maugeri, M., Nanni, T., Schöner, W., 2001. Regional temperature variability in the European Alps: 1760-1998 from homogenized instrumental time series. *International Journal of Climatology* 21, 1779–1801.
- Chang, M., 2006. *Forest hydrology: an introduction to water and forests*. CRC Press, Boca Raton, 474 pp.
- Davidson, D., Williamson, T., Parkins, J., 2003. Understanding climate change risk and vulnerability in northern forest-based communities. *Canadian Journal of Forest Research* 33, 2252–2261.
- Gabler, K., Schadauer, K., 2006. *Methoden der Österreichischen Waldinventur 2000/02*. BFW Berichte vol. 135, Bundesforschungs- und Ausbildungszentrum für Wald, Naturgefahren und Landschaft, Vienna, 132 pp.
- Hasenauer, H., Merganicova, K., Petritsch, R., Pietsch, S., Thornton, P., 2003. Validating daily climate interpolation over complex terrain in Austria. *Agricultural and Forest Meteorology* 119, 87–107.
- Haylock, M., Nofstra, N., Klein-Tank, A., Klok, E., Jones, P., New, M., 2008. A European daily high-resolution gridded data set of surface temperature and precipitation for 1950-2006. *Journal of Geophysical Research* 113.
- Mitchell, T., Carter, T., Jones, P., Hulme, M., New, M., 2004. A comprehensive set of high-resolution grids for Europe and the globe: the observed record (1901-2000) and 16 scenarios (2001-2100). Working Paper 55, Tyndall Centre for Climate Change Research, Norwich, 25 pp.
- Mummery, D., Battaglia, M., 2004. Significance of rainfall distribution in predicting eucalypt plantation growth, management options, and risk assessment using the process-based model CABALA. *Forest Ecology and Management* 193, 283–296.
- Patton, D., 2010. *Forest wildlife ecology and habitat management*. CRC Press, Boca Raton, 292 pp.
- Petritsch, R., 2002. *Anwendung und Validierung des Klimainterpolationsmodells DAYMET in Österreich*. Master's thesis, University of Natural Resources and Life Sciences, Vienna, 95p.
- Petritsch, R., Hasenauer, H., 2007. Interpolating input parameters for large scale ecosystem models. *Austrian Journal of Forest Science* 124, 135–151.

- Pielke, R. S., Marland, G., Betts, R., Chase, T., Eastman, J., Niles, J., Niyogi, D., Running, S., 2002. The influence of land-use change and landscape dynamics on the climate system: relevance to climate-change policy beyond the radiative effect of greenhouse gases. *Philosophical Transactions of the Royal Society of London A* 360, 1705–1719.
- Placer, K., Schneider, J., 2001. Arbeit zur Kartierung der trockenen Deposition in Österreich. Federal Environment Agency, Austria.
- Pretzsch, H., 2009. Forest dynamics, growth and yield. Springer-Verlag, Berlin, 664 pp.
- Schneider, J., 1998. Kartierung der nassen Deposition in Österreich. Umweltbundesamt, Wien, 24 pp.
- Schöner, W., Auer, I., Böhm, R., Brunetti, M., Mauger, M., Mestre, O., 2000. Homogenisation and gridding of a Central European temperature data set. Proceedings of the 3rd seminar for Homogenization and quality control in climatological databases, September 25-29, Budapest, Hungary. Online at http://www.met.hu/omsz.php?almenu_id=omsz&pid=seminars&pri=13&mpx=1&sm0=0&tfi=schoner Accessed 03 November 2010.
- Teich, M., Bebi, P., 2009. Evaluating the benefit of avalanche protection forest with GIS-based risk analyses-A case study in Switzerland. *Forest Ecology and Management* 257(9), 1910–1919.
- Thornton, P., 1998. Description of a numerical simulation model for predicting the dynamics of energy, water, carbon and nitrogen in a terrestrial ecosystem. Ph.D. thesis, University of Montana, Missoula, MT, 280p.
- Thornton, P., Hasenauer, H., White, M., 2000. Simultaneous estimation of daily solar radiation and humidity from observed temperature and precipitation: an application over complex terrain in Austria. *Agriculture and Forest Meteorology* 104, 255–271.
- Thornton, P., Running, S., White, M., 1997. Generating surfaces of daily meteorological variables over large regions of complex terrain. *Journal of Hydrology* 190, 214–251.
- Zeide, B., 1993. Analysis of growth equations. *Forest Science* 39(3), 594–616.

Biases in Volume Increment Estimates Derived from Successive Angle Count Sampling

Chris S. Eastaugh and Hubert Hasenauer

Abstract: Several large-scale forest inventories are now being conducted using angle count sampling, and the method is commonly used for timber cruising and corporate forest assessment. The calculation of basal area or volume increment from angle count sample data is not trivial, and three alternative methods are currently in common use: the difference method, the starting value method, and the end value method. This article develops the hypothesis that in various circumstances these methods are susceptible to bias as a result of measurement error and mis-sampling of trees. After reviewing prior work in angle count mathematics and developing the theoretical basis of our hypothesis, we present a supporting example based on a large permanent sampling plot at Hirschlacke in northern Austria. Our results suggest that the errors resulting from using calculation methodologies susceptible to bias from measurement error may in practical circumstances be more than 10% of volume increment, which could have ramifications for sustainable forest management or carbon sequestration budgeting. FOR. SCI. ■(■):000–000.

Keywords: point sample, angle count, sampling error, Bitterlich, inventory

ACCURATE ASSESSMENTS OF FOREST volume increment are becoming increasingly important within natural resource management. Apart from the obvious relevance to determining sustainable forest resource utilization, an increasing focus on using forest inventory data to assess the carbon sequestration potential of forests is taking forest growth assessment issues beyond the forest sector into a far wider policy environment. This suggests that consistent forest information is of increasing concern and any increment estimations derived from forest inventory data (e.g., timber volume, biomass, or carbon) that forest agencies provide to governments must therefore be as accurate and unbiased as possible to ensure their credibility and to allow support of rational policy development.

Forest inventories in some form have been in place in some jurisdictions since the 15th century (Schadauer et al. 2007). Until recently, inventories were conducted solely as a means of determining what resource was present in a region, generally to determine its immediate extractive capacity. Today, however, national forest inventories form an integral part of the way that many nations determine their national carbon balance, and inventories are used to estimate forest growth increment as a means of monitoring their value as a carbon sink.

Since the early 1990s, regular forest inventories have been established in many countries, often using a permanent plot design to reduce the sampling error of the resulting increment calculations (Tomppo et al. 2010). The remeasurement interval ranges from 5 to 10 years, and a common

sampling method in many jurisdictions is angle count sampling (Bitterlich 1948).

Angle count samples, also referred to as sampling proportional to size, horizontal point samples, or Bitterlich plots, are considered to be an unbiased estimate of stand volume (Grosenbaugh 1958) and have been demonstrated to be a superior method of forest inventory under many circumstances (Whyte and Tennent 1975, Scott 1990). In terms of increment assessment, they have high variance (Hradetzky 1995), although they are generally considered to be unbiased estimators of increment (Van Deusen et al. 1986). Three different methods for estimating volume increment from successive angle count samples are in common use, attributed by Hradetzky (1995) to Van Deusen et al. (1986), Grosenbaugh (1958), and Roesch et al. (1989), respectively.

1. Difference method (Z^D). This method calculates increment as the standing volume estimate at time 2 minus the volume estimate at time 1, plus the removals.
2. Starting value method (Z^S). This method selects only those trees present at both times and calculates stand increment as the increment of the selected trees multiplied by the estimated number of trees of that size in the stand in time 1, plus new trees entering the stand.
3. End value method (Z^E). All trees present in time 2 are considered, and the stand increment as the increment of the selected trees multiplied by the estimated number of trees of that size in the stand in time 2 is

Manuscript received January 14, 2011; accepted September 28, 2011; published online February 9, 2012; <http://dx.doi.org/10.5849/forsci.11-007>.

Chris S. Eastaugh, Universität für Bodenkultur (BOKU), Peter Jordan Str. 82, A1190 Vienna, Austria—Phone: 43 (147) 654-4050; chris.eastaugh@boku.ac.at. Hubert Hasenauer, Universität für Bodenkultur (BOKU)—hubert.hasenauer@boku.ac.at.

Acknowledgments: This work is part of the project “Comparing satellite versus ground driven carbon estimates for Austrian Forests” (MOTI). We are grateful for the financial support provided by the Energy Fund of the Federal State of Austria, managed by Kommunalkredit Public Consulting GmbH under Contract K10AC1K00050. We thank Prof. Hubert Sterba for comments on an earlier version of this manuscript and helpful review comments by the Associate Editor and two anonymous reviewers served to substantially improve the article.

Copyright © 2012 by the Society of American Foresters.

calculated. Note that the end value method requires the estimation of prior dimensions of trees, which may not have been recorded at time 1.

Published literature on deriving increments from angle count sampling distinguishes between “survivors,” “ingrowth,” “ongrowth,” and “nongrowth” trees (cf. Martin 1982), depending on whether they were above or below a particular dbh in the period preceding the current measuring period and whether they were counted “in” or “out” of the angle count in the preceding period. Hradetzky (1995) avoids this issue by noting that ingrowth and ongrowth trees are in fact quite rare when relatively low dbh thresholds are used and so only survivors and nongrowth need be considered. To simplify our theoretical discussions the dbh threshold was defined as 0. All trees sampled must thus be either survivors, nongrowth, or ongrowth. The difference method in this case treats ongrowth and nongrowth identically, as does the end value method. In his discussion of the starting value method Grosenbaugh (1958) also uses a dbh threshold of 0 and so did not need to distinguish between ingrowth and ongrowth. Both Van Deusen et al. (1986) and Roesch et al. (1989) separate survivor increment from ingrowth in their theoretical discussions, but this is an unnecessary complication if the dbh threshold is 0. If Hradetzky’s (1995) formulation of their methods is followed then all tree classes are included. Van Deusen et al. (1986) demonstrated that each of the three methods is theoretically an unbiased estimator of volume increment but did not account for the errors that are inevitably part of any forest inventory. Thus, for practical purposes the proof of Van Deusen et al. (1986) proof should be reexamined.

The purpose of this study was to develop the mathematical basis for proving the systemic biasing effect of inventory error on angle count increment calculations and to determine how these effects manifest differently for the various estimators. Errors in angle count inventories may involve the misestimation of tree dimensions (measurement errors), may be cases in which trees are incorrectly recorded as either in or out of the sample (summation errors), or may arise from the use of skewed samples (sampling bias errors). In this article, we systematically analyze the biasing effect of all aspects of inventory error on the three currently used increment estimation methods based on angle count sampling. We demonstrate the practical outcomes of measurement and summation errors using long-term permanent sampling plot data covering 5-year measurements from 1977 to 2007. The angle count sampling plot data for this study are derived from individual tree observations obtained from a large long-term permanent research plot and may be seen as a “controlled experiment” to explicitly address the increment estimation by each method with the corresponding errors resulting from elliptical tree boles, misestimation of boundary trees, and hidden or missed trees.

Methods

Nomenclature and Mathematical Background

Research into the statistical properties of angle count sampling is made somewhat more complicated because of a

lack of standardized terminology and nomenclature in the published literature. Thus, we first define the nomenclature (Appendix 1) as it is used throughout this article. Our choice of nomenclature is based on international convention, Van Deusen et al. (1986) and Hradetzky (1995). Note that the variables used here may represent different values in other reports, including those that we refer to.

Next we develop our mathematical proofs from first principles to present previously published work in a common frame (see Appendix 2). Appendix 2 leads to the proof of Van Deusen et al. (1986) that the expected increment estimate obtained from the difference method $E(Z^D)$ is equal to the true increment Z :

$$\begin{aligned} E(Z^D) &= K \sum_{i=1}^N \frac{g_i}{K} \left[\frac{v_i^*}{g_i^*} - \frac{v_i}{g_i} \right] + \frac{g_i^* - g_i}{K} \frac{v_i^*}{g_i^*} \\ &= \sum_{i=1}^N (v_i^* - v_i) = Z \end{aligned} \quad (1)$$

Although this (and equivalent derivations for the other methods) proves angle count increment estimates to be unbiased, it assumes that all trees are correctly counted and measured and are perfectly round in cross section. In practice, this, of course, is not always the case; discussions of angle count volume estimation errors and biases may be found in Grosenbaugh (1958), Holgate (1967), and Schieler (1997). Possible differences between the increment estimators may arise from three sources: measurement or estimation errors, summation errors (miscounting of trees), and sample biasing errors.

Measurement Errors

The proofs for lack of bias assume that the tree radius r^R apparent to the observer via the prism or relascope is exactly equal both to $\sqrt{g^M/\pi}$ (using the basal area calculated from physical tree measurements) and to the true radius r^T . Cases in which $r^R \neq \sqrt{g^T/\pi}$ may result in trees being incorrectly tallied in or out of the sample and are examined later in this paper under Summation Errors. For the following discussion of measurement error, we will assume that the basal area calculated with r^R is an unbiased estimator of the true basal area g^T .

Volume may be expressed as the product of basal area (g), height (h), and a form factor (f). Reformulating Equation 1 to reflect the sources of the basal area terms and the expansion of v we find

$$\begin{aligned} E(Z^D) &= K \sum_{i=1}^N \frac{g_i^T}{K} \left[\frac{f_i^* h_i^* g_i^{*M}}{g_i^{*M}} - \frac{f_i h_i g_i^M}{g_i^M} \right] + \frac{g_i^{*T} - g_i^T}{K} \frac{f_i^* h_i^* g_i^{*M}}{g_i^{*M}} \\ &= \sum_{i=1}^N g_i^T f_i^* h_i^* - g_i^T f_i h_i + g_i^{*T} f_i^* h_i^* - g_i^T f_i h_i \\ &= \sum_{i=1}^N (v_i^{*T} - v_i^T) = Z \end{aligned} \quad (2)$$

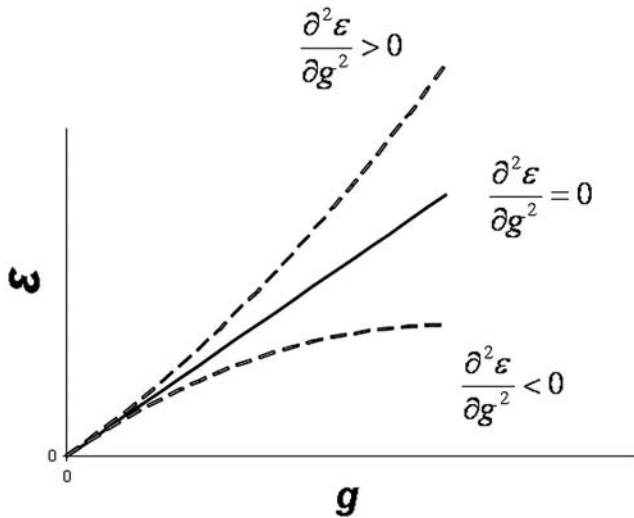


Figure 1. Bias will occur in the starting value and end value estimates if the second derivative of the measurement error ε with respect to basal area g is not zero.

This proves that Z^D is a theoretically unbiased estimator of true stand volume increment, regardless of errors in the measurement of g . In the case of Z^S we can develop

$$E(Z^S) = K \sum_{i=1}^N \frac{g_i^T}{K} \left[\frac{f_i^* h_i^* g_i^{*M}}{g_i^M} - \frac{f_i h_i g_i^M}{g_i^M} \right]$$

$$= \sum_{i=1}^N \left(g_i^T f_i^* h_i^* \frac{g_i^{*M}}{g_i^M} - v_i^T \right)$$

Defining single-tree basal area error as $\varepsilon = g^M - g^T$,

$$E(Z^S) = \sum_{i=1}^N \left(g_i^T f_i^* h_i^* \frac{g_i^{*T} + \varepsilon_i^*}{g_i^T + \varepsilon_i} - v_i^T \right) \quad (3)$$

Similarly for Z^E ,

$$E(Z^E) = K \sum_{i=1}^N \frac{g_i^T}{K} \left[\frac{f_i^* h_i^* g_i^{*M}}{g_i^{*M}} - \frac{f_i h_i g_i^M}{g_i^{*M}} \right]$$

$$+ \frac{g_i^{*T} - g_i^T}{K} \left[\frac{f_i^* h_i^* g_i^{*M}}{g_i^{*M}} - \frac{f_i h_i g_i^M}{g_i^{*M}} \right]$$

$$= \sum_{i=1}^N g_i^T f_i^* h_i^* - g_i^T f_i h_i \frac{g_i^M}{g_i^{*M}} + g_i^{*T} f_i^* h_i^* - g_i^{*T} f_i h_i \frac{g_i^M}{g_i^{*M}}$$

$$- g_i^T f_i^* h_i^* + g_i^T f_i h_i \frac{g_i^M}{g_i^{*M}}$$

$$= \sum_{i=1}^N \left(v_i^{*T} - g_i^{*T} f_i h_i \frac{g_i^M}{g_i^{*M}} \right)$$

$$= \sum_{i=1}^N \left(v_i^{*T} - g_i^{*T} f_i h_i \frac{g_i^T + \varepsilon_i}{g_i^{*T} + \varepsilon_i} \right) \quad (4)$$

From Equations 3 and 4 it is apparent that Z^S and Z^E can

only be unbiased estimators of Z if $\varepsilon = 0$ or if ε is linearly related to g , that is, that the second derivative of ε with respect to g is 0 (Figure 1).

It is necessary then to look at the nature of measurement errors to estimate the behavior of ε with respect to g . Here we examine measurements made with a diameter tape. Similar proceedings could be followed for caliper measurements, but for demonstration purposes we concentrate here on tape measurements. Measurement errors made with diameter tapes fall into five categories: (1) data recording or transcription error; (2) incorrect tape tension; (3) incorrect vertical positioning of diameter measurement; (4) noncircular cross sections; and (5) nonperpendicular alignment of tape. For reasons of space we present full analyses and results only for elliptical cross-section errors.

The measurement unit of a diameter tape is the tree bole circumference C^M , intended to reflect the true circumference C^T . The measured basal area $g^M = C^M/4\pi$. The true basal area of an elliptical tree cross section $g^T = \pi ab$ and the ellipticity (λ) is a/b , so $g^T = \pi a^2/\lambda$ or $g^T = \pi b^2\lambda$. Eccentricity (e) is formally defined as

$$e = \frac{\sqrt{a^2 - b^2}}{a} = \sqrt{1 - \frac{1}{\lambda^2}} \quad (5)$$

Calculating the circumference of an ellipse requires an approximation to

$$C = -2\pi a \sum_{i=0}^{\infty} \frac{e^{2i}}{2i-1} \prod_{j=1}^i \left(\frac{2j-1}{2j} \right)^2$$

or in expanded form, if we define

$$\Gamma = \left[1 - \left(\frac{1}{2} \right)^2 e^2 - \left(\frac{1 \cdot 3}{2 \cdot 4} \right)^2 e^4 - \left(\frac{1 \cdot 3 \cdot 5}{2 \cdot 4 \cdot 6} \right)^2 e^6 - \dots \right] \quad (6)$$

then $C = 2\pi a\Gamma$ and $g = \pi a^2\Gamma^2$. The error in basal area measurement then may be stated as

$$\varepsilon = g^T(\lambda\Gamma^2 - 1) \quad (7)$$

Using Ramanujan's first approximation for the circumference of an ellipse, $C = \pi[3(a+b) - \sqrt{(a+3b)(3a+b)}]$ the estimated basal area g^M will be

$$g^M = \pi \left[\frac{3(\lambda b + b) - \sqrt{(\lambda b + 3b)(3\lambda b + b)}}{2} \right]^2 \quad (8)$$

and the basal area overestimation proportion is approximated as

$$\frac{g^M}{g^T} = \frac{(3\lambda + 3 - \sqrt{3\lambda^2 + 10\lambda + 3})^2}{4\lambda} \quad (9)$$

From Equations 5–7, it is apparent that if λ remains constant, then e and Γ will also remain constant and ε will be a linear function of g^T , nonbiasing to Z^S and Z^E . Tree cross-section irregularity, however, usually increases with

age or size (Saint-André and Leban 2000, Moran and Williams 2002). If λ is any positive function of g^T , then the second derivative of Equation 7 must be positive, and the error will impart a positive bias to Z^S and Z^E .

Other types of measurement error may be similarly analyzed, but in all cases the difference method is resistant to bias (Equation 2 contains no error term). The impact of measurement errors on the starting value and end value methods depends on how the error relates to the basal area measurement. If that relationship is not linear, the error will impart a bias to the estimated increment.

Summation Errors

A further source of error comes from trees being incorrectly counted as being in or out of the angle count sample. Ignoring for the moment the circumstance of trees being removed, there are several possibilities for how these errors may impart bias to increment estimations.

All trees at some time will have been outside the angle count sample, which we shall denote c_O . Unless they remain correctly tallied as outside, at some subsequent time they will be counted either correctly inside the sample (c_I), incorrectly inside (I_I), or incorrectly outside (I_O). Incorrectly recorded trees may then be continued to be counted incorrectly but presumably at some time will be counted correctly in. This may be visualized in Figure 2, with the pathways between states labeled, and described in Table 1. The biasing effects described in Table 1 are developed from a simple consideration of how basal area increment would be affected by having too many or too few trees tallied. A tree incorrectly counted in will affect the difference and end value methods, but in the case of the difference method this will be counteracted at a later inventory, when the tree should be considered “new” but is not. Similar logic applies to the other circumstances.

Following all possible pathways between c_O and c_I , we find that Z^D has no or compensatory biases in all circumstances. An initial error incorrectly counting a tree in the angle count sample imparts an overall positive bias to Z^S

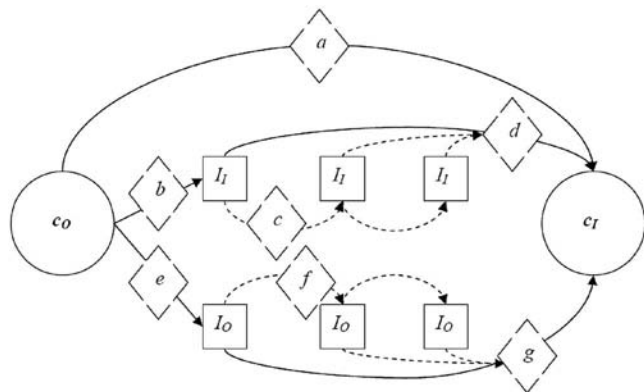


Figure 2. Pathways of possible angle count summations. c_O , tree correctly recorded as out; c_I , tree correctly recorded as in; I_I , tree incorrectly recorded as in; I_O , tree incorrectly recorded as out. Pathways a to g are various possible links between c_O and c_I , summarized in Table 1.

Table 1. Increment estimate effects of summation errors on the difference method (Z^D), the starting value method (Z^S), and the end value method (Z^E).

Pathway	Description	Angle-count error		Increment biasing effect		
		Time 1	Time 2	Z^D	Z^S	Z^E
a	c_O to c_I	0	0	0	0	0
b	c_O to I_I	0	+++	+++	0	+
c	I_I to I_I	+++	+++	0	+	+
d	I_I to c_I	+++	0	---	+	0
e	c_O to I_O	0	---	---	0	-
f	I_O to I_O	---	---	0	-	-
g	I_O to c_I	---	0	+++	-	0

+ and - are small positive and negative errors; +++ and --- are large errors. c_O is tree correctly recorded as out, c_I is correctly recorded as in, and I_I and I_O are incorrectly recorded as in and out, respectively. Pathways a to g are various possible links between c_O and c_I , represented in Figure 2.

and Z^E , whereas initially incorrectly counting out gives an overall negative bias.

With the assumption that modern, slope-compensating instruments are used and properly angled with the lean of the target, trees may be incorrectly counted because of the following:

Elliptical cross sections. Angle count sampling relies on the fact that for any tree $g/s = K$. Whereas this is true for perfectly round tree boles, it is not the case for trees with elliptical cross sections. It can be shown (Appendix 3) that the ratio p^e of the “relascope” probability to the “true” probability as a function of true basal area is

$$p^e = \frac{\lambda + 1}{2} \quad (10)$$

This is not biasing to Z^D (due to compensating effects in subsequent periods), but Z^S and Z^E will have a summation component of positive bias ε^p due to ellipticity of

$$\varepsilon^p = \frac{\lambda + 3}{4} \quad (11)$$

Misestimation of “borderline” trees. If there is doubt as to whether a tree should be tallied as in or out, manual distance and diameter measurements should be made. If this is not done the likelihood of a tree with a circular bole being mistakenly included would appear to be a matter of individual operator bias. Operators tend to be relatively consistent in the direction of their biases (Brack 1999), although some consistently overestimate and others consistently underestimate.

Hidden, missed, or double-counted trees. Hidden or otherwise missed trees are incorrectly counted out. Double-counted trees are a special case, not considered in Figure 2. After first being incorrectly counted in (pathway b from Table 1), if records were not updated when the error was noticed in a subsequent inventory, they would be presumed to be “removed” trees. The effect would be to give a large positive bias to Z^D , a small positive bias to Z^E , and (assuming that the error was noticed in the first subsequent inventory) no bias to Z^S .

Given, however, that for volume calculations all trees in the sample must be individually measured and recorded, double-counting of trees is effectively impossible.

Where trees are removed from the plot after following pathway b or e (Table 1), further error can be introduced. Trees on pathway c were counted incorrectly in the angle count sample, having already passed through pathway b. They, therefore, have contributed a large positive error to Z^D and a small positive error to Z^S and Z^E . If removed before being counted correctly in, the compensatory effect of pathway d will not apply to Z^D , leaving a large net positive error. Z^S and Z^E are not directly affected by the removal but will have a reduced error if the removal prevents trees from following pathway c. The converse of these arguments applies to trees initially counted incorrectly out.

Calculation of angle count increments requires that trees are numbered or have locations recorded so that survivors can be differentiated from nongrowth and survivor increment calculated in Z^S and Z^E and removal volumes estimated for Z^D . Trees that are “lost” from the database (due to misrecording of locations or an apparent “shrinking” of dbh, for example) will register with Z^D as removals and impart a positive error. Such trees will then not have their increment included in Z^S and Z^E , which will reduce the increment estimate in the current period. These “false removals,” however, may have been incorrectly recorded in in the prior measurement period, giving a positive bias to Z^D and a smaller positive bias to Z^E .

Sample Biasing Errors

Although the difference method may be applied to any plot, the starting value method is limited to those plots that have trees present in both periods, whereas the end value method requires trees to be present in the second measurement period. In studies comparing increment derived from inventory with that from other methods (i.e., modeling or remote sensing), it may be tempting to exclude those plots for which it is not possible to estimate an increment with Z^S or Z^E . This approach is statistically invalid, and such plots should be included and considered as having an increment of 0.

Trees may be either present or not present in time 1 and, if removed, either may or may not be replaced within the sample by new trees. There are then four possibilities, some of which will differently affect increment calculations using different methods (Table 2). Where no trees are present in time 2, the effect on the increment estimate is the same for

Table 2. Increment recorded by the difference method (Z^D), the starting value method (Z^S), and the end value method (Z^E), where no trees are present in one or both sampling periods.

Time 1	Time 2 (new trees)	Increment estimates		
		Z^D	Z^S	Z^E
0	0	0	0	0
0	>0	+++	0	+
>0	0	0	0	0
>0	>0 (original removed and replaced)	+++	0	+

Small increments are denoted +; large increments are denoted +++.

all methods (increment = 0). Where Z^S records no increment due to the removal or lack of trees sampled in time 1, but new trees are present in time 2, Z^D and Z^E would still record some growth. The exclusion of these plots from an aggregate of samples would increase the average increment determined with Z^S , but the effect on Z^D and Z^E is less certain. In a general case, it would seem likely that plots recording no trees due to low stocking would have a low increment and thus their exclusion would give a higher aggregated mean result to Z^D and Z^E , whereas if the lack of trees is due to harvest or mortality, then the effect would depend on the relative increment of these plots to the overall mean increment. A plausible case could be made that harvest is more likely on plots with higher increment, but it is difficult to be definitive.

Example Data

As an example to demonstrate the conceptual differences and how these affect a potential bias we obtain data from the 3.47-ha Hirschlacke long-term forest growth monitoring site in northern Austria. The stand was almost pure 110-year-old Norway spruce (*Picea abies* L. Karst) in 1977 and since then has been managed under a target diameter harvesting regime (Sterba and Zingg 2001) aimed to produce an equilibrium dbh distribution. All trees of more than 5.0-cm dbh have been measured for both diameter and height at 5-year intervals since 1977 and their location coordinates precisely recorded.

Since 1977, the stand structure has changed from having 1,510 trees with a mean dbh of 34.6 cm (SD 14.3 cm) to 2,820 trees with mean dbh of 18.2 cm (17.5 cm) in 2007. Mean tree heights have followed a similar pattern, from 25.8 m (8.9 m) in 1977 to 14.8 m (12.7 m) in 2007. This has been achieved by the removal of an average of 74 m³ of timber in each inventory period (timber volumes calculated according to the allometrics of Pollanschütz 1974).

We use the Hirschlacke data set as a means of mimicking a large-scale national inventory. Because all trees in the plot are repeatedly remeasured, we are able to simulate what increments would be determined using angle counts, assuming perfect measurements and also with a range of simulated error conditions. The data set is thus an ideal means of demonstrating the potential biases that may be apparent in angle count based inventories containing error. Through applying fixed measurement and summation errors to known data, we are able to show the effects of elliptical tree boles, mis-estimation of boundary trees, and hidden or missed trees. Sample biasing errors are not relevant to this example because of the density of trees on the example plot.

Example Results and Analysis

Increment Estimation by Method

We start our analysis by estimating the periodic volume increment by each of the three methods. Using our long-term research plot data we construct a pattern of 750 points at a 5 × 5 m spacing within the plot, such that no point is within 30 m of the plot boundary. We then simulate an angle count sample at each of the 750 points in each of the seven

measurement periods. The grid is repeated 1, 2, 3, and 4 m both northward and/or eastward to give 16 grids. Knowing the diameters of all trees in each period allows us to determine which new trees in a remeasurement from each sample point in each period are “nongrowth.” With a dbh threshold of 5.0 cm, we are not able to distinguish ingrowth from ongrowth, but this is not required for the methods examined here. We are, however, able to test Hradetzky’s (1995) assumption of the practical irrelevance of ingrowth/ongrowth when low dbh thresholds are used. Starting value increment is calculated as the sum of (survivor_i increment × $n_{i(t1)}$) plus ingrowth and ongrowth volumes (Beers and Miller 1964). End value increment is the sum of (survivor_i and nongrowth_i increment × $n_{i(t2)}$) plus (nongrowth_i increment × $n_{i(t2)}$) plus ingrowth and ongrowth volumes (Roesch et al. 1989). The results by period and method are given in Table 3.

Elliptical Tree Boles

We adjust the recorded data in the Hirschlacke database to reflect an ellipticity of 1.1. We assume here that the dbh figures recorded in the Hirschlacke database give a correct reflection of geometric mean diameter and apply a multiplication of 1.00341 to all basal areas to reflect the simulated ellipticity (Equation 9). To account for the increased chance of an elliptical tree being counted in the angle count sample, Equation 10 is applied to increase the probability of a tree being counted in the sample by 1.05 (increasing the critical distance for each tree by a factor of 1.01247, the square root of the required probability increase). Results of this test are shown in Table 4.

A further test is applied whereby the ellipticity rises linearly with basal area, from $\lambda = 1.0$ at 5.0-cm dbh to $\lambda = 1.3$ at a dbh of 100 cm ($\lambda = 0.000038293g + 0.9992484$). This test is applied both without (Table 5 left-hand panel) and with (Table 5, right-hand panel) the attendant probability increase.

Misestimation of Borderline Trees

Misestimating borderline trees gives rise to substantial errors under certain circumstances. We test the effects of misestimated borderline trees through maintaining correct measurement in all years except 1982, when critical distances are increased by 5% (trees mistakenly counted in the samples) in one test and then reduced by 5% (multiplier of 0.95) in the next. As expected from Figure 2 and Table 1, when a tree is first counted incorrectly in (pathway b), a

large overestimation is imparted to Z^D and a smaller overestimation to Z^E (Table 6, left-hand panel). Z^S should theoretically be unaffected at this stage, and the very small underestimation in the first increment period in Table 6 is a result of an apparently shrinking tree. Most large inventory databases will contain some examples of apparently shrinking trees, for which the dbh recorded at time 2 is slightly less than that at time 1. Although rare and of small magnitude, in our simulation it may be possible for this error to cause a tree to be counted in at time 1 but out at time 2, giving a presumption of tree removal. If false removals are avoided through either counting incorrectly in trees as continually incorrectly in (Figure 2, pathway c) or waiting until they are correctly in (pathway d), then the compensatory effect on Z^D is apparent in Table 6 (right-hand panel). A similar effect is found in the test applying an underestimation of critical distance (Table 7).

Hidden or Missed Trees

The effect of hidden or missed trees is tested through maintaining correct measurement in 1977, 1987, 1992, and 2007 but excluding a random selection of 10% of the new trees in the angle count samples (either ingrowth or nongrowth) from other years. A different random selection is made for each of the 16 iterations of each test. Hidden trees will impart a small negative bias to Z^S and Z^E (Table 8), except in the first period when the trees are missed for Z^S and in the subsequent year for Z^E , following the expectations of Table 1.

To determine the effect of removed (harvested) trees on the theories presented here, we repeat this test on a database in which any removed trees are replaced, with diameters and heights linearly extrapolated from their recorded values. To avoid shrinking trees being extrapolated we enforce a minimum dbh growth trend of 0.1 cm per period. If no removals occur, then the overall bias in Z^D (summed over all periods between the first and final correct measurements) is 0. This may be clearly seen in Table 8, considering that the periods from 1977 to 1992 and from 1987 to 2007 began and ended without any hidden trees.

Example Analysis

Ellipticity, if constant, produces results as expected. If only the basal area estimate error is considered, disregarding the increased probability of a tree being included in the

Table 3. Components of growth.

Period	Difference method Total	Starting value method			End value method			
		Survivors	Ingrowth + ongrowth	Total	Survivors	Nongrowth	Ingrowth + ongrowth	Total
1977–1982	64.26 ± 1.17	63.01 ± 0.48	0.00 ± 0.00	63.01 ± 0.48	58.92 ± 0.44	4.09 ± 0.14	0.00 ± 0.00	63.01 ± 0.46
1982–1987	80.40 ± 1.48	80.33 ± 0.46	0.00 ± 0.00	80.33 ± 0.46	72.93 ± 0.42	7.44 ± 0.19	0.00 ± 0.00	80.37 ± 0.44
1987–1992	64.35 ± 1.26	62.83 ± 0.40	0.12 ± 0.04	62.95 ± 0.40	58.32 ± 0.37	4.41 ± 0.14	0.12 ± 0.04	62.85 ± 0.39
1992–1997	64.72 ± 1.24	64.06 ± 0.40	0.58 ± 0.07	64.65 ± 0.40	59.42 ± 0.35	4.66 ± 0.15	0.58 ± 0.07	64.67 ± 0.37
1997–2002	83.66 ± 1.45	82.19 ± 0.52	0.83 ± 0.08	83.02 ± 0.52	75.67 ± 0.47	6.55 ± 0.18	0.83 ± 0.08	83.05 ± 0.50
2002–2007	56.67 ± 1.29	54.43 ± 0.47	1.02 ± 0.08	55.44 ± 0.48	49.75 ± 0.43	4.74 ± 0.15	1.02 ± 0.08	55.50 ± 0.46

Values are means ± 99% confidence interval for timber increment in each 5-year period, in m³/ha/period.

Table 4. Overpredictions resulting from a constant tree ellipticity of $\lambda = 1.1$.

Period	Difference method			Starting value method			End value method		
	Error	%	Sig	Error	%	Sig	Error	%	Sig
1977–1982	0.96	1.50	*	1.61	2.55	***	1.57	2.50	***
1982–1987	2.76	3.44	***	2.00	2.49	***	2.07	2.57	***
1987–1992	0.382	0.593	NS	1.611	2.559	***	1.530	2.434	***
1992–1997	1.938	2.995	***	1.649	2.550	***	1.636	2.530	***
1997–2002	2.490	2.976	***	2.062	2.483	***	2.100	2.529	***
2002–2007	1.522	2.686	***	1.379	2.488	***	1.453	2.618	***
Mean		2.36			2.52			2.53	

Errors are shown as the absolute overprediction in $\text{m}^3/\text{ha}/\text{period}$ and as a percentage of the “nonerror” values. The results here include consideration of both tree basal area misestimation and the increased probability of trees being counted in the angle count sample, but results for the probability increase alone are identical. Significance levels (Sig): NS, not significant; * $P < 0.1$; ** $P < 0.01$; *** $P < 0.0001$.

Table 5. Overpredictions resulting from increasing ellipticity linearly with basal area ($\lambda = 0.000038293g + 0.9992484$), considering only the error resulting from volume overestimation of individual trees and both the error resulting from volume overestimation of individual trees and the increased likelihood of trees being included in the samples.

Period	With only volume error component									With both volume and probability error components								
	Difference method			Starting value method			End value method			Difference method			Starting value method			End value method		
	Error	%	Sig	Error	%	Sig	Error	%	Sig	Error	%	Sig	Error	%	Sig	Error	%	Sig
1977–1982	0.00	0.00	NA	4.36	6.91	***	3.86	6.13	***	3.02	4.70	***	6.37	10.11	***	6.00	9.52	***
1982–1987	0.00	0.00	NA	8.18	10.19	***	7.13	8.87	***	5.35	6.66	***	10.99	13.69	***	10.24	12.74	***
1987–1992	0.000	0.000	NA	5.618	8.925	***	5.005	7.963	***	2.541	3.949	***	7.920	12.581	***	7.345	11.686	***
1992–1997	0.000	0.000	NA	5.803	8.976	***	5.209	8.055	***	4.281	6.614	***	8.163	12.628	***	7.735	11.960	***
1997–2002	0.000	0.000	NA	7.666	9.234	***	6.703	8.071	***	5.457	6.522	***	10.890	13.117	***	10.195	12.276	***
2002–2007	0.000	0.000	NA	5.546	10.004	***	4.988	8.988	***	3.148	5.555	***	7.532	13.585	***	7.104	12.801	***
Mean		0.00			9.04			8.01			5.67			12.62			11.83	

Units and significance are found in the footnote to Table 4. NA, not applicable.

sample, then the increment estimate by any method is unaffected because of the compensating effect of a lower estimated stem number per hectare (results not shown). Table 4, however, shows that the probability increase has a significant impact on results: for a constant ellipticity of 1.1, an overestimation of approximately 2.5% can be expected in all methods, which agrees well with the expectations of Equation 11 for Z^S and Z^E . The roughly equal overestimations in Z^D align with the constant overestimation of stand volume, ranging from 2.44 to 2.60% (results not shown). This degree of volume overestimation is consistent with correction tables developed by Grosenbaugh (1958), who advised that volume estimates from angle count samples be adjusted to compensate for ellipticity.

Where ellipticity rises linearly with basal area, substantial errors are imparted to the starting value and end value results. The difference method is self-compensating for errors in basal area estimation (Table 5, left panel), but retains some error resulting from the increased probability of elliptical trees being counted in the sample (Table 5, right panel).

Misestimation of borderline trees gives rise to substantial errors under certain circumstances. As expected from Figure 2 and Table 1, when a tree is first counted incorrectly in (pathway b) a large overestimation is imparted to Z^D and a smaller overestimation to Z^E (Table 6, left panel). Z^S should theoretically be unaffected at this stage, and the very small underestimation in the first increment period in Table 6 is a result of an apparently shrinking tree.

The effect of shrinking trees on the unmodified data set is small and of inconsistent sign (-0.6 to $+0.8\%$), without any clear effect of estimation method. The apparent shrinking will have other impacts on estimation errors, depending on whether such trees are presumed removed in the subsequent inventory, grow to be counted correctly in, or remain incorrectly in. If the incorrectly counted trees are presumed removed in the subsequent inventory, then the underestimation in Z^D in that period is not sufficient to compensate for the previous overestimation and an overall positive error is retained. Z^S will include a positive error of approximately the same magnitude as the error in Z^E in the previous period.

If false removals are avoided through counting incorrectly in trees as either continually incorrectly in (Figure 2, pathway c) or waiting until they are correctly in (pathway d), then the compensatory effect on Z^D is apparent in Table 6, right panel. The original estimation is not, however, fully compensated for because of some trees being removed and thus never following pathway d. The continuing small overestimations in Z^S and Z^E along pathway c are also apparent in the right panel of Table 6. In the case of no “true” removals (results not shown), the summed error in Z^D reduces to $7.22 \text{ m}^3/\text{ha}$, whereas for Z^S and Z^E the errors rise to 11.70 and $9.06 \text{ m}^3/\text{ha}$, respectively. Although theory suggests that the sum of errors in Z^D should be 0, this will not occur until all trees have followed pathway d.

With negative misestimations of borderline trees, those trees initially counted incorrectly out (pathway e) impart a strong negative bias to Z^D and a smaller negative bias to Z^E

Table 6. Errors resulting from misestimated borderline trees, positive inclusion error.

Period	With false removals						Without false removals											
	Difference method			Starting value method			End value method			Difference method			Starting value method			End value method		
	Error	%	Sig	Error	%	Sig	Error	%	Sig	Error	%	Sig	Error	%	Sig	Error	%	Sig
1977–1982	78.81	122.65	***	-0.01	-0.02	***	6.41	10.17	***	78.81	122.65	***	-0.01	-0.02	***	6.41	10.17	***
1982–1987	-53.87	-67.01	***	7.01	8.72	***	0.000	0.000	NA	-53.51	-66.55	***	8.26	10.29	***	1.18	1.47	***
Subsequent periods	0.000	0.000	NA	0.000	0.000	NA	0.000	0.000	NA	-11.680	-18.170	***	1.135	1.806	***	0.153	0.244	***
Sum	24.93			6.99			6.41			-2.968	-4.622	***	0.296	0.455	***	0.062	0.095	***
										-0.625	-0.749	***	0.114	0.138	***	0.052	0.062	***
										-0.450	-0.796	***	0.029	0.051	***	0.005	0.009	*
										9.58	9.58		9.82	9.82		7.86	7.86	

A 5% overestimation in critical distance is applied in 1982. False removals are included in the left-hand panel, but in the right-hand panel a tree once counted in the sample remains in until removed in fact. Units and significance are found in the footnote to Table 4. NA, not applicable.

Table 7. Errors resulting from misestimated borderline trees, negative inclusion error.

Periods	With false removals						Without false removals											
	Difference method			Starting value method			End value method			Difference method			Starting value method			End value method		
	Error	%	Sig	Error	%	Sig	Error	%	Sig	Error	%	Sig	Error	%	Sig	Error	%	Sig
1977–1982	-37.76	-58.76	***	-2.52	-4.00	***	-6.17	-9.79	***	-36.43	-56.70	***	-0.01	-0.02	***	-3.78	-5.99	***
1982–1987	67.69	84.19	***	-7.84	-9.76	***	0.00	0.00	***	32.38	40.27	***	-4.02	-5.00	***	0.003	0.003	ns
Subsequent periods	0.000	0.000	NA	0.000	0.000	NA	0.000	0.000	NA	0.062	0.097	**	-0.005	-0.008	*	-0.002	-0.003	ns
Sum	29.93			-10.36			-6.17			0.022	0.034	*	-0.001	-0.001	ns	0.000	0.001	ns
										0.002	0.002	*	0.002	0.002	*	0.002	0.002	*
										0.000	0.000	NA	0.000	0.000	NA	0.000	0.000	NA
										-3.97	-3.97		-4.04	-4.04		-3.77	-3.77	

A 5% underestimation in critical distance is applied in 1982. False removals are included in the left-hand panel, but in the right-hand panel a tree once counted in the sample remains in until removed in fact. Units and significance are found in the footnote to Table 4. NA, not applicable.

Table 8. Errors resulting from hidden or missed trees.

Period	With removals						Without removals											
	Difference method			Starting value method			End value method			Difference method			Starting value method			End value method		
	Error	%	Sig	Error	%	Sig	Error	%	Sig	Error	%	Sig	Error	%	Sig	Error	%	Sig
1977–1982	-3.77	-5.86	***	0.00	0.00	NA	-0.40	-0.63	***	-3.82	-5.92	***	0.00	0.00	NA	-0.41	-0.64	***
1982–1987	3.34	4.16	***	-0.43	-0.54	***	0.00	0.00	ns	3.82	4.34	***	-0.52	-0.59	***	0.00	0.00	ns
1987–1992	0.000	0.000	NA	0.000	0.000	NA	0.000	0.000	NA	0.000	0.000	NA	0.000	0.000	NA	0.000	0.000	NA
1992–1997	-4.418	-6.826	***	-0.045	-0.070	***	-0.528	-0.817	***	-5.414	-6.584	***	-0.052	-0.063	***	-0.617	-0.747	***
1997–2002	-1.895	-2.265	***	-0.670	-0.806	***	-0.786	-0.946	***	-2.428	-2.177	***	-0.794	-0.717	***	-0.975	-0.881	***
2002–2007	5.123	9.040	***	-0.551	-0.994	***	0.000	0.000	*	7.842	8.327	***	-0.814	-0.871	***	0.000	0.000	ns
Sum	-1.61			-1.70			-1.71			0.00			-2.18			-2.00		

10% of new trees are missed in 1982, 1997, and 2002. Units and significance are found in the footnote to Table 4. NA, not applicable.

(Table 7). The negative bias in Z^S in the first period in the left panel of Table 7 is a result of some misestimated trees dropping out of the sample and being presumed removed and not counted as survivors (false removals). If this circumstance is avoided (forcing such trees to remain on pathway f) then the initial error in Z^S is reduced to that resulting from shrinking trees in the original data set (Table 7, right panel).

In the period subsequent to the misestimation, pathway g can overcompensate for the initial underestimation in Z^D (Table 7, left panel). Trees that went from correctly in in 1977 to incorrectly out in 1982 were assumed removed and thus did not affect the increment calculation in the first period. In 1987, these trees are all assumed to be new, and thus their volume is double-counted. The error of -37.76 m^3 in the first period results from trees not recorded in 1977 incorrectly not entering the count in 1982. Without false removals, this double counting does not occur. Where neither false nor true removals are simulated, the summed error in Z^D is reduced to 0, with -4.57 and $-3.76 \text{ m}^3/\text{ha}$ for Z^S and Z^E , respectively (results not shown).

Hidden trees will impart a small negative bias to Z^S and Z^E (Table 8), except in the first period when the trees are missed for Z^S and in the subsequent year for Z^E , following the expectations of Table 1. As with border misestimations, where removals have occurred from the plot, Z^D is not able to fully compensate for the initial underestimation, but if no removals occur, then the overall bias in Z^D (summed over all periods between the first and final correct measurements) is 0. This may be clearly seen in Table 8, considering that the periods from 1977 to 1992 and from 1987 to 2007 began and ended without any hidden trees. Where a long series of periods all have hidden trees (results not shown), the biases in Z^S and Z^E are always negative (although small, 0.6 – 1.0%), but the errors in Z^D are inconsistent in sign. This will depend on whether the compensatory effect of previously hidden trees being discovered in a subsequent inventory is greater or lesser than the underestimation resulting from trees being hidden in the current period.

Example Discussion

The results of the examples presented above support our theoretical development. Although we have not examined all possible sources of errors, the resistance of Z^D to bias from measurement error is confirmed. All methodologies are vulnerable to positive bias from summation error where ellipticity causes too many trees to be counted in the sample, but if ellipticity increases as trees grow, then Z^S and Z^E are susceptible to substantially greater positive bias than Z^D . The overestimation of increment where ellipticity is constant is predictable, because this derives from the 2.4 – 2.6% overestimation of volume and removals in each period. Where ellipticity increases with tree size, however, the volume estimation error ranged only from 3.2 to 4.4% , but increment biases were much higher.

Summation errors from misestimated borderline trees had an extremely large impact on Z^D in some of our example simulations, but these cases are unlikely to be relevant in practical operations. The large overestimations are due to

the assumption that trees present in a sample at time 1 but not at time 2 must be removals and thus add to the increment estimated with Z^D . If it is recognized that these are false removals, resulting from errors, then the overestimation in Z^D is greatly reduced.

Common practice in inventory sampling is to tag all trees sampled and so the occurrence of false removals should be extremely rare. In some inventories, however, trees are not tagged, and the recognition that a tree either was or was not in the previous sample depends on the recorded location. Because there is a large possibility of error in these data (particularly if field crews do not have access to prior records), it is often difficult to determine whether a particular tree has been removed and replaced in the sample by another or whether records with slightly different location data in two periods refer to the same tree. Given the substantial errors in increment calculation that can result, clear protocols should be developed to deal with such cases in prior inventories and in the future tagging should be considered mandatory.

Over a series of measurements, the difference method will compensate for misestimated borderline trees or hidden trees unless these trees are removed from the plot before they can be correctly counted. Alternative methods have smaller initial errors but are unable to compensate, leading to positive bias if too many trees are counted or negative bias if trees are missed. Errors and biases due to hidden or misestimated borderline trees may be minimized through greater attention to detail in the field, and if trees are tagged to avoid false removals, then the relative biases of each method depend on the extent of true removals from the sample. If no removals occur, Z^D is more accurate than Z^S or Z^E . In the case of Hirshlacke (managed to maintain roughly constant standing volume), Z^E is the most resistant to border tree misestimation and Z^S is the least resistant. Total biases from hidden trees are small for all methods if the count in the final measurement period is correct; otherwise some underestimation will remain in Z^D .

The magnitudes of the errors applied in our examples are arbitrary but within practical bounds. Our constant ellipticity of 1.1 compares with published figures of 1.0 to 1.25 (reviewed by Todoroki et al. 2007). From two sample sets Saint-André and Leban (2000) found that 16 and 20% of Norway spruce cross sections had an ellipticity >1.1 . The 5% errors we applied to critical distances to simulate border tree misestimations gave total volume errors of from -4.6 to $+10.3\%$, comparable with the range of basal area percentage errors reviewed and reported by Omule (1978). Volume estimation errors in the hidden tree simulations were all less than 1%. Table 7 may also be compared with results from Thomas and Roesch (1990), who found that recording too few trees as in in the first remeasurement of a statewide inventory in Alabama resulted in a 37% overestimation in Z^D and an 11% underestimation in Z^S , whereas Z^E was accurate. The analogous case in our example is the period 1982–1987, which suggests that a 5% underestimation in critical distance can give a 40.3% overestimation in Z^D and a 4.0% underestimation in Z^S , with Z^E unaffected in that period.

Discussion and Conclusions

The difference method has been shown to be resistant to measurement error because any misestimation of basal area is compensated for by an equivalent but opposite error in the estimated number of trees per unit area. Effectively, the positive measurement error is counterbalanced by a precisely equivalent negative error. The starting value and end value methods, however, do not have this feature and are thus susceptible to retaining a positive bias from the erroneous measurements. Where such cases are likely to occur (for example, where higher tree ellipticity is expected due to steep slopes or particular species compositions), then significant positive bias should be expected and taken into consideration.

In professionally conducted inventories, overall increment estimation biases due to summation errors are likely to be small, depending on the balance between trees counted incorrectly in or incorrectly out of the sample. However, errors do occur. Over the course of several inventories, a comparison of results obtained from each of the three methods can indicate where problems may occur. Given the clear difference in bias behavior between the three alternative methods, there is potential for this to be used as an auditing aid for national forest inventories, as originally suggested by Thomas and Roesch (1990). It could be used to identify geographic regions where the three methods give significantly different increments and thus allow more efficient inventory remeasurement programs to be devised. Where longer time series of measurements are available, a close examination of the results obtained can give insights into what possible measurement and summation errors may be present. Comparing those results with the series of tables supplied in this article may permit the deduction of which errors have occurred in which years and the most bias-resistant estimator used in each increment period.

Although sample biasing errors were not demonstrated in our example, in some circumstances there is substantial potential for poor conclusions to be drawn if this aspect of error is not considered when angle count inventory data are used. Although the results for the plots used may be correct, limiting the sample to those plots that only display an increment with one particular method will give a skewed sample not representative of the overall forest condition.

The variance in results obtained using the difference method is generally higher than that from the other methods, as described theoretically by Hradetzky (1995). With a large number of samples, this variance may still be within reasonable bounds and if only two inventory periods are available, the difference method should be preferred because of its greater resistance to bias in most circumstances. In environments in which strong tree ellipticity is expected and such ellipticity increases with tree size, positive biases of more than 10% of volume increment are likely to occur in the starting value and end value methods and perhaps 5% in the difference method. Although the precise magnitudes of these biases are impossible to determine without knowledge of local ellipticity, when angle count-based increment information is used or compared with results from other

sources, the likelihood of significant positive bias must be considered.

Increments obtained from angle count inventories are often reported without reference to the calculation methods used, even though the choice of method will affect the results. Users of such data should be aware of the limitations and wherever possible examine the results obtained through all three calculation methods to gain at least some estimate of the data reliability. In an era when forest increment rates are becoming an integral part of international environmental, energy, and broader economic policy, it is essential that increments derived from angle count inventories be analyzed with a range of methods, rather than the results of one method being uncritically accepted as a measured fact.

Literature Cited

BEERS, T.W., AND C.I. MILLER. 1964. *Point-sampling: Research results, theory and applications*. Res. Bull. 786, Purdue University Agricultural Experimental Station, West Lafayette, IN. 55 p.

BITTERLICH, W. 1948. Die Winkelzählprobe. *Allg. For. Holzwirtschaft. Zeit.* 59(1-2):4-5.

BRACK, C. 1999. *Forest measurement and modelling*. Australian National University, Canberra. Available online at fenner school-associated.anu.edu.au/mensuration/home.htm; last accessed December 3, 2010.

GROSENBAUGH, L.R. 1952. Plotless timber estimates—New, fast, easy. *J. For.* 50:173-192.

GROSENBAUGH, L.R. 1958. *Point-sampling and line-sampling: Probability theory, geometric implications, synthesis*. US For. Serv. South Forest Experimental Station Occasional Paper 160. 34 p.

HOLGATE, P. 1967. The angle-count method. *Biometrika* 54 (3-4):615-623.

HRADETZKY, J. 1995. Concerning the precision of growth estimation using permanent horizontal point samples. *For. Ecol. Manag.* 71:203-210.

MARTIN, G.L. 1982. A method for estimating ingrowth on permanent horizontal sample points. *For. Sci.* 28:110-114.

MORAN, L.A., AND R.A. WILLIAMS. 2002. Comparison of three dendrometers in measuring diameter at breast height. *North. J. Appl. For.* 19(1):28-33.

OMULE, S.A. 1978. *Analysis of measurement errors associated with variable-radius plot forest sampling*. M.Sc. thesis, Univ. of British Columbia, Department of Forestry, Vancouver, BC, Canada. 59 p.

PALLEY, M.N., AND L.G. HORWITZ. 1961. Properties of some random and systematic point sampling estimators. *For. Sci.* 7(1):52-65.

POLLANSCHÜTZ, J. 1974. Formzahlfunktionen der Hauptbaumarten Österreichs. *Allg. Forstzeit.* 85:341-343.

ROESCH, F.A., E.J. GREEN, AND C.T. SCOTT. 1989. New compatible basal area and number of tree estimators from remeasured horizontal point samples. *For. Sci.* 35:281-293.

SAINT-ANDRÉ, L., AND J.M. LEBAN. 2000. An elliptical model for tree ring shape in transverse section. Methodology and case study on Norway Spruce. *Holz Roh. Werkst.* 58:368-374.

SCHADAUER, K., T. GSCHWANTNER, AND K. GABLER. 2007. Austrian National Forest Inventory: Caught in the past and heading towards the future. P. 47-53 in *Proc. of the Seventh annual forest inventory and analysis symposium*, McRoberts, R.E., G.A. Reams, P.C. Van Deusen, and W.H. McWilliams (eds.). US For. Serv. Gen. Tech. Rep. WO-77.

SCHIELER, K. 1997. *Methode der Zuwachsberechnung der Österreichischen Waldinventur*. Ph.D. thesis, Univ. of Natural Resources and Applied Life Sciences, Institute of Forest Growth, Vienna, Austria. 99 p.

SCOTT, C.T. 1990. An overview of fixed versus variable-radius plots for successive inventories. P. 97-104 in *State-of-the-art methodology of forest inventory: A symposium proceedings*, LaBau, V.J., and T. Cunia (eds.). US For. Serv. Gen. Tech. Report PNW GTR 263.

STERBA, H., AND A. ZINGG. 2001. Target diameter harvesting—A strategy to convert even-aged forests. *For. Ecol. Manag.* 151(1-3):95-105, 2001.

THOMAS, C.E., AND F.A. ROESCH. 1990. Basal area growth estimators for survivor component: A quality control application. *South. J. Appl. For.* 14(1):12-18.

TODOROKI, C.L., R.A. MONSERUD, AND D.L. PARRY. 2007. Lumber volume and value from elliptical western hemlock logs. *For. Prod. J.* 57(7/8):76-82.

TOMPO, E., T. GSCHWANTNER, M. LAWRENCE, AND R.E. MCROBERTS. 2010. *National Forest Inventories: Pathways for common reporting*. Springer, Berlin, Germany. 610 p.

VAN DEUSEN, P., T.R. DELL, AND C.E. THOMAS. 1986. Volume growth estimation from permanent horizontal plots. *For. Sci.* 32(2):415-432.

WHYTE, A.G.D., AND R.B. TENNENT. 1975. Improving estimates of stand basal area in working plan inventories. *N. Z. J. For.* 20(1):134-147.

Appendix 1: Commonly Used Variables and Superscripts

Variables

<i>C</i>	bole circumference at breast height, cm
<i>g_i</i>	Basal area of tree <i>i</i>
<i>G</i>	stand basal area
<i>K</i>	metric basal area factor
<i>n</i>	number of trees in a single angle count sample
<i>N</i>	total number of trees in a stand
<i>p_i</i>	probability that tree <i>i</i> will be included in an angle count sample
<i>s</i>	Effective plot area
<i>v_i</i>	volume of tree <i>i</i>
<i>V</i>	stand volume of all trees with dbh >0
<i>Z</i>	stand volume increment, m ³ /ha/time period

Superscripts

^	estimated value using angle-count sampling
*	variable relating to a subsequent measurement period
D	variable relating to the difference method
S	variable relating to the starting value method
E	variable relating to the end value method
M	value derived from measured values
T	assumed true value

Appendix 2: Mathematical Background of Angle Count Sampling

Bitterlich (1948) demonstrated that for any given angle, the ratio of the radius (*r*) of a tree that optically appears to be just within the wedge formed by that angle at a distance

(R) is a constant dependent on the angle. For such a tree, let Θ be the angle of the wedge in degrees:

$$\sin \frac{\Theta}{2} = \frac{r}{R}, \rightarrow \sin^2 \frac{\Theta}{2} = \frac{r^2}{R^2}.$$

r is half of the dbh (normally measured in centimeters) and R usually measured in meters, so

$$10000 \sin^2 \frac{\Theta}{2} = \frac{dbh^2}{4R^2} = \text{the metric basal area factor (K)}.$$

As the basal area (g) of a tree is $\pi(\text{dbh}/2)^2$, if the effective plot size (s) is that area within a circle of radius R , then for any tree $g/s = K$. In a fixed-area plot, the basal area of a stand (G) would be estimated as the sum of the in-plot tree basal areas divided by the plot area, multiplied by the stand area. Similarly with angle count samples, per hectare $\hat{G} = \sum_{i=1}^n (g_i/s_i)$, which reduces to $\hat{G} = Kn$.

The probability of any tree i being within a sample is proportional to the relationship between its effective plot size s and the stand area A , i.e., $p_i = s_i/A$; thus, for a per hectare estimate $p_i = g_i/K$.

Grosenbaugh (1952) extended Bitterlich's reasoning to volume (or other stand characteristics), showing that the estimator for basal area may be multiplied by the relationship of volume to basal area (v_i/g_i) to obtain the volume estimator $\hat{V} = \sum_{i=1}^n (v_i/p_i)$, hence

$$\hat{V} = K \sum_{i=1}^n \frac{v_i}{g_i} \quad (2.1)$$

Palley and Horwitz (1961) formulated this using an indicator variable Y_{ij} , which takes the value of 1 if the i th tree is included in the j th angle count sample. If (as commonly recommended) several (m) angle count samples are made in a stand and the results are averaged, then

$$\hat{V} = \frac{K}{m} \sum_{j=1}^m \sum_{i=1}^N \frac{v_i}{g_i} Y_{ij} \quad (2.2)$$

The expectation $E(Y_{ij})$ is the probability that a tree will fall within a sample, g_i/K . The expectation of the volume estimator can thus be described as

$$E(\hat{V}) = \frac{K}{m} \sum_{j=1}^m \sum_{i=1}^N \frac{v_i}{g_i} \frac{g_i}{K} \quad (2.3)$$

Summing over all trees and all points, this reduces to $E(\hat{V}) = \sum_{i=1}^N v_i = V$, following the demonstration of Palley and Horwitz (1961) that $E(\hat{G}) = G$ and proving the theoretically bias-free nature of angle count samples for volume.

Denoting measurements made in a subsequent inventory period by $*$, ignoring tree removals from the plots, and

following Hradetzky (1995), the mathematical form of the three increment estimation methods may be presented as

$$Z^D = \frac{K}{m} \sum_{j=1}^m \sum_{i=1}^n \frac{v_i^*}{g_i^*} - \frac{K}{m} \sum_{j=1}^m \sum_{i=1}^n \frac{v_i}{g_i} + \frac{K}{m} \sum_{j=1}^m \sum_{i=n+1}^{n^*} \frac{v_i^*}{g_i^*} \quad (2.4)$$

$$Z^S = \frac{K}{m} \sum_{j=1}^m \sum_{i=1}^n \frac{v_i^*}{g_i^*} - \frac{K}{m} \sum_{j=1}^m \sum_{i=1}^n \frac{v_i}{g_i} \quad (2.5)$$

$$Z^E = \frac{K}{m} \sum_{j=1}^m \sum_{i=1}^n \frac{v_i^*}{g_i^*} - \frac{K}{m} \sum_{j=1}^m \sum_{i=1}^n \frac{v_i}{g_i^*} + \frac{K}{m} \sum_{j=1}^m \sum_{i=n+1}^{n^*} \frac{v_i^*}{g_i^*} - \frac{K}{m} \sum_{j=1}^m \sum_{i=n+1}^{n^*} \frac{v_i}{g_i^*} \quad (2.6)$$

Hradetzky (1995) shows the applicability of the three methods in estimating basal area increment, but to be strictly correct, the increments measured with Hradetzky's formulation of the difference and end value methods is the increment of all trees in the stand with a dbh over the threshold at time 2, whereas his starting value method estimates the increment of only those trees with a dbh over the threshold at time 1. This does not affect the validity of Hradetzky's work, but it is an important factor to consider when the methods are applied to inventory data. The term $\sum_{i=n+1}^{n^*}$ in Equations 2.4 and 2.6 describes the new trees entering a sample in the subsequent measurement period and thus includes nongrowth, ongrowth, and ingrowth. The ingrowth and ongrowth components must be added separately to Equation 2.5.

Van Deusen et al. (1986) showed that for the difference method, if we define X_{ij} as an indicator variable similar to Y_{ij} but applying only to trees present in the subsequent sample that were not present in the first, then the expectation of the increment estimate may be formulated as

$$E(Z^D) = E \left\{ \frac{K}{m} \left[\sum_{j=1}^m \sum_{i=1}^N Y_{ij} \left(\frac{v_i^*}{g_i^*} - \frac{v_i}{g_i} \right) + \sum_{i=n+1}^{n^*} X_{ij} \frac{v_i^*}{g_i^*} \right] \right\}$$

As $E(Y_{ij}) = g_i/K$, $E(X_{ij}) = (g_i^* - g_i)/K$. This allows us to reproduce the proof of Van Deusen et al. (1986) that

$$E(Z^D) = K \sum_{i=1}^N \frac{g_i}{K} \left[\frac{v_i^*}{g_i^*} - \frac{v_i}{g_i} \right] + \frac{g_i^* - g_i}{K} \frac{v_i^*}{g_i^*} = \sum_{i=1}^N (v_i^* - v_i) = Z \quad (2.7)$$

Similar reasoning proves the theoretical lack of bias in Z^S and Z^E .

Appendix 3: Summation Biasing Effect Due to Ellipticity

If an observer were to walk around an elliptical tree, keeping the apparent optical width of the bole constant, the shape traversed will be a wide “figure of 8.” The area of this shape is impossible to calculate precisely, but may be approximated by

$$\hat{s} = \frac{\kappa^2 \pi \left(\frac{D^2 + d^2}{2} \right)}{4}$$

(Grosenbaugh 1958), where κ is Grosenbaugh’s basal area factor ($\kappa = 1/\sqrt{K}$ in our terminology) and D and d are the major and minor axes of the ellipse. We may reformulate this as

$$\hat{s} = \frac{\pi \alpha^2 \left(1 + \frac{1}{\lambda} \right)}{2K} \quad (3.1)$$

If we define the probability error as $p^e = p^R/p^T$ (the ratio of the relascope probability to the true probability as a function of true basal area), then, recalling that $g^T = \pi \alpha^2/\lambda$ and $p^T = g^T/K$ for a per hectare value,

$$p^e = \frac{\lambda g^T + g^T}{2g^T} = \frac{\lambda + 1}{2} \quad (3.2)$$

As λ is equal to 1 only for perfectly round trees and >1 otherwise, the probability error is always positive and tree ellipticity leads to trees being incorrectly counted in to the angle count sample. The indicator variable Y_{ij} must be replaced with an indicator that reflects this error, so we make $Y_{ij} = (g_i/K)p_i^e$. The expectation of volume then becomes

$$E(\hat{V}) = \frac{K}{m} \sum_{j=1}^m \sum_{i=1}^N \frac{v_i g_i}{g_i K} p_i^e = \bar{p}^e V,$$

which in the circumstance with trees of high average ellipticity will result in a substantial overestimation of stand volume. Note that this is in addition to the volume overestimation resulting from the assumption of circular boles when the relationship of volume to measured basal area (arising from Equation 9) is calculated.

For determination of increment bias with the inclusion of the possibility of trees being mistakenly counted in due to ellipticity, we must consider all applicable pathways in Figure 2. For pathway b the trees counted at time 1 are presumed to be correctly counted, and the new trees in time 2 may contain errors. p^e thus equals 1, whereas p^{*e} may be

>1 . With $X_{ij} = (p_i^{*e} g_i^* - p_i^e g_i)/K$, Equation 1 is now adapted to

$$\begin{aligned} E(Z_b^D) &= K \sum_{i=1}^N \frac{g_i}{K} \left[\frac{v_i^*}{g_i^*} - \frac{v_i}{g_i} \right] + \frac{p^{*e} g_i^* - g_i v_i^*}{K g_i^*} \\ &= \sum_{i=1}^N p_i^{*e} v_i^* - v_i \end{aligned}$$

With the assumption that pathway b is followed by pathway d, the error will now be in the first period of the current increment pair and we will assume that the final period has a correct count. Denoting values applying to the third inventory with the superscript **, $p^{***} = 1$, whereas p^{*e} may be >1 . Now $Y_{ij} = (g_i^*/K) p_i^{*e}$ and $X_{ij} = (p_i^{*e} g_i^* - p_i^{*e} g_i)/K$. Reformulating Equation 2 to take this into account we find

$$E(Z_d^D) = \sum_{i=1}^N v_i^{**} - p_i^{*e} v_i^*$$

Across both pathways, with the assumption that the mean stand ellipticity across all stands (as opposed to single tree ellipticity) remains constant,

$$E(2Z^D) = \sum_{i=1}^N v_i^{**} - v_i = 2Z$$

If, however, the incorrect tree is incorrectly counted in more than one inventory (pathway c), then both p^{**} and p^* will be >1 and

$$E(Z_c^D) = \sum_{i=1}^N p_i^{***} v_i^{**} - p_i^{*e} v_i^*$$

Pathway d then, however, would apply to the fourth inventory (superscript ***), and thus

$$\begin{aligned} E(3Z^D) &= \sum_{i=1}^N p_i^{*e} v_i^* - v_i + p_i^{***} v_i^{**} - p_i^{*e} v_i^* \\ &\quad + v_i^{***} - p_i^{***} v_i^{**} = 3Z \end{aligned}$$

It can be seen then that for a given plot, Z^D is eventually unbiased under any circumstances of trees being incorrectly counted in due to ellipticity. However, because new trees are continually being added to the sample, some positive bias will most likely be present when averaged over all plots in an inventory.

Similar logic may be applied to demonstrate that under pathway b $E(Z_b^S) = \sum_{i=1}^N v_i^* - v_i$ and $E(Z_b^E) = \sum_{i=1}^N p_i^{*e} v_i^* - p_i^e v_i$. Conversely, for pathway d $E(Z_d^S) = \sum_{i=1}^N p_i^{***} v_i^{**} - p_i^{*e} v_i^*$ and $E(Z_d^E) = \sum_{i=1}^N v_i^{**} - v_i^*$. The combined pathways in each case (assuming p^e is constant) sum to

$$E(2Z^S) \text{ or } E(2Z^E) = \sum_{i=1}^N p_i^e v_i^{**} - p_i^e v_i^* + v_i^* - v_i \quad (3.3)$$

Analysis of the error in this case requires that we define a

new variable for the ratio of the increments in the two increment periods:

$$q = \frac{v^{**} - v^*}{v^* - v} \text{ and } Q = \frac{V^{**} - V^*}{V^* - V} \quad (3.4)$$

Equation 3.3 may then be rearranged as:

$$\begin{aligned} E(2Z^S) \text{ or } E(2Z^E) &= \sum_{i=1}^N (v_i^* - v_i)(q_i p_i^\varepsilon + 1) \\ &= (V^* - V)(Q p^\varepsilon + 1) \end{aligned} \quad (3.5)$$

The true stand increment ($2Z = V^{**} - V$) may be described as $2Z = V^{**} - V^* + V^* - V$ or hence as

$$2Z = (V^* - V)(Q + 1) \quad (3.6)$$

Dividing Equation 3.5 by Equation 3.6 we find

$$E(2Z^S) \text{ or } E(2Z^E) = \frac{Q p^\varepsilon + 1}{Q + 1} 2Z \quad (3.7)$$

If trees are incorrectly counted in across several inventory periods (pathway c), then the formulation of Equations 3.4 and 3.6 remain the same (because other terms cancel). Equation 3.4 must, however, be adapted so that the final volume terms (v^{**} and V^{**}) apply to the final volume term in pathway d. All other terms remain unchanged. For a single increment period, Q may be considered equal to 1 and hence the biasing effect is $(p^\varepsilon + 1)/2$. Referring to Equation 3.2, we find that Z^S and Z^E will have a summation component of positive bias ε^p due to ellipticity of

$$\varepsilon^p = \frac{\lambda + 3}{4}. \quad (3.8)$$

Research Article

Assessing Forest Production Using Terrestrial Monitoring Data

Hubert Hasenauer and Chris S. Eastaugh

Department of Forest and Soil Sciences, Institute of Silviculture, BOKU University of Natural Resources and Life Sciences, Vienna, Peter Jordan Street 82, A-1190 Vienna, Austria

Correspondence should be addressed to Hubert Hasenauer, hubert.hasenauer@boku.ac.at

Received 20 October 2011; Revised 12 December 2011; Accepted 5 January 2012

Academic Editor: Timo Pukkala

Copyright © 2012 H. Hasenauer and C. S. Eastaugh. This is an open access article distributed under the Creative Commons Attribution License, which permits unrestricted use, distribution, and reproduction in any medium, provided the original work is properly cited.

Accurate assessments of forest biomass are becoming an increasingly important aspect of natural resource management. Besides their use in sustainable resource usage decisions, a growing focus on the carbon sequestration potential of forests means that assessment issues are becoming important beyond the forest sector. Broad scale inventories provide much-needed information, but interpretation of growth from successive measurements is not trivial. Even using the same data, various interpretation methods are available. The mission of this paper is to compare the results of fixed-plot inventory designs and angle-count inventories with different interpretation methods. The inventory estimators that we compare are in common use in National Forest Inventories. No method should be described as “right” or “wrong”, but users of large-scale inventory data should be aware of the possible errors and biases that may be either compensated for or magnified by their choice of interpretation method. Wherever possible, several interpretation methods should be applied to the same dataset to assess the possibility of error.

1. Introduction

National forest inventories are an expensive and time-consuming operation, particularly in large, remote, and inhospitable regions. There is therefore great interest in alternative measures to estimate forest growth, such as remote sensing [1] or mechanistic process modeling [2]. These methods, however, are not a direct measurement of the same physical characteristics as in an inventory, and it is reasonable to suggest that estimates made with these alternatives should be shown to be unbiased with reference to ground data.

In the near future, national forest inventories will form an integral part of the way that many nations determine their national carbon balance, and inventories are used to estimate forest increment as a means of monitoring their value as a carbon sink. Relatively minor errors in current standing volume estimates may have little practical or policy impact, but these may translate to substantial errors and biases in the estimate of forest increment. In some cases, these biases may mean the difference between forest areas being assessed as a sink or a source of CO₂ or could result in erroneous

(but substantial) financial penalties to countries signing up to successor agreements to the Kyoto protocol. Conversely, countries may claim carbon credits for a degree of forest sequestration that does not in fact exist.

Until recently, inventories were conducted solely as a means of measuring the timber resource present in a region, generally in order to determine its immediate extractive capacity. The inventories were optimized to most efficiently estimate a particular forest parameter, current standing volume. This was and still is important, as it describes a crucial aspect of forested landscapes. The carbon sink strength of forests is not, however, directly related to standing volume, but is a function of forest increment. Mathematically, increment is simply the difference in standing volume between two periods, plus the volume of any removals from the growing stock. In practice however this is not so simple, as sample designs or locations may vary between increments, forest area may change and some inventory designs use a nonadditive method of increment estimation (where, at the individual plot level, increment does not equal the difference in standing volumes) [3].

In recent decades, regular forest inventories have been established in many countries using a permanent plot design to reduce the sampling error of the resulting increment calculations [4]. Remeasurement intervals range from 5 to 10 years and either fixed area plots or angle-count sampling [5] may be used. In the latter case, three common methods may be applied to repeated measurements in order to estimate forest increment: the difference, starting value or end-value methods. Upscaling plot-level increments from fixed-plot inventories or using any three of the angle-count estimation methods produces mathematically unbiased estimates of increment [6–8]. It has been shown, however, that measurement error affects the various estimators differently, and thus different estimators will produce different results [6]. It has been suggested that comparing the results of different estimators can indicate the presence of measurement error and thus be used as an inventory auditing tool [6, 9].

In a theoretical simulation study using plausible estimates of measurement errors Eastaugh and Hasenauer [6] reported possible biases in angle count-derived increment estimates of up to ± 0.4 – $1.0 \text{ m}^3/\text{ha}/\text{yr}$ when averaged over 30 years, depending on the nature of the error and the estimation method used. The key findings of that study were that errors can result in different magnitudes of increment bias and may manifest in either the period in which the error occurred or in subsequent periods, depending on the increment estimation method used. Thomas and Roesch [9] applied different interpretation methods to large-scale inventory data from the southern United States and found that an up to 48% difference in increment estimation was present between methods, which they attributed to trees being missed (not counted) in the first inventory period. The Eastaugh and Hasenauer [6] study found that a 44.3% increment difference could result from inventory errors that gave rise to an only 4.6% error in volume estimation.

Applying several methods to the same dataset can, however, give substantially different results due to sampling variation, even in the absence of error. The different results are all equally valid estimators, but precision may be poor if relatively few plots are sampled. In such cases, it may be difficult to determine which (if either) of the estimators may be error affected and doubts can be raised over which estimated value should be accepted. Similarly, if inventory data is to be used as a baseline to compare against modeled or remote-sensed estimates of forest characteristics, then it is important to first ensure the integrity of the inventory estimate. This can be done by applying more than one estimation method and ensuring that the final results are within a predetermined range of each other.

In this study, we mimic a large scale forest inventory through simulating 12000 fixed area and angle count samples inside a large long term forest monitoring plot at Hirschlacke in northern Austria, over 7 measurement periods from 1977 to 2007. We are interested in how such errors may be detectable in mean increment estimates with high variance. Our primary purpose is to confirm the non-biased nature of each of the increment estimators in the absence of measurement error and determine the minimum

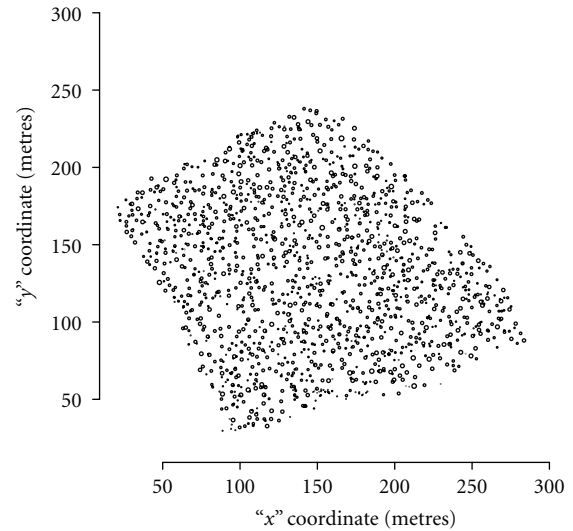


FIGURE 1: Stand layout at the Hirschlacke long-term forest monitoring plot. Sizes of circles are proportional to diameter at breast height, ranging from 5 to 75 cm. Axis coordinates are in metres.

number of such sample plots necessary to support the concordance of different combinations of estimators.

2. Data and Methods

We obtain data from the 3.47 hectare Hirschlacke long-term forest growth monitoring site in northern Austria [10]. When first measured in 1977, the stand was almost pure 110-year-old Norway spruce (*Picea abies* L. Karst) and has since then been managed under a target diameter harvesting regime [11] designed to produce an equilibrium dbh distribution. All trees of over 5.0 cm dbh have been measured for both diameter and height at five yearly intervals since 1977 and their location coordinates are precisely recorded. Figure 1 depicts the stand layout in 1977.

Since 1977, the stand structure has changed from having 1510 trees with a mean dbh of 34.6 cm (standard deviation 14.3 cm) to 2820 trees with mean dbh 18.2 cm and standard deviation 17.5 cm in 2007. Mean tree heights have followed a similar pattern, from 25.8 m (standard deviation 8.9 m) in 1977 to 14.8 m (standard deviation 12.7 m) in 2007. This has been achieved by the removal of an average of 74 m^3 of timber in each inventory period (timber volumes calculated according to the allometrics of Pollanschütz [12]). Under this permanent-cover management system, the standing volume on the site remains relatively constant over time, although diameter distribution is currently quite different to that in 1977, providing a diverse sampling space across time.

We use the Hirschlacke dataset as a means of mimicking a large-scale national inventory. As all trees in the plot are repeatedly remeasured, we are able to simulate what increments would be determined using angle counts or small fixed-area sample plots assuming perfect measurements and also with a range of simulated error conditions. The dataset is thus an ideal means of demonstrating the potential

biases that may be apparent in angle-count-based inventories containing error [6], or in this study, comparing the results of different increment estimation methods.

We construct a pattern of 12 000 points at a 1×1 meter spacing within the Hirschlacke plot, such that no point is within 30 meters of the plot boundary. We then simulate a fixed area plot of 200 m^2 and an angle-count sample with a basal area factor of 4 at each point in each of the seven measurement periods. This mimics the plot size used as part of the Swiss National Forest Inventory [13] and the basal area factor used in Austria [14].

Increments are estimated four ways.

- (1) Differences between time 1 and time 2 volumes determined from fixed-area plots, plus removals (fixed-plot method).
- (2) Differences between time 1 and time 2 volumes determined from angle-count plots, plus removals (difference method).
- (3) The recorded increment of the trees within the angle-count sample multiplied by the estimated number of trees of that size in the stand in time 1, plus the volume of the new trees entering the stand. (starting value method).
- (4) The recorded increment of the trees within the angle-count sample multiplied by the estimated number of trees of that size in the stand in time 2. (end value method). This method requires the estimation of prior dimensions of trees which (in a practical inventory situation) may not have been recorded at time 1.

Much of the published literature on deriving increments from angle-count sampling distinguishes between “survivors”, “ingrowth”, “ongrowth”, and “nongrowth” trees (cf. Martin 1982 [15]), depending on whether they were above or below a particular diameter at breast height in the period preceding the current measuring period and whether they were counted “in” or “out” of the angle count in the preceding period (Table 1).

Defining the following variables.

Z = volume increment per hectare, with superscripts F for fixed area plots, D for difference method, S for starting value method, and E for end value method;

m = Number of sample plots;

n_j = Number of trees in each sample j ;

v_i = volume of individual tree i ;

a_j = area of fixed area plot j ;

K = basal area factor;

g_i = basal area of individual tree i . and denoting measurements made in a subsequent inventory period by $(*)$, ignoring tree removals from the plots and following Hradetzky (1995) [16] and Eastaugh and Hasenauer [6], the mathematical form of the four methods may be presented as:

$$Z^F = \frac{10000}{m} \sum_{j=1}^m \sum_{i=1}^{n_j} \frac{v_{ji}^*}{a_j} - \frac{10000}{m} \sum_{j=1}^m \sum_{i=1}^{n_j} \frac{v_{ji}}{a_j}, \quad (1)$$

$$Z^D = \frac{K}{m} \sum_{j=1}^m \sum_{i=1}^{n_j} \frac{v_{ji}^*}{g_{ji}^*} - \frac{K}{m} \sum_{j=1}^m \sum_{i=1}^{n_j} \frac{v_{ji}}{g_{ji}^*} + \frac{K}{m} \sum_{j=1}^m \sum_{i=n_j+1}^{n_j^*} \frac{v_{ji}^*}{g_{ji}^*}, \quad (2)$$

$$Z^S = \frac{K}{m} \sum_{j=1}^m \sum_{i=1}^{n_j} \frac{v_{ji}^*}{g_{ji}^*} - \frac{K}{m} \sum_{j=1}^m \sum_{i=1}^{n_j} \frac{v_{ji}}{g_{ji}^*} + \frac{K}{m} \sum_{j=1}^m \sum_{i=n_j+1}^{n_j^*, g_{ji} < 19.63} \frac{v_{ji}^*}{g_{ji}^*}, \quad (3)$$

$$Z^E = \frac{K}{m} \sum_{j=1}^m \sum_{i=1}^{n_j} \frac{v_{ji}^*}{g_{ji}^*} - \frac{K}{m} \sum_{j=1}^m \sum_{i=1}^{n_j} \frac{v_{ji}}{g_{ji}^*} + \frac{K}{m} \sum_{j=1}^m \sum_{i=n_j+1}^{n_j^*} \frac{v_{ji}^*}{g_{ji}^*} - \frac{K}{m} \sum_{j=1}^m \sum_{i=n_j+1}^{n_j^*} \frac{v_{ji}}{g_{ji}^*}. \quad (4)$$

The term $\sum_{i=n_j+1}^{n_j^*}$ in (2) and (4) describes the “new” trees entering a sample in the subsequent measurement period and includes nongrowth, ongrowth, and ingrowth. In this formulation of the difference and end value methods, the three types of new tree need not be distinguished. The starting value method does not include nongrowth, so only those new trees with a previous dbh of less than 5.0 cm (basal area less than 19.63 cm^2) are included in (3).

Mean per hectare volume and increment estimates (without errors) for each plot across each and all time periods are compared with paired t -tests. In these examples, we use 84 000 paired data points for volume calculations and 72 000 for increment, thus even very small differences may be deemed to be statistically “significant”. In practical applications, however, given the large variances in increment estimation, the null hypothesis (that the means are the same) is difficult to reject even if the mean values appear quite different. If differences due to measurement errors were present, we are interested to determine a minimum number of samples necessary to detect that difference. To do this, we estimate the population mean increment and standard deviation through lumping data from all periods and applying standard statistical procedures [17] to find the minimum number of paired samples that will give a t -test with 90% confidence that the means are within 5%, with 95% power.

$$n = \frac{s_d^2}{\delta^2} (t_{\alpha(2),v} + t_{\beta(1),v})^2, \quad (5)$$

where: n = required minimum sample size, s_d^2 = variance of the differences, δ = maximum allowable error, $t_{\alpha(2),v}$ = t statistic at significance α , two tailed, and degrees of freedom v , $t_{\beta(1),v}$ = t statistic for power $1-\beta$, one tailed, and degrees of freedom v .

These minimum sample sizes are then tested by drawing that many random plots from the data and comparing the appropriate increment estimators with a paired t -test. This is repeated 1000 times, and we report the number of times where a statistically significant difference of greater than 5%

TABLE 1: Components of growth in angle-count sampling.

Tree classification	dbh in measurement period 1	dbh in measurement period 2	Presence in Angle-count sample, period 1	Presence in Angle-count sample, period 2
Survivors	>threshold	>threshold	IN	IN
Ingrowth	<threshold	>threshold	IN	IN
Ongrowth	<threshold	>threshold	OUT	IN
Nongrowth	>threshold	>threshold	OUT	IN

appears to be present. These routines are implemented in the “sample size” package in the “R” programming environment [18]. Users of this package should note that it assumes one-sided tests, thus the value of α must be adapted to the two-tailed equivalent.

3. Results

3.1. Standing Volume and Volume Increment. The mean volume estimated across all plots and time periods using fixed area methods was 775.5 m³/ha, with a standard deviation of 244.8 m³/ha. Using angle counting, the mean was estimated as 779.8 m³/ha, with a standard deviation of 168.2 m³/ha. The difference of 0.55% of mean volume is statistically significant at 95%, $P = 3 \times 10^{-5}$. This statistical significance is a result of the very large number of data points (Figure 2). A breakdown of volumes estimated in each period is given in Table 2. The mean increment estimated across all plots and time periods with the four available estimation methods is given in Table 3. All differences were significant at $P < .001$.

3.2. Minimum Number of Plots Required to Detect Differences. The procedure for determining the minimum number of plots needed depends on the variance of the differences between the two methods to be compared, as per (5). This is given in the lower left portion of Table 4. The upper right portion of Table 4 gives the minimum number of plots required to detect a 5% difference in increment estimates using different methods at 90% confidence, with 95% power in a paired t -test. Randomly selecting these numbers of plots from the dataset and comparing increment estimates with a t -test shows that in less than 0.1 percent of 1000 repetitions a spurious difference of greater than 5% is found between the estimates (bracketed values, Table 4).

4. Discussion

The data we amass from the Hirschlacke stand provides us with 12 000 simulated plots over 7 years, which ranged from zero to 1800 m³/ha (Figure 2). The size and spread of this dataset is comparable to that of the Austrian National Forest Inventory, comprising 9182 plots containing trees in the 2007–2009 period with angle-count volume estimates ranging from 1 to 1806 m³/ha, with a mean of 344 m³/ha and a standard deviation of 241.5 m³/ha (Eastaugh, unpublished data). Even though a plot of only 3.47 ha cannot of course

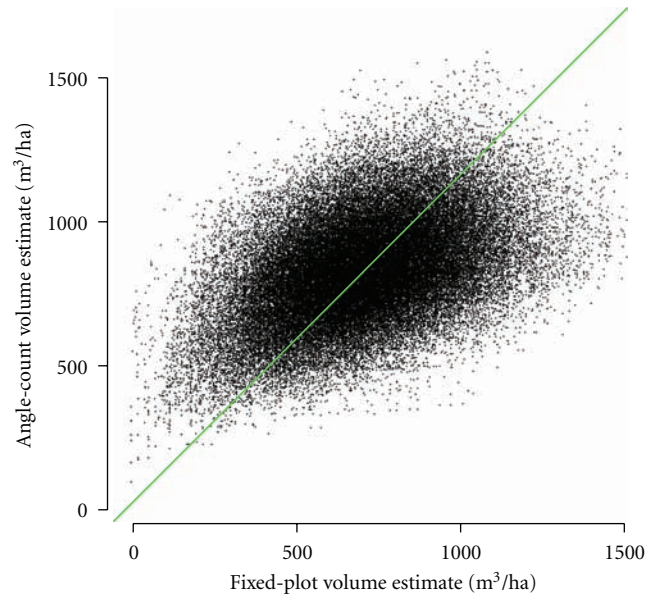


FIGURE 2: Comparison of fixed area and angle-count estimates of stand volume. Each point represents the sample measurement at each of the 12 000 simulated plots in one of the seven measurement years (84 000 data points).

represent the variability across the whole forest estate, Figure 2 shows how much variation can be found between plots even in such a small area. Examination of Table 2 shows that although the means are substantially different, the variation around the mean in our simulation is comparable to that from the real NFI. This suggests that a substantial portion of the variability in an inventory is due to the fine-scale estimation variability between plots, even plots within the same stand, rather than to the true broad-scale differences between forest stands in different areas. The synthetic dataset that we construct mimics an NFI and allows the exploration of theoretical aspects of inventory sampling without the added complications of measurement error issues.

It is important to recognize that the dataset we construct is a hypothetical forest inventory and is not validly comparable with any comprehensive calculations of volume or increment from the Hirschlacke stand. A valid sampling design would require that all points in the stand have an equal possibility of sampling. Although in theory, it

TABLE 2: Comparison of fixed-area and angle-count estimates of stand volume, for the 12 000 plots simulated in each measurement year.

Measurement year	Fixed-area volume estimate		Angle-count volume estimate	
	Mean (m ³ /ha)	Std. dev.	Mean (m ³ /ha)	Std. dev.
1977	759.0	231.3	762.5	172.4
1982	769.3	226.3	774.6	161.9
1987	772.7	225.3	775.2	155.1
1992	818.2	241.2	822.4	163.9
1997	798.6	242.5	806.0	158.7
2002	775.5	259.0	780.8	168.0
2007	735.3	275.5	737.1	181.9

TABLE 3: Comparison of fixed-area and angle-count estimates of stand increment per 5 years, for the 72 000 data points simulated in each measurement year.

Method	Increment estimate, m ³ /ha/5 years	
	Mean	Std. dev.
Fixed-area plots	67.88	28.14
Angle counts, difference method	69.01	56.97
Angle counts, starting Value method	68.23	21.89
Angle counts, end Value method	68.24	21.13

would be possible to extend our sample grid to encompass the whole stand, problems then arise with the boundary overlap problem, where some sample plots extend to outside the stand. Solutions to this may exist [19] but would be computationally extremely expensive to institute in our simulation. Our purpose in this paper, however, is not to assess the accuracy of each inventory method in estimating the values of a true stand, but to compare the estimates made with different methods from the same set of points.

The apparent statistically significant differences in volume results from different methods arise from the large number of plots. However, at 0.55% of volume and a maximum of 1.66% of increment, these differences are not functionally significant [20]. This difference does not arise in a properly conducted inventory, as both fixed-area plots and angle-count plots are unbiased sampling procedures. In this respect, our hypothetical inventory may be slightly flawed, as we effectively sample from a forest stand without edges and the population sampled with angle counts is slightly different to that sampled with fixed-area plots, even though both use the same plot centres. Nevertheless, significance testing with sufficiently large samples will always find “some” significant difference, even if the null hypothesis that the sample means are equal is actually true [21]. Given that the effect size is so small, we believe that this difference does not invalidate our sample collection for the purposes of this paper. Moreover, the (hypothetical) populations sampled for analysis with the three angle-count-based increment estimators are identical and thus validly comparable.

A single fixed-plot will measure different trees to an angle count with the same centre and thus high variance in the difference between each individual plot is to be expected. Interestingly, the behaviour at the extremes appears to be quite different, as the fixed plot estimates appear to give

higher values than the angle counts in denser portions of the forest but lower values in regions with lower density (Figure 2).

The difference method of increment estimation has very high variance in itself (ref. Table 3), as it is dependent mostly on how many new trees (either ingrowth, ongrowth or nongrowth) enter a sample in a remeasurement period. Multimethod estimation comparisons involving either of these two methods will thus require a large number of plots (Table 4). When comparing the starting value and end value methods, most trees that make up the increment estimate are the same trees, the only difference in the sample is due to the nongrowth trees that enter the sample in the remeasurement. This explains the plotwise intermethod variance of only 7.39 m³/ha/5 years. It is important, however, to note that the end value method requires knowing or estimating the dimensions of nongrowth trees in the period prior to when they entered the sample. In our example studied here this information was known from the long-term monitoring records, but in real inventories it is usually estimated with regression equations. This may change the variance in the estimates in comparison with other methods. The inclusion of nongrowth trees enlarges the sample and so in principle the estimate should be more precise. This effect is, however, lessened by the fact that the covariance is greater as the survivor estimates are calculated using their inclusion probabilities at time 2, when the basal areas are larger [16]. Hradetzky [16] derived equations showing that increments derived from the end value method would have “slightly” less variance than the starting value method, if prior tree dimensions were known. Roesch et al. [22] and Heikkinen and Henttonen [23] however give details of empirical studies showing that the standing volume at the time of first measurement can be substantially more precisely estimated

TABLE 4: Minimum number of plots required to detect a 5% difference in increment estimates using different methods at 90% confidence, with 95% power in a paired t -test. Numbers in italics are the standard deviation of the differences between each pair of methods, numbers in normal text are the required numbers of plots. Values in brackets are the number of times that a t -test using the appropriate number of plots (randomly selected) incorrectly suggested that a significant difference of greater than 5% existed, from 1000 iterations.

Method	Fixed plot	Difference	Starting value	End value
Fixed plot	—	3204 (8)	491 (2)	490 (2)
Difference	<i>59.34</i>	—	3032 (4)	2416 (6)
Starting value	<i>23.19</i>	<i>57.72</i>	—	52 (2)
End value	<i>23.17</i>	<i>51.53</i>	<i>7.39</i>	—

by regressing information available only at time two. Our results in Table 2 (with perfectly known tree volumes prior to their first-angle-count measurement) support Hradetzky's view, leading to the conclusion that a modeled estimate of time one volume made with an angle count from a particular point may in fact be more precise than the actual observation made from that point. To the best of our knowledge, this artificial reduction in sampling variability has not yet been formally justified from a conceptual standpoint. At issue is which sampling method best represents the true variability of the stand, which would first require defining stand variability at a scale compatible with the scale-indeterminate samples. This, we suggest, is a problem for another day.

In real inventory situations, both fixed-area estimates and angle counts are not likely to be available for the same region in one-time period. If our comparisons of increment estimation here are to be applied to National Forest Inventories, then this will be limited to those inventories based on angle counting (i.e., Finland, Germany, and Austria).

All efforts at assessing large-scale ecosystem productivity will be estimates, whether they depend on “top down” approaches from satellite data [24] or use “bottom up” methods from terrestrial samples (inventories). Although advances have been made in linking these two approaches [25, 26], success will depend on having a clear understanding of the variability, biases, and limitations of each method. As shown in this paper, confidence in the concordance of estimates derived with different calculation methods is largely an issue of scale.

5. Conclusions

Forest inventories are measured data and thus other forest growth estimation methods such as remote sensing or modeling must be shown to be consistent with accurate inventories in order to claim to represent reality. Inventories, however, are not a full measurement of the whole forest but are an estimate, a statistical model. We have shown here that different inventory interpretation methods can give different results, even though all are mathematically unbiased. If sufficiently large numbers of samples are available then all methods can be shown to agree, but with less than this number, a range of equally plausible estimates could be made.

It is inevitable that any forest measurement program will contain some degree of error, hopefully (but not certainly) small. These errors have different effects on increment

estimation, depending on what inventory interpretation methods are used. If two different methods are applied to the same dataset, over a sufficient number of samples, then the integrity of the inventory can be proven. In the case of National Forest Inventories based on angle-count sampling, the procedures in this paper can be easily applied and should be a precondition of using inventory data to validate other approaches to forest-growth estimation.

Appendix

It has been suggested that the slight difference between the volume estimates made with fixed-area plots or angle-count samples may be due to differences in stand density towards the edges of the plot. The fixed area plots are limited to trees within a radius of 7.98 metres of the plot centres, but an angle count will count trees further away than this if they are over 28.2 cm dbh. As the angle count method in our example gave results a little higher than the fixed area plots, this initially seems to imply that the density of the forest in the zone just outside the limitations of the fixed area plots must be higher and that this could easily be tested with our available data. However, the edges of our study area were found to be less dense than the inner parts. The explanation for the slightly higher volume estimates with angle-count sample plots becomes evident from the following example.

Consider a stand of 4 trees, each of dbh 56.4 cm, in an area of 625 m² (Figure 3(a)). A fixed-area plot of radius 14.1 m and an angle-count plot of BAF = 4 m²/ha are established in the centre of the stand. The true stand density is 16 m²/ha, and both the fixed area plot and the angle count will arrive at the same conclusion.

If our stand was in fact a little larger (Figure 3(b)), it might include one larger tree of dbh 80 cm and 2 small trees of dbh 10 cm. Assuming a radius of 18 m, the total stand area is now 1017 m². The angle count detects the larger tree, and so the density estimate is 20 m²/ha. The fixed-area plot estimate is the same 16 m² as before, but the true stand density is 14.9 m²/ha, with 16 m²/ha in the “inner” zone and 13.2 m²/ha in the outer boundary zone. Even though the outer zone is less dense than the inner and the angle count “sees” further, the angle count appears to result in higher basal area estimate than a fixed area plot with the same centre point.

The differences in volume estimates in the body of this paper do not arise from differences in stand density in different zones of the forest, but are a result of the fact that the

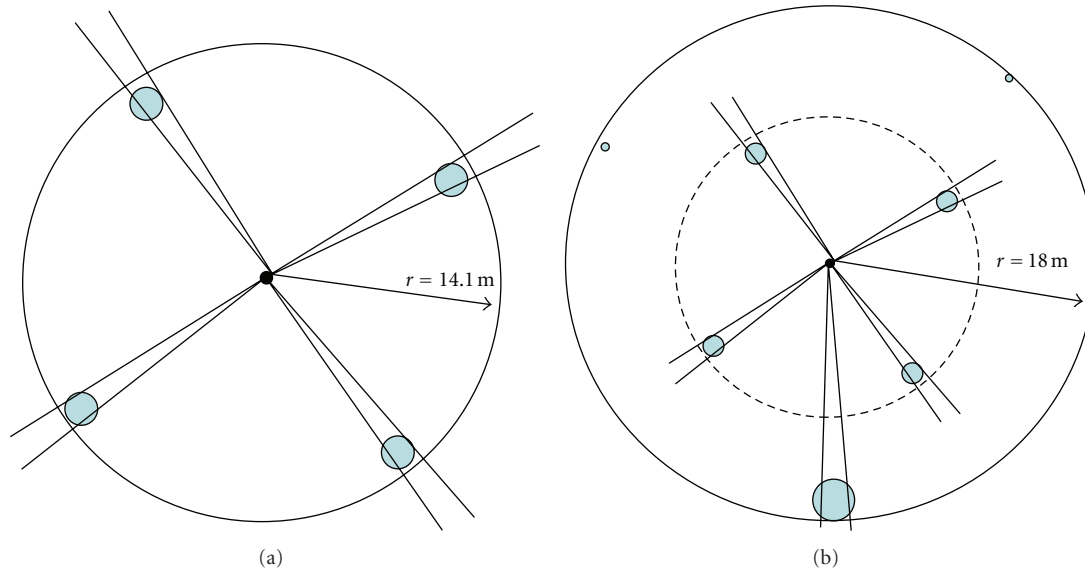


FIGURE 3: (a) Four trees each of basal area 2500 cm^2 in an area of 625 m^2 . A fixed-area plot of 625 m^2 or an angle count with $\text{BAF} = 4$ will agree that the stand density is $16 \text{ m}^2/\text{ha}$. (b) A stand of 1018 m^2 , including the same four trees as (a) plus one tree of basal area 5027 cm^2 and two of 78.5 cm^2 each. The true stand density is now $14.9 \text{ m}^2/\text{ha}$, but the fixed-area plot sees $16 \text{ m}^2/\text{ha}$ and the angle count $20 \text{ m}^2/\text{ha}$.

precise area being sampled has not been defined. It would be possible to obtain equal results from each sampling method in our small example in this appendix if we adhered to the following strictures.

- (i) The area to be sampled must be strictly defined in space.
- (ii) A very large number of plots must be used and aggregated.
- (iii) Plot locations must be random, with any point in the defined area having an equal or known probability of selection (including near the edges).
- (iv) Estimates from plots where the plot boundary (or the tree's inclusion zone) overlaps the edge of the sampling area must be appropriately adjusted. For angle counts, this is not yet a fully solved problem [19].

For perfect mathematical precision, future simulation studies will need to either develop new, computationally efficient methods to deal with the boundary overlap problem or project their simulated forest onto a sphere thus eliminating boundaries. The purpose of this current paper, however, was to compare collections of point samples, not to assess their accuracy in estimating stand densities in any defined area.

Acknowledgments

This work was funded by the project "Comparing Satellite Versus Ground Driven Carbon Estimates for Austrian Forests" (MOTI). The authors are grateful for the financial support provided by the Energy Fund of the Federal State of Austria managed by Kommunalkredit Public Consulting GmbH under contract number K10AC1K00050. The authors

thank Hubert Sterba for providing the excellent Hirschlacke dataset for this study. Insightful review comments were provided by Timo Pukkala and three anonymous reviewers.

References

- [1] H. K. Gibbs, S. Brown, J. O. Niles, and J. A. Foley, "Monitoring and estimating tropical forest carbon stocks: making REDD a reality," *Environmental Research Letters*, vol. 2, no. 4, Article ID 045023, 2007.
- [2] G. M. J. Mohren, "Large-scale scenario analysis in forest ecology and forest management," *Forest Policy and Economics*, vol. 5, no. 2, pp. 103–110, 2003.
- [3] C. T. Scott, "An overview of fixed versus variable-radius plots for successive inventories," in *State-of-the-Art Methodology of Forestry Inventory. A Symposium Proceedings. July 30-August 5, 1989*, V. J. LaBau and T. Cunia, Eds., Syracuse, NY, USA, 1990.
- [4] E. Tomppo, T. Gschwantner, M. Lawrence, and R.E. McRoberts, *National Forest Inventories: Pathways for Common Reporting*, Springer, Berlin, Germany, 2010.
- [5] W. Bitterlich, "Die Winkelzählprobe," *Allgemeine Forst- und Holzwirtschaftliche Zeitung*, vol. 59, no. 1-2, pp. 4–5, 1948.
- [6] C.S. Eastaugh and H. Hasenauer, "Biases in volume increment estimates derived from successive angle count sampling," *Forest Science*. In press.
- [7] L. R. Grosenbaugh, "Point-sampling and line-sampling: probability theory, geometric implications, synthesis," USDA Forest Service South Forest Experimental Station Occasional Paper 160, pp. 34, 1958.
- [8] F. A. Roesch, E. J. Green, and C. T. Scott, "New compatible basal area and number of tree estimators from remeasured horizontal point samples," *Forest Science*, vol. 35, pp. 281–293, 1989.
- [9] C. E. Thomas and F. A. Roesch, "Basal area growth estimators for survivor component: a quality control application," *Southern Journal of Applied Forestry*, vol. 14, no. 1, pp. 12–18, 1990.

- [10] H. Sterba, "20 Years target diameter thinning in the "Hirschblacke", forest of the monastery of Schögl," *Allgemeine Forst- und Jagdzeitung*, vol. 170, no. 9, pp. 170–175, 1999.
- [11] H. Sterba and A. Zingg, "Target diameter harvesting—a strategy to convert even-aged forests," *Forest Ecology and Management*, vol. 151, no. 1–3, pp. 95–105, 2001.
- [12] J. Pollanschütz, "Formzahlfunktionen der Hauptbaumarten Österreichs," *Allgemeine Forstzeitung*, vol. 85, pp. 341–343, 1974.
- [13] P. Brassel and H. Lischke, *Swiss National Forest Inventory: Methods and Models of the Second Assessment*, WSL Swiss Federal Research Institute, Birmansdorf, Switzerland, 2001.
- [14] K. Gabler and K. Schadauer, *Methoden der Österreichischen Waldinventur 2000/02*, vol. 135 of *BFW Berichte*, Bundesforschungs- und Ausbildungszentrum für Wald, Naturgefahren und Landschaft, Vienna, Austria, 2006.
- [15] G. L. Martin, "A method for estimating ingrowth on permanent horizontal sample points," *Forest Science*, vol. 28, no. 1, pp. 110–114, 1982.
- [16] J. Hradetzky, "Concerning the precision of growth estimation using permanent horizontal point samples," *Forest Ecology and Management*, vol. 71, no. 3, pp. 203–210, 1995.
- [17] J. H. Zar, *Biostatistical Analysis*, Prentice Hall, Englewood Cliffs, NJ, USA, 1999.
- [18] R Development Core Team, *R: A Language and Environment for Statistical Computing*, R Foundation for Statistical Computing, Vienna, Austria, 2011.
- [19] M. J. Ducey, J. H. Gove, and H. T. Valentine, "A walkthrough solution to the boundary overlap problem," *Forest Science*, vol. 50, no. 4, pp. 427–435, 2004.
- [20] S. T. Ziliak and D. N. McCloskey, *The Cult of Statistical Significance: How the Standard Error Costs Us Jobs, Justice and Lives*, University of Michigan Press, Ann Arbor, Mich, USA, 2008.
- [21] J. Cohen, "The earth is round ($P < 0.05$)," *American Psychologist*, vol. 49, no. 12, pp. 997–1003, 1994.
- [22] F. A. Roesch, E. J. Green, and C. T. Scott, "A test of alternative estimators for volume at time 1 from re-measured point samples," *Canadian Journal of Forest Research*, vol. 23, pp. 598–604, 1993.
- [23] J. Heikkinen and H. Henttonen, "Re-measured relascope plots in the assessment of inventory update methods," in *Nordic Trends in Forest Inventory, Management Planning and Modelling. Proceedings of SNS meeting in Solvalla, Finland. April 17–19, 2001*, J. Heikkinen, K. T. Korhonen, M. Siitonen, M. Strandström, and E. Tomppo, Eds., Finnish Forest Research Institute, 2001, Research Papers 860.
- [24] R. Päivinen and P. Anttila, "How reliable is a satellite forest inventory?" *Silva Fenica*, vol. 35, no. 1, pp. 125–127, 1998.
- [25] R. Petritsch, C. Boisvenue, S. W. Running, and H. Hasenauer, "Assessing forest productivity: satellite versus terrestrial data-driven estimates in Austria," in *Forest Growth and Timber Quality: Crown Models and Simulation Methods for Sustainable Forest Management Proceedings of an International Conference, Portland, OR, USA, August 7–10, 2007*, Dennis P. Dykstra and Robert A. Monserud, Eds., pp. 211–216, United States Department of Agriculture Forest Service Pacific Northwest Research Station, 2009, General Technical Report PNW-GTR-791.
- [26] R. A. Houghton, D. Butman, A. G. Bunn, O. N. Krankina, P. Schlesinger, and T. A. Stone, "Mapping Russian forest biomass with data from satellites and forest inventories," *Environmental Research Letters*, vol. 2, no. 4, Article ID 045032, 2007.

FIRE SIZE/FREQUENCY MODELLING AS A MEANS OF ASSESSING WILDFIRE DATABASE RELIABILITY

Eastaugh CS^{1,*} and Vacik H¹

¹ Institute of Silviculture, Department of Forest and Soil Sciences, BOKU University of Natural Resources and Life Sciences Vienna, Peter Jordan Str. 82, A-1190 Wien, Österreich.

* Corresponding author: chris.eastaugh@boku.ac.at

Submitted to PloS ONE 05/04/2012

ABSTRACT

Many jurisdictions around the world have recently begun compiling databases of wildfire records, in an effort to determine patterns, quantify risks and detect possible changes in fire regimes. Such datasets, if valid and comprehensive, could be used for fire hazard model validation, detection of trends and risk modelling under current and future climatic conditions. It may be however that data quality issues can hinder these efforts. In particular, older records may be less comprehensive, and smaller fires may have a greater chance of being unrecorded. A database of Austrian wildfires has been compiled, based on historic documentary records from a variety of sources that cover different time periods or geographical regions. The non-comprehensive and non-random nature of this dataset (both spatially and temporally) makes the direct analysis of wildfire patterns impossible, necessitating the use of models to identify trends and patterns. If properly validated, models using climatic and non-climatic input data can serve as proxies for the true probability of wildfire occurrence. It is likely however that small fires are substantially underreported, particularly in early decades. We test this proposition by examining the fire size/ frequency distribution of all fires with recorded areas. The thesis behind the work is that we may compare the fire size/frequency relationships in the data across different time periods and that anomalies in the fire size/frequency distribution may indicate weak parts of the dataset.

INTRODUCTION

Many national jurisdictions around the world have recently begun compiling databases of wildfire records, in an effort to determine patterns, quantify risks and detect possible changes in fire regimes. Examples are available from Switzerland [1,2], the USA [3], Canada [4] and Europe [5]. Such datasets, if valid and comprehensive, could be used for model validation, detection of trends and quantitative risk analyses. In some cases, historic fire databases have been used to demonstrate an apparent increase in fire danger, [5-8] but as is often pointed out [9-12], data quality issues can hinder these efforts. In particular, older records may be less comprehensive, and smaller fires may have a greater chance of being unrecorded [13]. This is not unique to wildfires, similar issues have been raised in the broader context of historical natural disaster records [14].

If fire databases are to be used for practical or research purposes every effort must be made to ensure the integrity of the dataset. Missing data from earlier periods may result in an apparent increase in the chance of fire ignition, where no such change has occurred. Similarly, if unreported fires are smaller than those recorded this may bias fire hazard models and risk assessments. It is difficult however to assess how many (if any) fire events are truly missing from a dataset in any given period, and what size they may have been.

One common approach to fire modelling involves determining fire size/frequency relationships. It is well accepted that smaller fires occur much more often than larger fires (a heavy tailed frequency distribution), and great effort has been put into defining the mathematical function of this relationship. Some previous work (i.e. [15,16]) suggests that the fire size/frequency relationship of larger fires might comply with a power law distribution, although this is not universally accepted [17]. Regardless of the form of this relationship, in most previous work it is assumed to be temporally stable (although this is rarely tested). Malamud et al. (2005) [16] did test this assumption and were unable to find a statistically significant difference in their power-law parameters across different time periods.

Our aim in this study is to develop methods to assess historical fire datasets and determine whether or not they contain anomalies that may adversely impact future work. To illustrate these methods we apply them to the database of Austrian wildfires compiled by the Institute of Silviculture at the University of Natural Resources and Life Sciences in Vienna [18,19]. The principle of our approach is that we compare the fire size/frequency relationships in the data across different time periods and that anomalies in the fire size/frequency distribution may indicate weak parts of the dataset that should be treated with especial caution. Our hypothesis is that changes in the size/frequency relationships are consistent with increasingly better reporting of smaller fires in more recent years. We test the dataset for its compliance with a power law distribution in the upper tail using the modern techniques of Clauset et al. (2007)[20], but the bulk of our analysis uses non parametric methods.

METHODS

Data

As part of the AFFRI and ALP FFIRS projects [21,22], a database of Austrian wildfires has been compiled, based on historic documentary records [18,19]. The database has been assembled with information from a variety of sources that cover different time periods or geographical regions. Records were collated from public online fire news platforms

‘www.wax.at’ and ‘www.feuerwehr-news.at’, from regional fire brigade records and through personal contact with the various Austrian municipalities and Federal government departments. The raw collated data as of April 2011 consisted of 2660 records. After removing repeated observations of the same fire event 2455 records remain, 1870 of which pertain to forest fires, the earliest being in the year 1874. 1012 of these have a value recorded for burnt area (the earliest in the year 1907), with values ranging from one square metre to 200 hectares, distributed as shown in figure 1.

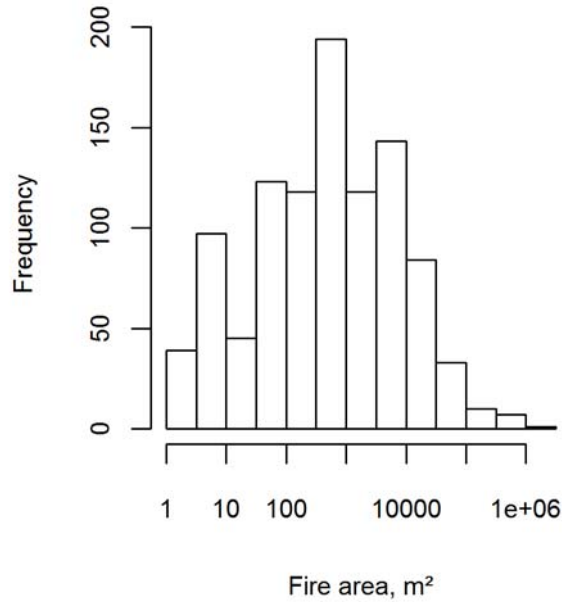


Figure 1 Frequency distribution of forest fires in Austria 1960-2010.

Methods

A power law distribution is one where $\Pr[X \geq x] = Cx^{-\alpha}$, C and α both > 0 . Newman (2005) [23] demonstrated that where $\alpha > 1$,

$$p(x) = \frac{\alpha - 1}{x_{\min}} \left(\frac{x}{x_{\min}} \right)^{-\alpha} \quad (1)$$

α and x_{\min} being constants. The power law parameters α and x_{\min} have commonly in the past been estimated graphically or with a least-squares regression, although these methods can introduce significant bias to power law parameter estimates [24,25]. Newman (2005) [23] gives a derivation for a Maximum Likelihood Estimation (MLE) estimation of α , arriving at Eq. 2.

$$\alpha = 1 + n \left[\sum_{i=1}^n \ln \frac{x_i}{x_{\min}} \right]^{-1} \quad (2)$$

To determine x_{\min} we follow Clauset et al. (2007) [20] and test the fit of the modelled distribution to the empirical data. Power law models are constructed with a range of possible values of x_{\min} , and a distance statistic determined for each model’s fit to the empirical data. We then select the x_{\min} from the model with the smallest distance between the observed and

modelled cumulative probability distributions that leaves a useful number of records above. The modelled cumulative probability curve (Pm_i) is calculated as

$$Pm_i = \left(\frac{x_i}{x_{min}} \right)^{-\alpha+1}, x_{min} \leq i \leq \max(x) \quad (3)$$

and the observed curve (PO_i) as the normalised ranks (R) of each observation

$$PO_i = \frac{Rx_i}{\max(Rx_i)}, x_{min} \leq i \leq \max(x) \quad (4)$$

The maximum difference between Pm_i and PO_i is the distance for the particular x_{min} tested.

Standard errors and 90% confidence limits around the estimates of α are estimated with a non-parametric bootstrapping procedure [26]. Estimates are made in the ‘R’ statistical package [27] (R Development Core Team 2011), using code kindly made public by Clauset et al. (2009) [28], available via <http://tuvalu.santafe.edu/~aaronc/powerlaws/>.

The database is divided into 6 subsets based on year of record, with each subset containing a comparable number of fires above x_{min} and (with one exception) at least 30 fires per period. The slope of the fire size/frequency relationship is calculated for each subset (using the global x_{min}), and compared graphically with the slope for all records subsequent to that period. Formal goodness of fit test results are calculated and consist of the standard error and bias of the slope estimate and the KS statistics for the fit of the data to the estimated power law model.

If record-keeping is consistent and the fire size/frequency distribution is temporally stationary, then there should be no significant difference between the size/frequency slope in any period and that from the combined records from subsequent periods. The significance of any apparent trend differences between each period and all subsequent periods is examined with a t-test and a likelihood ratio (LR) test. The LR tests the proposition that separate models for each period will perform better than one model for combined periods (a pooled model). If this is the case, then it appears likely that the distributions in each case are different. Ratios and p values are obtained from the ‘pchisq’ function in R

Given that some data subsets may fail formal goodness of fit tests when compared with a power law distribution, we also compare data from each subset with subsequent periods with a non-parametric Kolmogorov-Smirnoff (KS) test. As there are a large number of ‘ties’ in the data, we use the bootstrapping `ks.boot` algorithm in the `Matching` package [29]. This procedure compares the KS statistic from the original pair of datasets with that from a large number of samples drawn from a resampled pooled dataset. The p value reported is the proportion of times that the KS statistic from the generated samples is greater than that from the original [30]. A low p value suggests that the Null hypothesis that the datasets are drawn from the same distribution should be rejected.

Fires smaller than x_{min} are divided into three magnitude classes; from 1 to 100m², from 101 to 1000m² and from 1001 to the x_{min} previously determined. Fires of less than 100m² are possibly not ‘wild’ fires and so may exhibit different statistical behaviour. Figure 1 suggests that 1000m² is a possible break in the frequency distribution. No parametric testing is performed as these data subsets are arbitrarily truncated and parametric statistics are unlikely

to be meaningful. Differences between the data distributions from each period and its subsequent periods are analysed with the KS testing procedure outlined above, and detailed graphical representations supplied as supplementary figures.

RESULTS

Parametric comparisons

The optimal value for x_{min} was found to be 4500m² (fig 2), with this value giving a power law model for the fire database that most closely matches observations.

Table 1 gives a summary of the parameters and the formal goodness of fit statistics for each period.

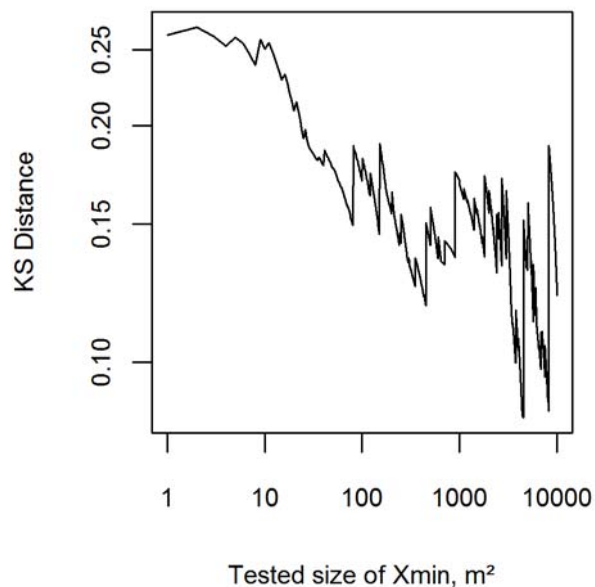


Figure 2 Test of possible values of x_{min} .

Kolmogorov Smirnov distances for possible values of x_{min} to fit a power law relationship to fires in the Austrian database. The smallest distance between the theoretical and observed distributions suggests the best fit, in this case 4500m².

Table 1 Goodness of fit of power law relationships for each period.

Period	1960-2010	< 1993	> 1992	1993-1994	> 1994	1995-2001	> 2001	2002-2004	> 2004	2005-2007	> 2007
n	260	29	231	46	185	45	140	55	85	47	38
alpha	1.784	1.619	1.811	1.945	1.784	1.796	1.780	1.739	1.808	1.877	1.737
SE	0.049	0.124	0.054	0.147	0.057	0.123	0.067	0.104	0.090	0.137	0.126
Bias	0.003	0.023	0.003	0.019	0.004	0.016	0.006	0.013	0.009	0.019	0.020
KS	0.165	0.109	0.178	0.160	0.184	0.204	0.178	0.191	0.170	0.163	0.182
p	0.000	0.697	0.000	0.041	0.000	0.005	0.000	0.002	0.000	0.032	0.033

n: number of fires in each period

alpha: best-fit power law exponent

SE: standard error of exponent estimate

Bias: bias of exponent estimate

KS: bootstrapped Komolgorov -Smirnov distance

p: p value for KS test. p values less than 0.1 suggest that the power law hypothesis should be rejected [29].

260 fires are recorded with a size of at least 4500m² since 1960. Dividing these into 6 time periods gives between 29 and 55 fires per period, with between 0 and 32 fires recorded per year (fig 3a).

The results of the t-tests and the likelihood ratios are in table 2. To interpret these results we consider the Null hypothesis that each pair of data subsets are in fact from distributions with the same parameters. H_0 cannot be rejected with greater confidence than the p_t or p_{LR} values in table 2.

Table 2 Results of comparisons for fires > 4499m²

1st period years	2nd Period		Slope difference	Slope difference significance			Likelihood ratios		
	n	years		n	t statistic	df	p	LR	p
< 1993	29	> 1992	231	0.193	1.415	256	0.158	2.032	0.154
1993-1994	46	> 1994	185	-0.161	1.033	227	0.303	1.235	0.266
1995-2001	45	> 2001	140	-0.017	0.119	181	0.905	0.015	0.902
2002-2004	55	> 2004	85	0.069	0.509	136	0.612	0.270	0.603
2005-2007	47	> 2007	38	-0.140	0.763	81	0.448	0.637	0.425

The estimated power law exponent (slope) for each period is tested against that for the years following that period. The differences in the slopes are tested for significance with t-tests and likelihood ratio tests.

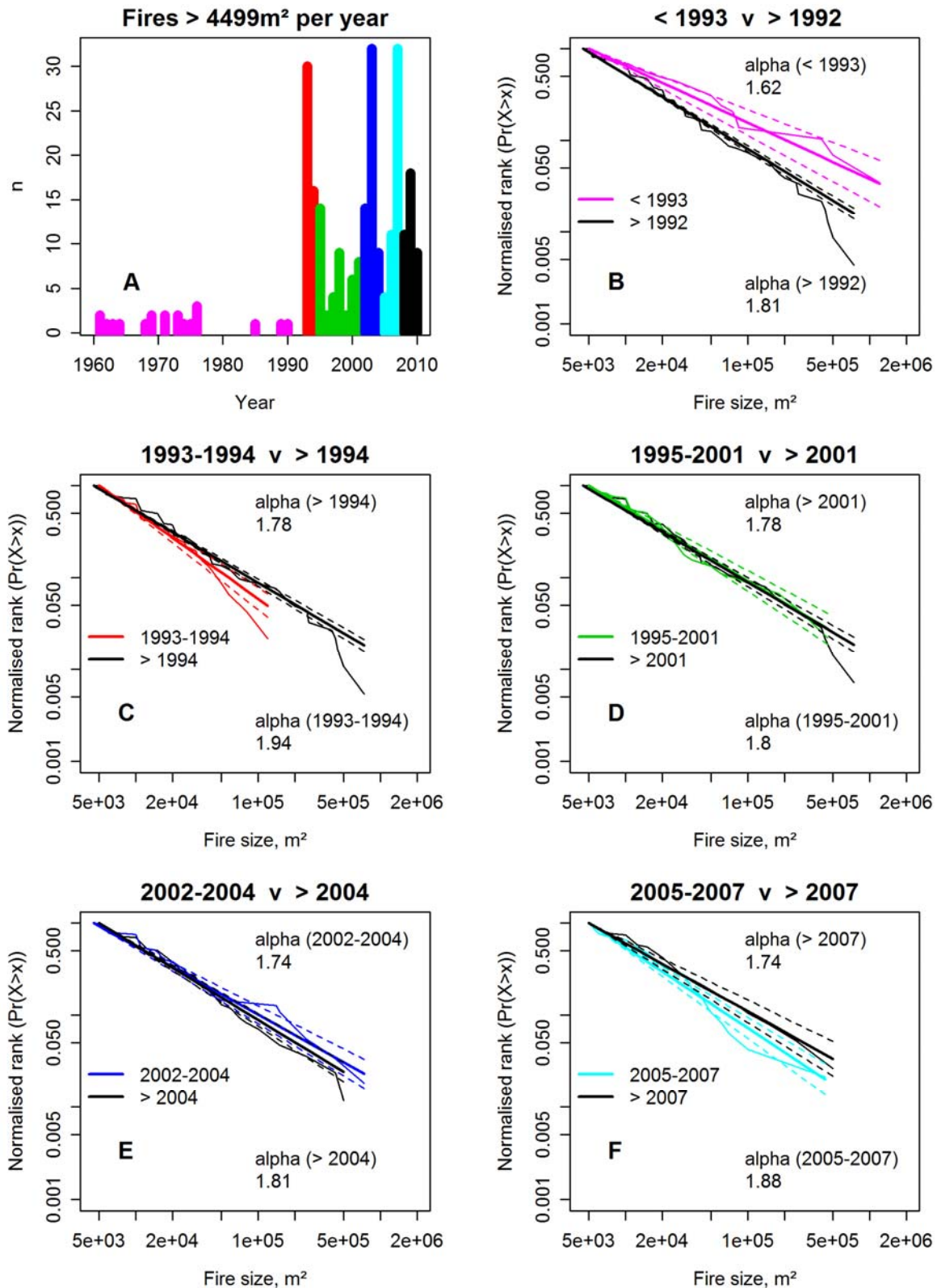


Figure 3 Recorded occurrence and size/frequency relationships of large fires.

Panel 'A' shows the number of fires each year in the database of at least 4500m² (the figure is truncated before 1960 for clarity). Panels 'B' to 'F' show the fire size/frequency relationships for each time period, and for all fires subsequent to that period. 'alpha' denotes the best-fit power law exponent for each curve. Note that in panels 'D', 'E' and 'F', the exponent for the period (in color) is closer to that for the subsequent years than is apparent in panels 'B' and 'C'.

Non-parametric comparisons

In table 3 are the results from the non-parametric bootstrapped KS tests. The p_{KS} values are the probability that a D statistic this high would be attained if the data subsets being compared were drawn from the same distribution.

Table 3 Komolgorov Smirnof statistics for comparing the size/frequency distributions of fires in each time period with that from subsequent periods

	Period 1	< 1993	1993-1994	1995-2001	2002-2004	2005-2007
Size	Period 2	> 1992	> 1994	> 2001	> 2004	> 2007
Large > 4449 m ²	n1	29	46	45	55	47
	n2	231	185	140	85	38
	D	0.185	0.133	0.079	0.080	0.111
	p	~~ 0.342	0.531	0.983 ##	0.983 ##	0.958 ##
Medium > 1000m ² , < 4500m ²	n1	34	21	18	22	25
	n2	102	81	63	41	16
	D	0.500	0.111	0.164	0.125	0.105
	p	~~ 0.000	0.986 ##	0.863 ##	0.978 ##	1.000 ##
Small > 100m ² , < 1001m ²	n1	61	28	32	52	77
	n2	251	223	191	139	62
	D	0.263	0.203	0.252	0.178	0.111
	p	~~ 0.002	~~0.257	~~ 0.062	~~ 0.180	0.791 ##
Tiny < 101m ²	n1	6	28	9	44	91
	n2	298	270	261	217	126
	D		0.674		0.172	0.100
	p		~~0.000		~~ 0.230	0.672

For each size class, the size/frequency distributions are compared using a bootstrapped Komolgorov Smirnof test. Statistics are not reported where less than ten fires occurred in either period.

n1, n2: number of fires in periods one and two

D: Komolgorov Smirnof D statistic

p: p values of the given D statistic. Low p values suggest rejection of the Null hypothesis of equal distributions.

. p values over 0.75

~~ p values under 0.5

DISCUSSION

Results in table 1 suggest that a power law is a poor model for fire size/frequency relationships of the documented fire records in Austria. Clausett et al. (2009) [28] suggest that a p value of 0.1 should be considered a minimum standard, which was achieved only in the pre 1993 period. This poor fit makes it difficult for the parametric t-test and LR test to find significant differences between periods (table 2). Graphically summarising the data as the slopes of best-fit power law relationships (figure 3) is however still a valid method of data exploration, as the line of best fit is rigorously obtained. If a ‘true’ size/frequency model does exist it would plot on these axes with a slight curve, but to the naked eye it would probably be indistinguishable from the straight lines that we show. A valid model however would have smaller standard errors and hence the t-test and LR tests would have greater power to distinguish differences between periods.

For fires in the largest size class (fig 3), two anomalies are apparent. In the pre-1993 period (fig 3b) there appears to be a flatter than normal size/frequency distribution, which is consistent with the thesis that the largest early fires are more likely to appear in the database. The 1993-1994 period (figure 3c) shows an α of 1.94, markedly higher than that across ensuing periods (1.78). This is especially curious considering that this period recorded a particularly high number of large fires in both years (fig 3a). At face value, it seems that this period experienced many fires in the lower end of the $\geq 4500\text{m}^2$ class, but few at the upper end (hence the high α). This however would imply that the size/frequency relationship is extremely non-stationary, which would be at odds with earlier work on the stability of these relationships [16]. The parametric tests in table 1 suggest that this difference is not formally significant, and the KS results in table 2 show that we cannot reject the hypothesis that the current data available from 1993-1994 are drawn from the same distribution as subsequent periods with greater than 53.1% confidence. Nevertheless, it is striking that in each of the three periods after 1994 the p value from the KS test is over 0.95. From 1995 onwards, the size/frequency relationship of large fires in all periods appears to be consistent, with overlapping 90% confidence limits for the estimates of α (fig 3d,e,f).

Referring to table 3 it is clear that in general, the conformity of the data increases as the periods examined are more recent (larger p values towards the right of the table), and as the size class of fires examined increases (larger values towards the top of the table). Fires in the $< 100\text{m}^2$ class showed very little concordance until 2005, and even then the p value is much less than that attained in larger size classes. None of the size classes prior to 1993 show similar distributions to later periods. Fires of up to 1000m^2 show very poor concordance until 2005. This is consistent with the thesis that fire reporting has shown continual improvement, and that underreporting is a greater problem for smaller fires than for larger ones.

The 1993-1994 period is anomalous, in that concordance for fires in the medium class appears good (0.986), but less so for larger fires (0.531). The data for the smallest fires is also clearly not concordant ($p = 1.909 \times 10^{-10}$). Unlike in all other periods, in this smallest size class no fires were recorded of less than 10m^2 (see supplementary figures S1, S2 and S3). There is no apparent physical reason as to why 1993-1994 should have had no fires of less than 10m^2 , very many fires near the lower end of the $\geq 5000\text{m}^2$ class and yet few at the higher end. A highly plausible explanation is that fires of less than 10m^2 have at some stage of the data reporting/recording/transcribing process been mistakenly listed with a size in hectares, rather than m^2 . Unfortunately this is impossible to confirm without access to long-lost original source documents. Although the concordance for medium fires in 1993-1994 is high, the far

lower concordance for larger fires makes the value of the medium fire data moot, as it is unlikely that it would be useful if the larger fire data was discarded.

Our attempt to fit Austrian forest fires to a power law relationship should be considered as a ‘failed hypothesis’. We present the results here both as a convenient means of summarising the data for larger fires in each period (in terms of the best-fit slope on logarithmic axes) and as support for earlier work that has questioned the assumption of power law behaviour [17,23,28]. Although it may be possible to find relationships that provide a better fit, this is beyond the scope of this paper. In any case, an accurate model must be based on accurate data, so a pre-screening of the type we demonstrate here should be a prerequisite. Our non-parametric testing has not conclusively proven data flaws in the 1993-1994 period to scientific standards, but enough suspicion is raised to advise not using this data in applications where the sizes of fires is an important factor. The p value cut off levels we show in the table (0.5 and 0.75) are arbitrary, but may be considered useful as an indication of the confidence we have in the integrity of the data subsets.

Our methods in this paper rely on the assumption of temporal stationarity in the fire size/frequency distribution. Given the relative stationarity of larger fires post 1994, this assumption seems reasonable, and agrees with the findings of Malamud (2005) [16]. It is not impossible that the assumption is flawed, and that physical or anthropogenic reasons for substantial non-stationarity exist. It is notable however that Europe’s most serious summer heatwave in living memory was in 2003, and it seems reasonable that if fire size/frequency distributions were not temporally stable over the past few decades then this is the period where we would expect to see evidence of this. We suggest then that the conservative course is to exclude that data we are not confident in where it may bias the results of future studies.

Where the data is not used to make distinctions regarding trends in fire occurrence or sizes over time, the full database can be used. If it is clear that neither the location, the year of occurrence nor the fire size are important to the conclusions then it is not invalid to consider the database as an effectively random subset of all fires that truly occurred. No inferences regarding temporal trends or patterns can be made, as these may simply be an artefact of the incomplete database. The collection of historical data is however ongoing, and as more sources become available it may be possible to extend the period of data confidence further back in time.

Cloppet and Regimbeau (2011) [31] noted that fire events databases are usually incomplete and inhomogeneous. Their approach to assessing past temporal trends in fire ignition danger in France was to model the danger with the Canadian Fire Weather Index, validating against fires from a recent period. The validated danger model could then be applied to earlier periods, overcoming the likelihood that apparent trends of increasing fire danger were a result of missing data from earlier periods. Arpaci et al. (2012, pers. comm.) test several models against the Austrian database, but exclude very small fires (< 100m²) due to the likelihood that these are not ‘wild’ fires and thus may not have the same dependence on meteorological conditions. Although a fuller reporting of historic fire occurrences would perhaps allow for the construction of a more-skilled model, the strength of the model inter-comparison [31] is not affected by the location or timing of unreported fires.

CONCLUSIONS

We have presented here a novel method of examining historical forest fire records in order to estimate the reliability of records from different time periods. The attempted fit to a power law distribution of the fire size/frequency relationship was very poor, but non-parametric methods were found to be sufficient to raise concerns about using the current database, particularly in earlier time periods and for smaller fires. For applications where historic Austrian fire size data are important, we suggest that based on the current database data for fires of greater than 100m² only be used from 2005 onwards, or data for fires greater than 1000m² from 1995 onwards. Although our analysis is limited to the Austrian forest fire database, the methods we have applied are easily transferable to any environment, and can give indications of where possible flaws may exist in any historic fire dataset.

ACKNOWLEDGEMENTS

The dataset used in this analysis was jointly collated by Dipl.- Ing. Mortimer Müller and Dipl.- Ing. Natalie Arndt of the Institute of Silviculture, University of Natural Resources and Life Sciences, Vienna.

REFERENCES

- [1] Conedera M, Marcozzi M, Jud B, Mandallaz D, Chatelain F et al. (1996) Incendi boschivi al Sud delle Alpi: passato, presente e possibili sviluppi futuri. NRP 31 report. Zurich, vdf Hochschulerverlag and ETH. 143 pp. [in Italian]
- [2] Conedera M (1999) Forest Fires. In: Minor H, editor, Coping study on disaster resilient infrastructure. Zurich, VAW, Laboratory of Hydraulics, Hydrology and Glaciology of the Swiss Federal Institute of Technology. pp 71-76.
- [3] Brown TJ, Hall BL, Mohrle CR, Reinbold HJ (2002) Coarse Assessment of Federal Wildland Fire Occurrence Data. Reno, Desert Research Institute. pp. 31
- [4] Stocks BJ, Mason JA, Todd JB, Bosch EM, Wotto BM et al. (2003) Large forest fires in Canada, 1959-1997. *Journal of Geophysical Research* 108(D1): 5.1-5.12.
- [5] EC (2008) Forest fires in Europe 2007. Report No8. European Commission, Joint Research Centre, Institute for Environment and Sustainability. Ispra, Italy. 80 p.
- [6] Seidl R, Schelhaas M-J, Lexer MJ (2011) Unraveling the drivers of intensifying forest disturbance regimes in Europe. *Global Change Biology* 17(9): 2842-2852.
- [7] Lorz C, Furst C, Galic Z, Matijasic D, Podrazky V et al. (2010): GIS-based Probability Assessment of Natural Hazards in Forested Landscapes of Central and South-Eastern Europe. *Environmental Management*. 46(6): 920-930.
- [8] UN (2002) Forest fires in Europe 1961-1998. *International Forest Fire News* 27: 76-80.
- [9] Podur JJ, Martell DL, Knight K (2002) Statistical quality control analysis of forest fire activity in Canada. *Canadian Journal of Forest Research* 32(2): 195-205.

- [10] Schelhass MJ, Schuck A, Varis S (2003) Database on forest disturbances in Europe (DFDE) – Technical description. European Forest Institute internal report 14, Joensuu, EFI. pp. 44.
- [11] Larjavaara M, Kuuluvainen T, Rita H (2005) Spatial distribution of lightning-ignited forest fires in Finland. *Forest Ecology and Management* 208: 177-188.
- [12] San-Miguel J, Camia A (2009) Forest fires at a glance: Facts, figures and trends in the EU. In: Birot Y, editor. *Living with wildfires: What science can tell us*. Joensuu, European Forest Institute. pp. 11-18.
- [13] Hall JR Jr, Harwood B (1989) The national estimates approach to U.S. fire statistics. *Fire Technology* 25(2): 99-113.
- [14] Kron W, Steuer M, Löw P, Wirtz A (2012) How to deal properly with a natural catastrophe database – analysis of flood losses. *Natural Hazards and Earth System Sciences* 12: 535-550.
- [15] Ricotta C, Avena G, Marchetti M (1999) The flaming sandpile: self-organised criticality and wildfires. *Ecological Modelling* 119: 73-77.
- [16] Malamud BD, Millington JDA, Perry GLW (2005) Characterizing wildfire regimes in the USA. *Proceedings of the National Academy of Sciences* 102(13): 4694-4699.
- [17] Reed WJ, McKelvey KS (2002) Power-law behaviour and parametric models for the size-distribution of forest fires. *Ecological Modelling* 150: 239-254.
- [18] Müller M, Vacik H, Diendorfer G, Arpaci A, Formayer H, Gossow H (2012) Analysis of lightning induced forest fires in Austria. *Theoretical and Applied Climatology*. In press DOI: 10.1007/s00704-012-0653-7.
- [19] Vacik H, Arndt N, Arpaci A, Koch V, Müller M et al. (2011) Characterisation of forest fires in Austria. *Austrian Journal of Forest Science* 128(1): 1-31.
- [20] Clauset A, Young M, Gleditsch KS (2007) On the frequency of severe terrorist events. *Journal of Conflict Resolution* 51(1): 58-88.
- [21] Valsecchi E, Beck A, Comini B, Conedera M, Cvenkel H et al. (2010) The Alpine Forest Fire Warning System (ALP FFIRS) project. In: Viegas DX, editor. *VI International Conference on Forest Fire Research*. p. 9. Online at http://www.alpffirs.eu/index.php?option=com_docman&task=doc_download&gid=239&Itemid
- [22] Vacik H, Gossow H (2011) Forest Fire Research and Management Options in Austria: Lessons Learned from the AFFRI and the ALPFFIRS Networks. In: Borsdorf A, Stötter J, Veulliet E, editors. *Managing Alpine Future II conference*, 21-23 November 2011, Innsbruck, Verlag der Österreichischen Akademie der Wissenschaften. pp 203-211.
- [23] Newman MEJ (2005) Power laws, Pareto distributions and Zipf's law. *Contemporary Physics* 46(5): 323-351.

- [24] Goldstein ML, Morris MA, Yen GG (2004) Problems with fitting to the power-law distribution. *European Physics Journal B* 41: 255-258.
- [25] White EP, Enquist BJ, Green JL (2008) On estimating the exponent of power-law frequency distributions. *Ecology* 88: 905-912.
- [26] Efron B (1987) Better bootstrap confidence intervals. *Journal of the American Statistical Association* 82(397): 171-185.
- [27] R Development Core Team (2008) R: A language and environment for statistical computing. Vienna, R Foundation for Statistical Computing.
- [28] Clauset A, Shalizi CR, Newman MEJ (2009) Power Law distributions in empirical data. *SIAM Review* 51(4): 661-703.
- [29] Sekhon JS (2011) Multivariate and Propensity Score Matching Software with Automated Balance Optimization: The Matching Package for R. *Journal of Statistical Software* 42(7): 1-52.
- [30] Abadie A (2002) Bootstrap tests for distributional treatment effects in instrumental variable models. *Journal of the American Statistical Association* 97(457): 284-292.
- [31] Cloppet E, Regimbeau M (2011) Fire Weather Index: From high-resolution climatology to Climate Change impact study. International Conference on current knowledge of Climate Change Impacts on Agriculture and Forestry in Europe COST-WMO Topolcianky, SK, 3-6 May 2011. Online at. <http://www.shmu.sk/File/akcie/Cloppet%20Emmanuel,%20Impact%20of%20climate%20change%20on%20fire%20weather%20index%20from%20high%20resolution%20climatology%20to%20Climate%20Change%20impact%20study.pdf> Accessed 2012 14 March.
- [32] Eastaugh CS, Arpaci A, Vacik H (2012) A cautionary note regarding comparisons of fire danger indices. *Natural Hazards and Earth System Sciences* in press. doi:10.5194/nhess-12-1-2012

SUPPLEMENTARY FIGURES

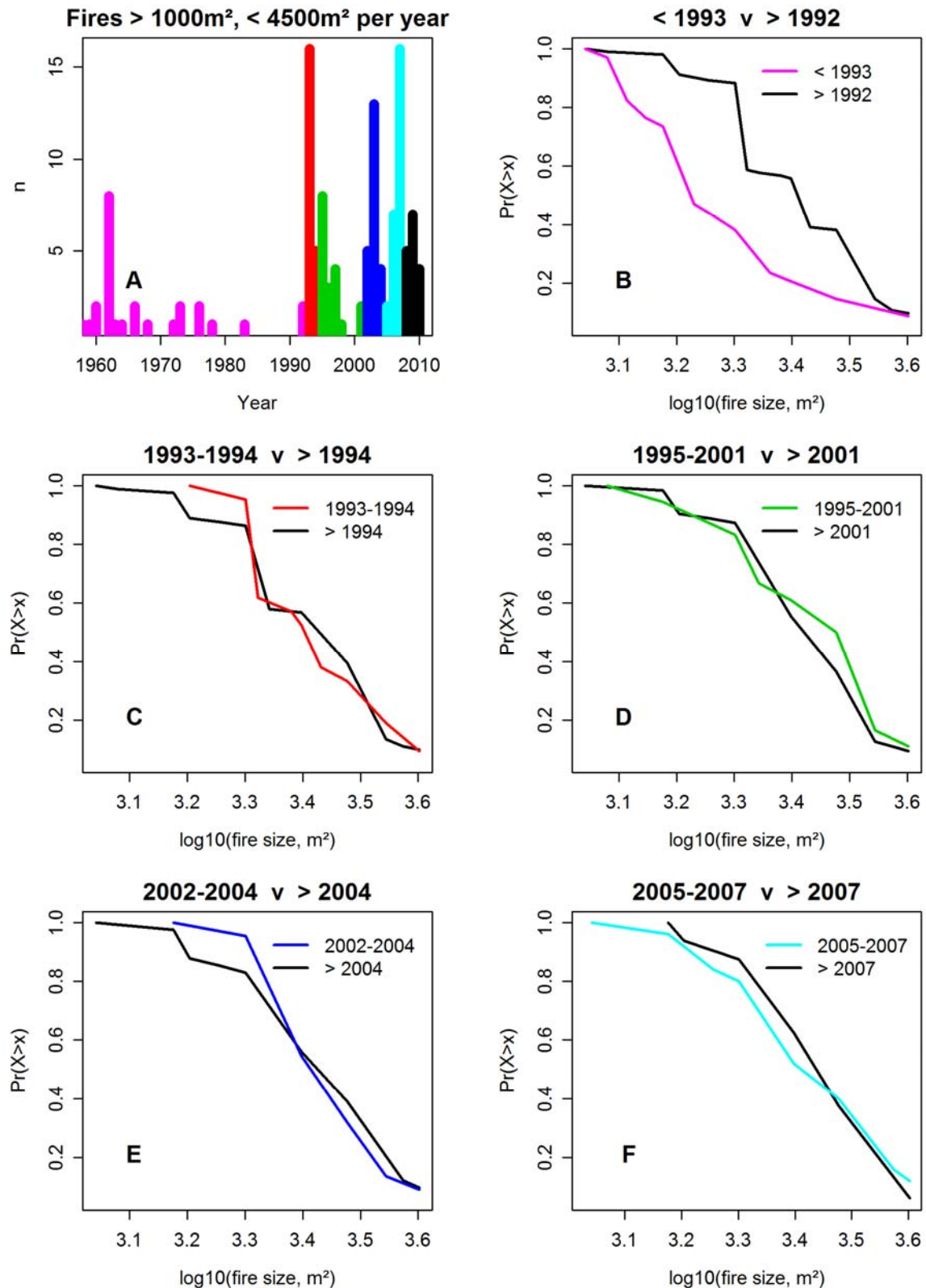


Figure S1 Recorded occurrence and size/frequency relationships of medium fires.

Panel 'A' shows the number of fires each year in the database of 1001 – 4499m² (the figure is truncated before 1960 for clarity). 136 fires are recorded with a size greater than 1000m² and less than 4500m² since 1960. Dividing these into 6 time periods gives between 16 and 34 fires per period, with between 0 and 16 fires recorded per year. Panels 'B' to 'F' show the fire size/frequency relationships for each time period, and for all fires subsequent to that period.

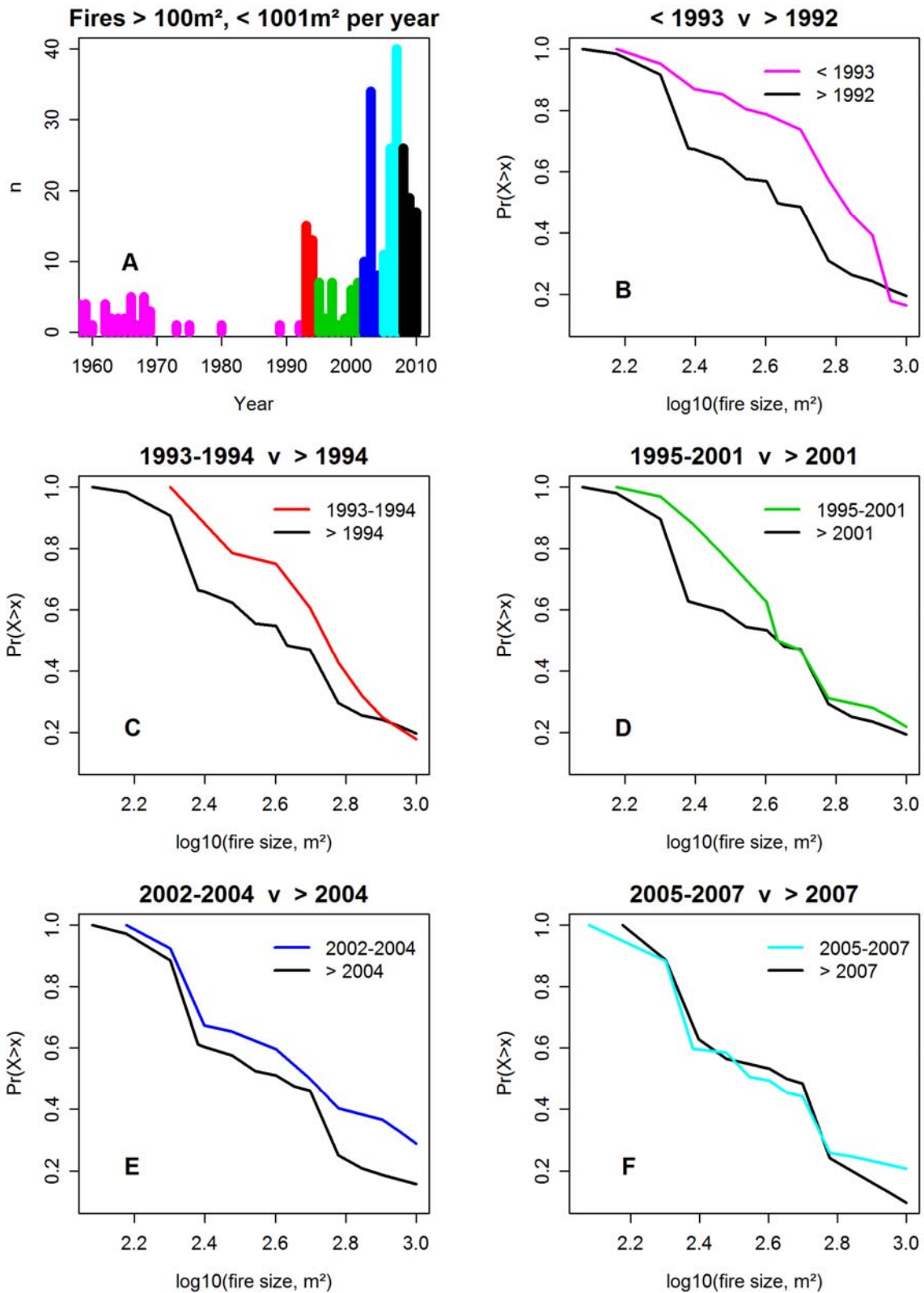


Figure S2 Recorded occurrence and size/frequency relationships of small fires.

Panel 'A' shows the number of fires each year in the database of 101 – 1000m² (the figure is truncated before 1960 for clarity). 312 fires are recorded with a size greater than 100m² and less than 1001m². Dividing these into 6 time periods gives between 32 and 77 fires per period, with between 0 and 40 fires recorded per year. Panels 'B' to 'F' show the fire size/frequency relationships for each time period, and for all fires subsequent to that period.

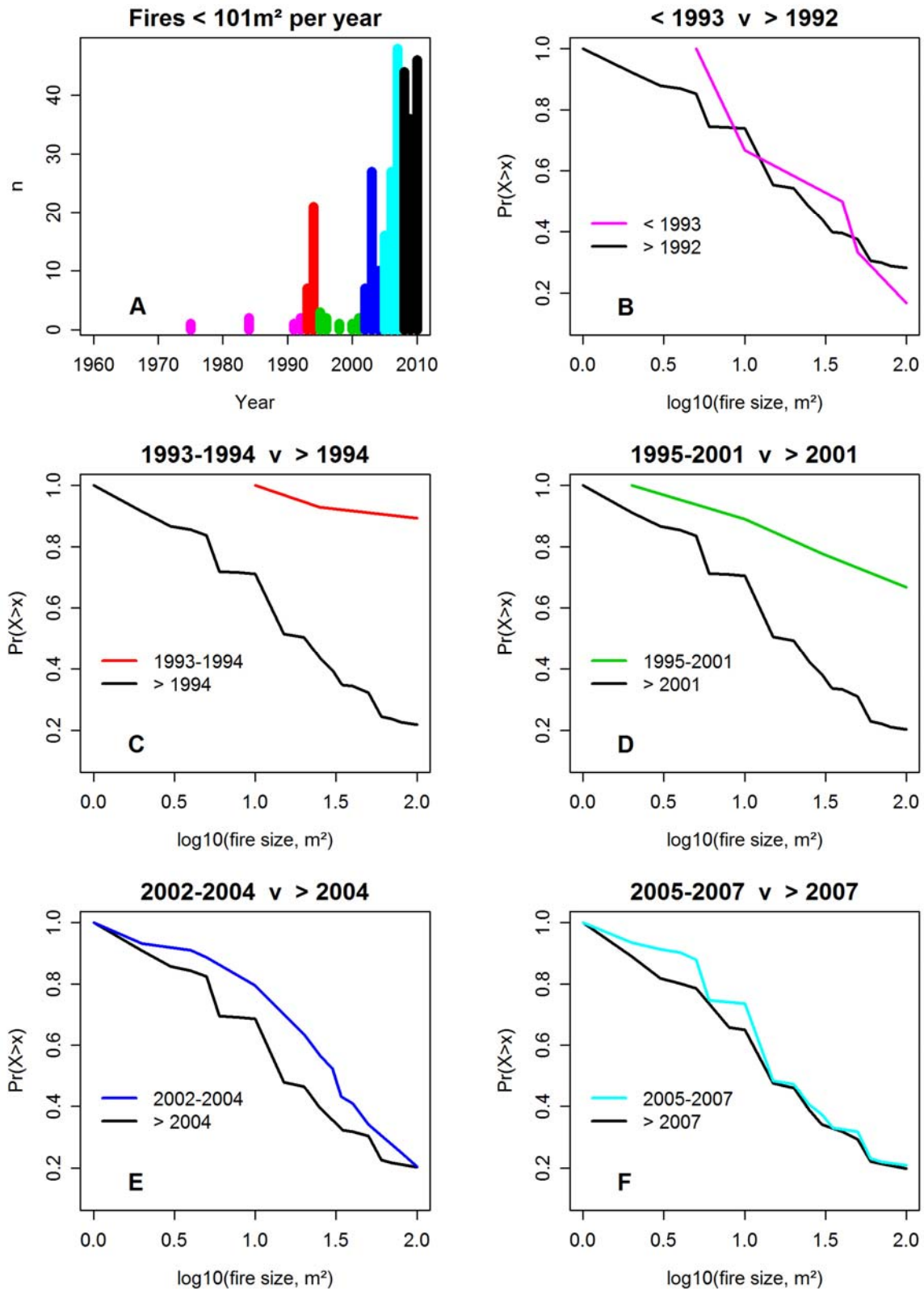


Figure S3 Recorded occurrence and size/frequency relationships of tiny fires.

Panel 'A' shows the number of fires each year in the database of 101 – 1000m² (the figure is truncated before 1960 for clarity). 304 fires are recorded with a size up to 100m². Dividing these into 6 time periods gives between 6 and 126 fires per period, with between 0 and 48 fires recorded per year. Panels 'B' to 'F' show the fire size/frequency relationships for each time period, and for all fires subsequent to that period.



A cautionary note regarding comparisons of fire danger indices

C. S. Eastaugh, A. Arpaci, and H. Vacik

Institute of Silviculture, Universität für Bodenkultur (BOKU), Peter-Jordan Strasse 82, Vienna 1190, Austria

Correspondence to: C. S. Eastaugh (chris.eastaugh@boku.ac.at)

Received: 10 August 2011 – Revised: 10 January 2012 – Accepted: 18 January 2012 – Published: 12 April 2012

Abstract. Over the past decade, several methods have been used to compare the performance of fire danger indices in an effort to find the most appropriate indices for particular regions or circumstances. Various authors have proposed comparators and demonstrated different responses of indices to their tests, but rarely has much effort been put into demonstrating the validity of the comparators themselves. We present a demonstration that many of the published comparators are sensitive to the different frequency distributions, that may be inherent in the performance of the different indices, and outline a non-parametric method that may be useful for future work. We compare four hypothetical fire danger indices, three of which are simple mathematical transformations of each other. The hypothesis tested is that the comparators often used in such studies may indicate spurious performance differences between these indices, which is found to be the case. Non-parametric methods are robust to differences in index value frequency distribution and may allow more valid comparisons of fire danger indices. The new comparison method is shown to have advantages over other non-parametric comparators.

1 Introduction

Recently much effort has been put into finding the “best” fire danger indices for particular regions. Indices with greater skill may allow for more efficient allocation of firefighting resources, more appropriate public warning systems and more precise research studies. Regional differences in index performance may be apparent at relatively small geographical scales (e.g., Padilla and Vega-García, 2011), and it is unlikely that there will ever be a “one size fits all” approach. The United States Forest Service maintains the “FireFamily Plus” computer programme, one component of which can be used to analyse the performance of a range of fire danger indices (Andrews et al., 2003), and similar efforts to systematically compare fire danger index performance are underway

in alpine Europe (e.g., Arpaci et al., 2010a, b). The comparison of fire danger indices is not trivial and the performance of indices must be tested according to high standards. Different indices may be discrete or continuous and may produce data across different ranges or follow different distributions in their frequency of occurrence throughout a year, all of which serves to complicate direct comparisons.

1.1 Fire danger indices

The fire danger indices we are concerned with here are those formed so as to assign some particular value to any day, with (usually) higher values indicating a greater chance of a fire occurring. These indices form the basis of public warning systems and are of increasing interest for fire planning and resource allocation.

A wide variety of indices have been developed, with different mathematical formulations and different input variables. Some of these use only the weather conditions on the days in question, such as the Angström index (I_A), which is dependent only on the relative humidity (R , %) and the temperature (T , °C):

$$I_A = \frac{R}{20} + \frac{29 - T}{10} \quad (1)$$

(note that in this case, lower values indicate higher fire danger).

Other indices also include information from previous days. The Nesterov index (I_N) is constructed using temperature and the dew point (D , °C), summed over the number of days since a rainfall of 3 mm was recorded (W):

$$I_N = \sum_{i=1}^W T_i (T_i - D_i) \quad (2)$$

The set of all daily values from some index over some time period define the “frequency distribution” of that index. Depending on the mathematical formulation of the index and the characteristics of its input variables, these frequency distributions can have markedly different shapes.

1.2 Parametric and non-parametric tests

Parametric statistical tests assume by definition that data follows some particular statistical distribution and are often invalid if those assumptions are not met. Although for some tests these conditions are well known (such as the assumption of a normal distribution in the calculation of t-tests), in complex procedures or statistical software packages the need for the data to meet certain conditions may not be immediately apparent. Consequently, the ensuing results are at best meaningless, or at worst dangerously misleading. Exploratory data analyses should always be performed before applying complex statistical procedures.

Using a simple set of hypothetical indices, we show here that these differences in frequency distributions can introduce spurious results into common index comparison methods. A non-parametric test (not affected by differences in frequency distribution) is introduced which can support comparative studies in future research. Although this paper serves to introduce the new method to the scientific community for further study, our main purpose is to elucidate the shortcomings of methods currently in use and, thus, demonstrate the necessity for the development of more descriptive non-parametric index comparison methods.

1.3 Previous approaches

Over the past decade or so several methods have been proposed to compare fire danger indices. For reasons of space these methods are only briefly described here; readers are asked to refer to the cited papers.

1.3.1 Mahalanobis distance

The Mahalanobis distance is a measure of the distance between two datasets. Viegas et al. (1999) applied this method in southern Europe, beginning by normalising their indices so that all will range from zero to 100. This is done linearly, with the normalised index

$$I'_x = 100(I_x - I_{\min}) / (I_{\max} - I_{\min}) \quad (3)$$

where I'_x is each individual normalised index value,
 I_x is the individual index value at its original scale
 I_{\min} is the minimum value of I_x in the full dataset, and
 I_{\max} is the maximum value of I_x in the full dataset.

The normalised indices are then grouped into ten categories ($I'_x = 0:10, 10:20$ etc.). Viegas et al. (1999, p. 240) recognised the possibility of error being introduced due to using equally spaced class limits, but proceeded due to the simplicity of this approach. After plotting the percentage of days in each class and the percentage of fire-days in each class, they calculated the Mahalanobis Distance (M_d) as a measure of the discrimination of days with higher or lower fire danger. The Mahalanobis Distance is calculated as:

$$M_d = [(X_1 - X_2) / \sigma]^2 \quad (4)$$

where X_1 is the mean index value on fire-days, X_2 is the mean index value on non-fire days and σ is the standard deviation of the index value on all days. A larger Mahalanobis Distance is presumed to represent greater differentiation of fire/nonfire-days. Note also that M_d gives the same result whether raw or normalised index values are used.

1.3.2 Percentile analysis

Andrews et al. (2003) described a “percentile analysis”, where, for a particular index, the index values at the 90th, 50th and 25th percentile are calculated for all days and compared with the corresponding percentile of that index value on fire-days. For example, the 90th percentile of some index across all days may have a value of 80, but when considering only fire-days a value in that index of 80 represents the 75th percentile, a difference of 15. The differences for each of the three given percentiles are summed and represent the shift in the distribution of index values between all days and fire-days. A greater distribution shift is taken to signal a better index. Using the 90th, 50th and 25th percentiles appears to be subjective; selecting a different set of percentiles would give different results.

1.3.3 Logistic regression

As the occurrence or non-occurrence of a fire is a binary event, it may be modelled with a logistic regression. Andrews et al. (2003) also used a logistic regression technique to model the probability of a day at a particular index value being a fire-day or a nonfire-day with the index values as independent variables. The indices are ranked according to the range of the fitted values (with wider ranges, beginning closer to zero being indicative of more sensitive models) and to the fit of the models to the observations using a pseudo R^2 value that they denote R_L^2 . A higher R_L^2 indicates a closer fit of the logistic regression to the observed data.

1.3.4 c-index

Verbesselt et al. (2006) also used a logistic regression model, but judged their models' performances using an adjusted chi-square form of Akaike's Information Criteria (AIC), where AIC_{χ^2} is the model likelihood ratio chi-squared statistic minus two times the degrees of freedom. With this form of the AIC, a higher value indicates better model fit. To represent the “discrimination power” of each model they calculated the “c-index”, which is equal to the area under a receiver operating characteristic (ROC) curve. An ROC curve is a graphical representation of how a model performs with regard to “true” or “false” positive predictions and “true” or “false” negative predictions. For each fire day, the index value is plotted according to its “sensitivity” or “true positives” (the index's ability to correctly determine that a fire might occur

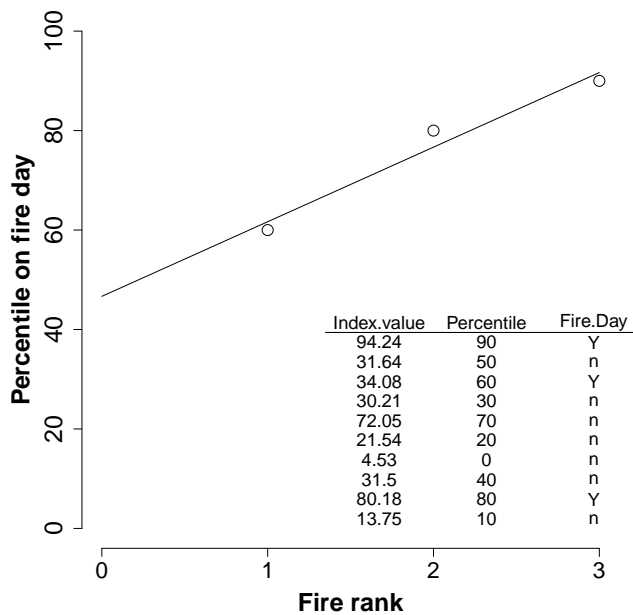


Fig. 1. Example figure for the proposed ranked percentile method of index comparison. Fire danger index values for every day are expressed as percentiles and those percentiles on days when fire occurs are plotted according to rank. The slope and intercept of a robust regression line through these points characterises the index.

at or above that value) and its “specificity” or “false positives” (the index’s propensity for false alarms at or below that value). Fawcett (2006) provides an excellent overview of the concept and notes that the area under the curve is equivalent to a non-parametric Wilcoxon test of ranks (Hanley and McNeil, 1982). A *c*-index of less than 0.5 indicates random predictions, whereas a “perfect” model would have a *c*-index of 1.0.

The *c*-index gives useful non-parametric information, but is not adequate to fully describe differences in the performance of competing indices. Two ROC curves may not be identical, yet have the same area beneath them.

2 Methods

2.1 Proposed new comparator

We present here an outline of a two-part descriptor of fire indices that may help to differentiate performance, based on the slope of the ranked fire-day percentiles and the “*y*” intercept of that slope. The daily values for each index are converted to individual percentiles across the full range of days in the dataset. Those index percentiles for fire-days are ranked from lowest to highest and plotted on the “*y*”-axis, with the “*x*”-axis indicating the rank. Figure 1 provides a small example, with three fires occurring within a timespan of ten days.

Considering that on this plot an index composed of random numbers would have an expected slope of 1.0 and an intercept of zero while a “perfect” index would have a slope

approaching zero and an intercept approaching 100, these two parameters together may usefully describe the performance of fire indices. To reduce the influence of outliers in the data, the slope is calculated with the Theil-Sen technique (Theil, 1950; Sen, 1968), which gives the median of all slopes from all points plotted to all other points. The intercept is the median of all of the possible individual intercepts of that slope, passing through each single point. Although the Theil-Sen method is well established in the hydrological sciences as a means of producing a robust regression (e.g., Granato, 2006), to the best of our knowledge we are the first to suggest that it may be applied in order to characterise a curve of ranked percentiles, and that such a curve can usefully describe the performance of a fire danger index.

2.2 Test and application example

To assess the robustness and usefulness of these index comparison methods, we firstly constructed a set of four hypothetical indices and applied them to a arbitrary year containing 10 fire days. The four hypothetical indices were assessed with the four previously published comparison methods and with our proposed new comparator. This is intended to demonstrate the need for non-parametric techniques.

The greater utility of our ranked-percentile method is shown through a brief application example. Meteorological data was obtained from the weather station in Graz (southern Austria) and used to derive values for the Angström and Nesterov indices for the surrounding region over the period 1978–2008. Twenty-one fires occurred in this time period. This data is a subset of an Austria-wide project examining the performance of 19 different indices including, for example, the Canadian FWI (Van Wagner, 1987), the M68 index (Käse, 1969) and the FMI of Sharples (2009).

Calculations of the hypothetical index values, the Mahalanobis Distance and the percentile scores for the theoretical examples in this paper were made in Excel 2003, and both these and the remaining tests were performed with the R statistical software v.13.1 (R Development Core Team, 2008), using the “glm” model (“binomial” family) to develop the logistic regressions, the “anova” function to derive the model likelihood ratio chi-squared statistic to calculate AIC and functions in the “pROC” package (Robin et al., 2011) to calculate the *c*-index and the “mblm” package for the Theil-Sen statistics. The use of both Excel and R is intended to explore what differences may potentially result from applying the tests under different software frameworks. R and all packages used are available via <http://cran.r-project.org/>. Calculations for the Graz application case are made solely in R.

2.3 Index value generation

Consider a hypothetical fire index (index “A”), that is based simply on the calendar day of a year. The index is formulated as:

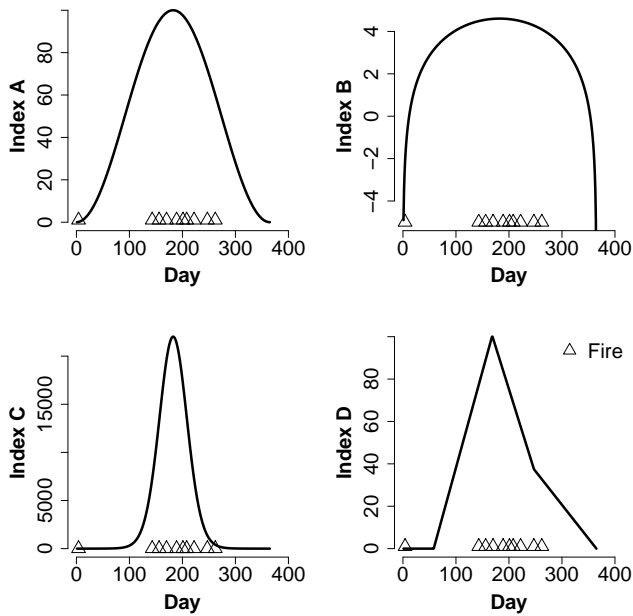


Fig. 2. Hypothetical fire danger index values over the course of one year. Index A is sinusoidal, as defined in Eq. (5) (in text). Indices B and C are respectively logarithmic and exponential transformations of index A, and index D is a discontinuous function described in Equation set 6 (in text). Triangles indicate fire occurrence days.

$$A = \sin\left(\frac{3\pi}{2} + \frac{2d\pi}{365}\right) \times 50 + 50 \quad (5)$$

with d being the day of year and the sin calculated with radians. The index is thus sinusoidal with a period of one year and a range of zero to 100. Two further indices are constructed as transformations of the first, with index “B” = $\ln(A)$ and index “C” = $e^{A/10}$. Finally, index “D” is independent and discontinuous, with:

$$\begin{aligned} D[d = 1 : d = 57] &= 0, \\ D[d = 58 : d = 168] &= (d - 58)/1.1, \\ D[d = 169 : d = 247] &= (294 - d) \times 0.8, \\ D[d = 248 : d = 365] &= (365 - d)/(365/116). \end{aligned} \quad (6)$$

Ten days are arbitrarily selected as “fire occurrence” days, 9 loosely centred around the middle of the year and one outlier. For this example, these are days 4, 143, 156, 170, 189, 201, 208, 222, 247 and 262.

2.4 Index characteristics

Figure 2 displays the daily values of the four indices and the fire occurrence days, while Fig. 3 shows the frequency distributions over all days. Index A values occur mostly at each extreme, while the mathematical transformations applied to create indices B and C causes the distributions to cluster towards one extreme.

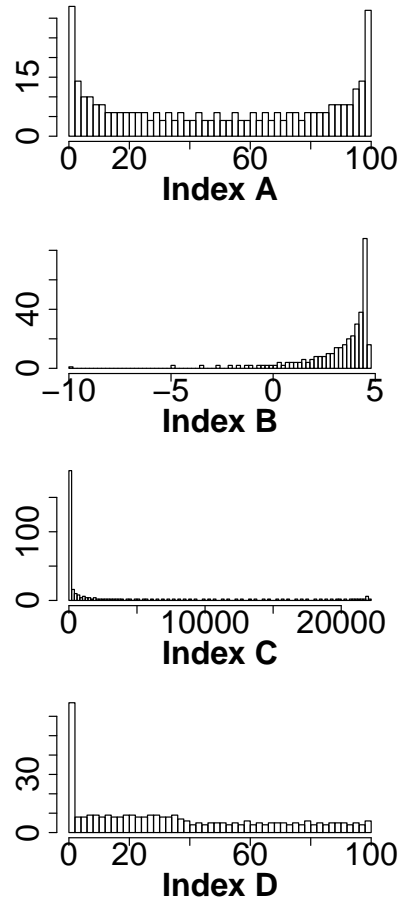


Fig. 3. Frequency distributions of the four hypothetical indices.

As the first three indices are simply mathematical transformations of each other (i.e., ranks are not changed through the transformation), it is reasonable to suppose that any valid method of comparing them should rank each index as equally useful, otherwise the comparison method may be ranking indices differently simply because the index values have different occurrence frequency distributions. This proposition will be tested for a number of different comparators that have been proposed in the literature, following procedures described by Viegas et al. (1999), Andrews et al. (2003) and Verbesselt et al. (2006).

3 Results

3.1 Hypothetical indices

Plotting the percentages of days that record index values in each “normalised” class (Fig. 4a) is sufficient to show that the indices are drawn from markedly different distributions. This should be a warning signal that perhaps parametric methods of index comparison may not be appropriate. Figure 4b is the percentage of days where fires occurred in each class and

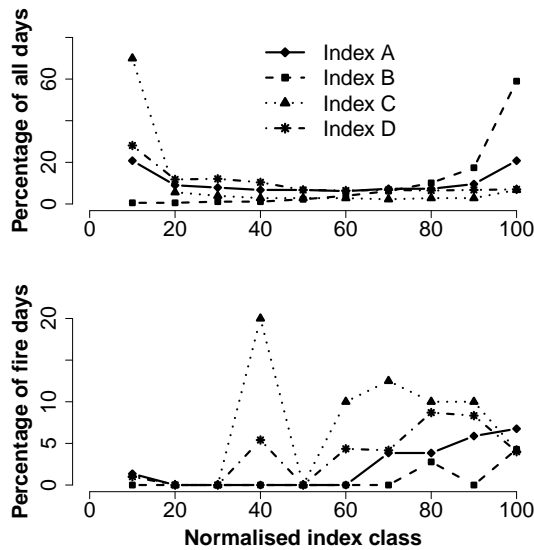


Fig. 4. Characteristics of normalised indices. Top figure shows the percentage of days falling in each index class, while the bottom figure is the percentage of the days in each class that recorded a fire occurrence.

shows little consistency between indices with regard to which “normalised” index class contains the highest proportion of fires.

Results for the Mahalanobis Distance, the percentile analysis, logistic regression statistics and the c-index are given in Table 1, along with the ranks of each index for each comparator. The only comparator that detects that indices A, B and C are effectively identical is the c-index. Also, c-index results are identical whether calculated using raw index values, “normalised” values or fitted values from the logistic regression, because the indicator uses ranks rather than values.

Ranking the fire-day percentiles of each index gives identical results for indices A, B and C, but some differences are apparent to index D (Fig. 5). Index D performs better at the fifth and tenth ranks, but poorer at all others. The Theil-Sen robust regression line summarises the performance difference, with indices A, B and C having a slope of 3.836 and an intercept of 58.90, and index D having a slope of 4.658 and an intercept of 52.60. Index D is, thus, concluded to have less skill than the others, which are of equal worth.

3.2 Application example

The results for the Graz application example are shown in Table 2. The c-index suggests that the indices are identical, while other methods may recommend either. The ranked percentile curves are shown in Fig. 6, demonstrating that the performances of the two indices are in fact different.

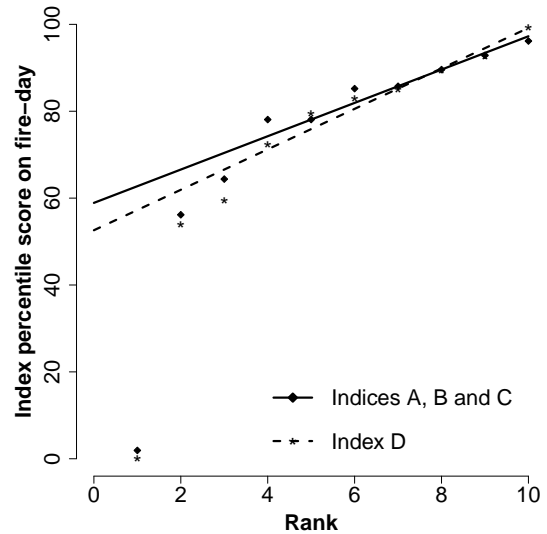


Fig. 5. Robust regression of ranked percentiles.

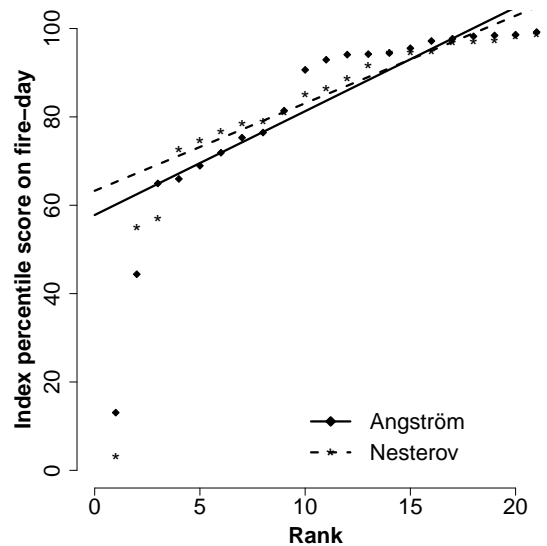


Fig. 6. Ranked percentile curve for the Angström and Nesterov indices, applied to the 21 fires that occurred in the Graz region, 1978–2008.

4 Discussion and conclusions

It has been argued that the transformations applied in our example are a valid means of developing improved indices, on the grounds that it is often necessary to transform input variables in order to better the fit of a function. This, however, is not the same thing as comparing transformed outputs. Figure 7a shows the comparison of indices A and B, on linear axes. A visual appraisal of this figure would suggest that index A is superior to index B, as index A appears to provide better discrimination between fire-days and non-fire days, because index B is commonly quite high on non-fire

Table 1. Comparator values and ranks for each index applied to the 4 hypothetical indices. Md = Mahalanobis distance; R_L^2 = Pseudo R^2 , as per Andrews et al. (2003); AIC = Akaike’s Information Criteria, r = rank. Bold numbers in the rank column indicate the “best” index according to each method

Index	Md ¹		percentiles ²		logistic regression ²					c-index ³		Rank-Percentile ⁴		
	r	Sum delta	r	model range	r	R_L^2	r	AIC	r	r	(slope,intercept)	r		
A	0.740	2	75.25	2	0.004–0.074	3	0.026	1	6.02	1	0.737	2	3.836, 58.90	2
B	0.116	4	67.85	4	0.002–0.037	4	0.008	4	–0.55	4	0.737	2	3.836, 58.90	2
C	0.855	1	83.3	1	0.015–0.109	1	0.016	3	4.32	3	0.737	2	3.836, 58.90	2
D	0.740	4	73.05	3	0.008–0.099	2	0.02	2	4.82	2	0.730	4	4.658, 52.60	4

¹ Viegas et al. (1999); ² Andrews et al. (2003); ³ Verbesselt et al. (2006); ⁴ this study.

Table 2. Comparator values and ranks for each index applied to Angström and Nesterov indices in the Graz area. Bold numbers in the rank column indicate the “best” index according to each method.

Index	Md		percentiles		logistic regression					c-index		Rank-Percentile		
	r	Sum delta	r	model range	r	R_L^2	r	AIC	r	r	(slope,intercept)	r		
Angström	1.053	2	119.92	1	0.000–0.029	2	0.011	1	26.79	1	0.816	1.5	2.350, 57.79	2
Nesterov	1.598	1	95.69	2	0.001–0.090	1	0.005	2	15.94	2	0.816	1.5	1.981, 63.28	1

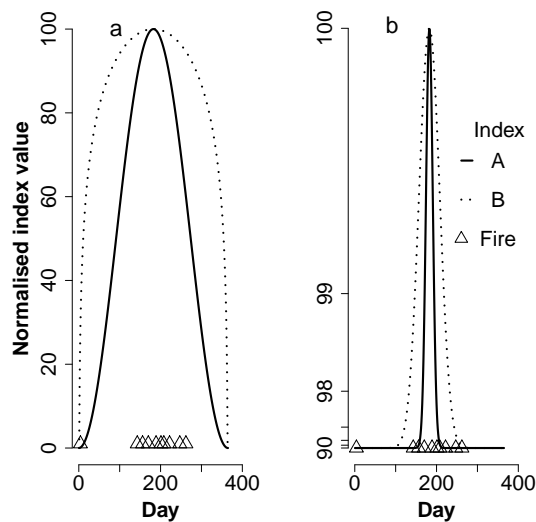


Fig. 7. Hypothetical fire danger index values over the course of one year, on linear (a) and exponential (b) “y”-axes.

days. Consider though, if the y-axes on the plots were displayed on a different scale. Figure 7b shows the identical indices on an exponential scale. The data and the relationship between each index and the day of year is identical to that in Fig. 7a, only the scale of the “y”-axis is changed. Yet now, it “appears” that index B has greater discriminatory power than index A, because index A is commonly low on fire days.

The parametric methods examined in this paper are essentially Euclidean distance-based, in linear space. As pointed out by Wu (2005), there is no a priori reason to suppose that linear scaling is necessarily superior. The differences that some comparators find between the transformed indices are a result of the distribution, just as the appearance in Fig. 7 is the result of the axis scale.

Apart from the c-index, all of the established fire index comparators that we examined here indicate different predictive power between the effectively identical indices A, B and C, suggesting that in many cases the differences they detect are spurious, resulting from the frequency distributions of the index values rather than from any real difference in predictive power.

The percentile analyses method of Andrews et al. (2003) is non-parametric, and should in theory give identical values for indices A, B and C. The large differences we reported for this method are an artefact of the way that Excel interpolates quantiles, strongly suggesting that Excel should not be used in this application. The R “quantile” function offers nine different ways of computing quantiles (see Hyndman and Fan, 1996), but it is unclear which would be appropriate for use within a fire index comparator, or if perhaps different methods should be used for indices with different distributions. Conducting the percentile analysis with all 9 computation methods in R shows that none of them produce simultaneously identical values for indices A, B and C. The problem with the Excel results may also be exacerbated by the low number of fire events in our example, as quantile calculation

methods involve some degree of interpolation between data points. In practical applications (with large numbers of fire-days) this particular shortcoming of the method is unlikely to cause problems if R is used rather than Excel, but may be important where smaller numbers of events (such as “multiple fire-days” or “large fire days”) are of interest. The choice of which quantiles to be compared is somewhat subjective and will sometimes influence the results of the comparisons. In our Graz application example, the percentile analysis method suggests that the Angström index is substantially better than the Nesterov (Table 2). The reason for this is apparent in Fig. 6. The 90th, 50th and 25th percentiles are used for comparison. While at the 50th and 25th percentile the curves for the two indices are at similar points, at the 90th percentile the Angström curve is higher. If the 75th percentile had been used instead of the 90th, the percentile analysis method would have determined the Nesterov to be the better index.

The non-parametric method that we outline appears to avoid some of the shortcomings of parametric methods, correctly determining that the hypothetical indices A, B and C have equal predictive power. The method is in agreement with the c-index, that index D is inferior to the other indices. The proposed method also offers an improvement over the c-index, in that it is able to distinguish differences between fire indices that have identical c-index scores, where such difference is real rather than an artefact of frequency distribution. Our Graz application case was selected to demonstrate this. The c-index for both the Angström and Nesterov indices is 0.816, yet the ranked percentile curves for each index have different characteristics. The higher intercept and flatter slope would lead us to accept the Nesterov as the better index in this application. Although from Fig. 6, we can see that the Angström works well at the very high values (above the 90th percentile), its performance below this level is comparatively poor, with several fires occurring when the index was between its 66th and 76th percentile levels. The Nesterov index for fires at the same ranks was between its 72nd and 79th percentiles. This is immediately clear from the figure, but this pattern is also inferable from the fact the Angström index has a lower intercept and a higher slope than the Nesterov.

Although substantial work remains to be done on determining acceptable methods for comparing fire indices, we have established that commonly used parametric methods may produce potentially spurious results. Our proposed two-part non-parametric comparator is robust to index distribution differences and can provide more useful information than current alternatives. Future investigations will be needed to determine its full worth, including indepth mathematical analyses and application studies over a range of real-world datasets.

Acknowledgements. This research has been conducted partly within the frame of the Austrian Forest Research Initiative (AF-FRI), which is funded by the Austrian Science Fonds (FWF) with the reference number L539-N14 and the European Project ALP FFIRS (Alpine Forest Fire Warning System), which is funded by the European Regional Development fund of the Alpine Space Program with the reference number 15-2-3-IT. We also acknowledge the helpful comments provided by participants at the 2011 European Geosciences Union general assembly, where a précis of this work was presented (Eastaugh et al., 2011). Insightful comments from three anonymous reviewers served to substantially improve the paper.

Edited by: R. Lasaponara

Reviewed by: three anonymous referees

References

- Andrews, P. L., Loftsgaarden, D. O., and Bradshaw, L. S.: Evaluation of fire danger rating indexes using logistic regression and percentile analysis, *Int. J. Wildland Fire*, 12, 213–226, 2003.
- Arpaci, A., Beck, A., Formayer, H., and Vacik, H.: Interpretation of fire weather indices as means for the definition of fire danger levels for different eco-regions in Austria, 6th international conference on Forest Fire Research, Coimbra, Portugal, 15–18 November, 2010, BP12, 2010a.
- Arpaci, A., Vacik, H., Formayer, H., and Beck, A.: A collection of possible Fire Weather Indices (FWI) for alpine landscapes, available at: http://www.alpffirs.eu/index.php?option=com_docman&&task=doc_download&&gid=240&&Itemid=21&&lang=en (last access: 6 March 2012), 2010b.
- Eastaugh, C. S., Arpaci, A., and Vacik, H.: Methods of comparing fire danger indices. European Geosciences Union general assembly, Vienna, Austria, 3–8 April 2011, EGU2011-9470, 2011.
- Fawcett, T.: An introduction to ROC analysis, *Pattern Recogn. Lett.*, 27, 861–874, 2006.
- Granato, G. E.: Kendall-Theil Robust Line (KTRLine – version 1.0) – A visual basic program for calculating and graphing robust nonparametric estimates of linear-regression coefficients between two continuous variables: Techniques and Methods of the US Geological Survey, book 4, chap. A7, 31 pp., 2006.
- Hanley, J. A. and McNeil, B. J.: The meaning and use of the area under a Receiver Operating Characteristic (ROC) curve, *Radiology*, 143, 29–36, 1982.
- Hyndman, R. J., and Fan, Y.: Sample quantiles in statistical packages, *Am. Stat.*, 50, 361–365, 1996.
- Käse, H.: Ein Vorschlag für eine Methode zur Bestimmung und Vorhersage der Waldbrandgefährdung mit Hilfe komplexer Kennziffern, Akademie Verlag, Berlin, 68 pp., 1969.
- Padilla, M. and Vega-García, C.: On the comparative importance of fire danger rating indices and their integration with spatial and temporal variables for predicting daily human-caused fire occurrences in Spain, *Int. J. Wildland Fire*, 20, 46–58, 2011.
- R Development Core Team: R: A language and environment for statistical computing, R Foundation for Statistical Computing, Vienna, Austria, 2008.
- Robin, X., Turck, N., Hainard, A., Tiberti, N., Lisacek, F., Sanchez, J.-C., and Müller, M.: pROC: an open-source package for R and

- S+ to analyze and compare ROC curves, *BMC Bioinformatics*, 12, p. 77, 2011.
- Sen, P. K.: Estimates of Regression Coefficient Based on Kendall's tau, *J. Am. Stat. Assoc.*, 63, 1379–1389, 1968.
- Sharples, J. J., McRae, R. H. D., Weber, R. O., and Gill, A. M.: A simple index for assessing fire danger rating, *Environ. Model. Softw.*, 24, 764–774, 2009.
- Theil, H.: A rank invariant method for linear and polynomial regression analysis, *Nederlandse Akademie van Wetenschappen Proceedings Series A*, 53, 386–392 (Part I), 521–525 (Part II), 1397–1412 (Part III), 1950.
- Van Wagner, C. E.: Development and structure of the Canadian forest fire weather index system, Canadian Forest Service, Ottawa, 48 pp., 1987.
- Verbesselt, J., Jönsson, P., Lhermitte, S., van Aardt, J., and Coppin, P.: Evaluating satellite and climate data-driven indices as fire risk indicators in savanna ecosystems, *IEEE T. Geosci. Remote*, 44, 1622–1632, 2006.
- Viegas, D. X., Bovio, G., Ferreira, A., Nosenzo, A., and Sol, B.: Comparative study of various methods of fire danger evaluation in southern Europe, *Int. J. Wildland Fire*, 9, 235–246, 1999.
- Wu, L.: Automated modeling and nonlinear axis scaling, Ph.D. thesis, School of Computer Science, Carnegie Mellon University, Pittsburgh, USA, 155 pp., 2005.



Research paper: part of a special section on adaptations of forest ecosystems to air pollution and climate change

Assessing the impacts of climate change and nitrogen deposition on Norway spruce (*Picea abies* L. Karst) growth in Austria with BIOME-BGC

Chris S. Eastaugh^{1,2}, Elisabeth Pötzelsberger¹ and Hubert Hasenauer¹

¹Institute of Silviculture, University of Natural Resources and Life Sciences (BOKU), Vienna, Austria; ²Corresponding author (chris.eastaugh@boku.ac.at)

Received October 8, 2010; accepted March 18, 2011; handling Editor Marc Abrams

The aim of this paper is to determine whether a detectable impact of climate change is apparent in Austrian forests. In regions of complex terrain such as most of Austria, climatic trends over the past 50 years show marked geographic variability. As climate is one of the key drivers of forest growth, a comparison of growth characteristics between regions with different trends in temperature and precipitation can give insights into the impact of climatic change on forests. This study uses data from several hundred climate recording stations, interpolated to measurement sites of the Austrian National Forest Inventory (NFI). Austria as a whole shows a warming trend over the past 50 years and little overall change in precipitation. The warming trends, however, vary considerably across certain regions and regional precipitation trends vary widely in both directions, which cancel out on the national scale. These differences allow the delineation of 'climatic change zones' with internally consistent climatic trends that differ from other zones. This study applies the species-specific adaptation of the biogeochemical model BIOME-BGC to Norway spruce (*Picea abies* (L.) Karst) across a range of Austrian climatic change zones, using input data from a number of national databases. The relative influence of extant climate change on forest growth is quantified, and compared with the far greater impact of non-climatic factors. At the national scale, climate change is found to have negligible effect on Norway spruce productivity, due in part to opposing effects at the regional level. The magnitudes of the modeled non-climatic influences on aboveground woody biomass increment increases are consistent with previously reported values of 20–40 kg of added stem carbon sequestration per kilogram of additional nitrogen deposition, while climate responses are of a magnitude difficult to detect in NFI data.

Keywords: biogeochemical modeling, climate zone, nitrogen deposition, regional climate change.

Introduction

Throughout the 1970s many researchers expected a forest growth decline in Europe due to air pollution (European Commission 1994), but from the early 1990s several studies noted an increase in forest growth across Europe and North America (e.g., Kauppi et al. 1992, Spiecker et al. 1996, Myneni et al. 1997, Hasenauer et al. 1999, Spiecker 1999, Boisvenue and Running 2006, McMahon et al. 2010). Increasing temperature was often mentioned as one likely contributing cause. Stand treatments such as increased thinning

intensity or fewer planted trees per unit area may have influenced the growth on a stand level, but do not explain the observed increment increase throughout Austria. In various other parts of the world, changes in climate (temperature and precipitation) and non-climatic factors such as increasing atmospheric CO₂, forest age effects (Schimel et al. 2000, Karnosky 2003, Churkina et al. 2007), increased nitrogen deposition (de Vries et al. 2008, 2009), reduced acid deposition and ozone concentration have been reported as driving productivity changes.

Increases in forest growth rates in Austria were apparent in National Forest Inventory (NFI) results from 1961 to 1990 (Schadauer 1996). The three most likely causal factors in this region are CO₂ fertilization, increasing nitrogen deposition and a possibly improving climate. CO₂ concentration has continuously increased globally (Keeling et al. 1995) and increasing nitrogen deposition rates in Europe have been evident since the early 1960s (Katzensteiner and Glatzel 1997, de Vries et al. 2009). The lengthening of the growing season as a result of warmer temperatures may be responsible for much of the observed growth increase; Hasenauer et al. (1999) reported that a warming climate trend had increased the average annual growing season in Austria by 11 days from 1961 to 1990 and Petritsch and Hasenauer (2009) found that since 1960 Austria has had a statistically significant trend to increasing growing season lengths of 0.34 days per year. The impacts of these factors cannot be individually distinguished with growth measurements alone, but mechanistic modeling offers an option for assessing the relative importance of those that may be expected to be major contributors.

At the national scale, climate change is apparent over Austrian forests from 1960 to 2008. The warming trend implies that the average national temperature has increased by 1.5°C since 1960, but precipitation is little changed (Eastaugh et al. 2010). There are, however, substantial regional differences in climate trends across Austrian forests. Nitrogen deposition has also shown a considerable and regionally variable increase in this period (Schneider 1998, Placer and Schneider 2001).

The mission of this study was to apply the species-specific parameterization of the biogeochemical ecosystem model BIOME-BGC (Thornton et al. 2002, Pietsch et al. 2005) as a diagnostic tool to gain insights into the likely effects of climate change and nitrogen deposition over the past half-century on Austrian Norway spruce (*Picea abies* (L.) Karst) forests, and seeks to explain the observed changes in forest growth increment rates in the Austrian NFI. Norway spruce was selected for this study due to its accounting for >60% of the growing stock in Austrian forests and the fact that it is present across most Austrian ecozones and thus provides a convenient means of studying possible regional differences in climatic impact on forests.

We are specifically interested in examining:

- (1) What changes in Norway spruce productivity are apparent at the national scale in currently available NFI data?
- (2) Are simulation studies a useful tool to separate the effects of climate from other impacting factors?
- (3) Are climate change-driven differences in regional forest growth trends likely to be of a magnitude that can be distinguished from the random error in NFI measurements?

Data

This paper relies on forest growth data from the Austrian NFI. Point-specific climate data are interpolated with the DAYMET algorithms of Thornton et al. (1997), and nitrogen deposition is calculated from Austrian national statistics of Schneider (1998) and Placer and Schneider (2001).

Austrian NFI

The Austrian NFI has been conducted in its modern form since the early 1980s, when a system of permanent plots replaced the earlier, temporary plot sample design. The 2224 tracts in the inventory are each made up of four plots, arranged in a square of sides 200 m. Each plot consists of an angle-count sample with a basal area factor of 4 for trees of >10.5 cm dbh and a fixed area plot of 5 m radius for trees of 5.0–10.4 cm dbh (Gabler and Schadauer 2006). Data made available for this study comprised one plot from each of the 1188 Norway spruce-dominated tracts in Austria.

Inventories are made with staggered timing, where only a percentage of plots are measured in any one year. Inventory measurements covered the periods 1981–85, 1986–90, 1992–96 and 2000–02. On any plot, the intervening increment periods are 5 years for the first inter-measurement period, 6 years for the second and variously 6, 7 or 8 years for the third. This staggered design complicates the comparison with model outputs, as the inventory volume or increment cannot be precisely determined for any single point in time. Our interpretation of the NFI data presumes that the inventory increments represent the period 1981–2002.

Climate data

Daily climate data from 1960 to 2008 covering precipitation and maximum and minimum temperatures were obtained from the Austrian Meteorological Service (ZAMG). In many cases, stations have been moved or do not cover the complete time period, so the precise number of stations available in any particular year varies, with only 93 stations available in 1960 and 270 in 1987 (Hasenauer et al. 2003). Also, many of the stations available in the early period were discontinued at some time and replaced by others. Although a total of ~1200 separate record series are available, in many cases these are of short duration, or represent separate records for similar locations due to minor station moves, instrument replacements, etc. (Petritsch 2008).

The change in station density and location over time complicates trend analysis, as <30 stations are available with consistent daily records over the entire time period of interest (Eastaugh et al. 2010). For this reason, we used the DAYMET interpolation tool (Thornton et al. 1997) to provide a sufficiently large number of consistent daily records to enable regional delineation of climatic regions. Interpolating to the locations of the Austrian NFI plots provided a spatially regular

network of daily climate records covering the entirety of Austria's forested area, while maximizing the use of available measured data.

Nitrogen deposition calculations

In natural ecosystems nitrogen can enter the system from the atmosphere in four different ways: by wet, dry and occult (fog-borne) deposition, and by biological nitrogen fixation. Occult deposition is a very local phenomenon and is not considered here further, while biological fixation is estimated as a constant value of $0.0003 \text{ kg N m}^{-2} \text{ year}^{-1}$.

Wet and dry nitrogen deposition rates for Austria were obtained from two studies conducted by the Austrian Federal Environment Agency (Umweltbundesamt, UBA) using national nitrogen emission and deposition databases. Schneider (1998) developed a method to interpolate wet nitrogen deposition from point measurements of nitrate and ammonium deposition and precipitation, with consideration of elevation dependencies. Dry deposition of the various relevant nitrogen compounds was determined by Placer and Schneider (2001), who interpolated this across Austria based on emission data, emission source, compound-specific dispersion models and land-cover-specific deposition velocities. The annual dry deposition of nitrate, nitrogen dioxide and nitric acid was calculated for 1998, whereas wet deposition was calculated for 1994.

Methods

We analyze the available NFI data for temporal trends in above-ground woody biomass increment, and compare this with a mechanistic ecosystem model simulation. To maximize the possibility of finding a climate signal in the data, we delineate the particular regions that exhibit climate trends from 1960 to 2008 that are substantially different from the national mean. The model is then applied as a diagnostic tool; by repeating the model simulation with a synthetic climate database without climate change, we are able to isolate the impact of climate change on Austrian spruce forests. As other model inputs are kept consistent between the two simulations, the portion of the increase in growth increment not attributable to climate is isolated and compared with the mean increase in nitrogen deposition in each region.

National Forest Inventory

Inventory measurements made with angle counts have high variance, and large numbers of plots must be aggregated to give usefully precise results. This is compounded in the case of increment measurements (Van Deusen et al. 1986). For this reason we aggregate those regions showing similar climate change characteristics, grouping together the substantially warming regions and the regions that show either increasing or decreasing precipitation trends.

Climate variables

The Austrian version of the climate interpolation model DAYMET (Thornton et al. 1997, 2000, Hasenauer et al. 2003) was applied to estimate daily climatic information for all 2224 NFI plots from 1960 to 2008. DAYMET interpolations are generated based on the geographic position, elevation, slope, aspect and angle to the horizon and climate records from several hundred climate stations in Austria and surrounding countries (Petritsch and Hasenauer 2007).

DAYMET interpolates the daily values of precipitation and maximum and minimum temperature based on a truncated Gaussian filter, using observations from surrounding stations within a particular radius. The filter weight is associated with a radial distance from the plot center (the point of interest). The size of the radius depends on the density of stations near the point of interest and on a predefined Gaussian shape parameter. Austrian forest climate development from 1960 to 2008 at the national level is summarized in Figure 1. These results are an annual summary of the daily climate conditions.

Solar radiation and water vapor pressure deficit (VPD) values are derived from daily temperature and precipitation values according to the methods of Thornton et al. (1997), validated for Austria by Hasenauer et al. (2003), and incorporate

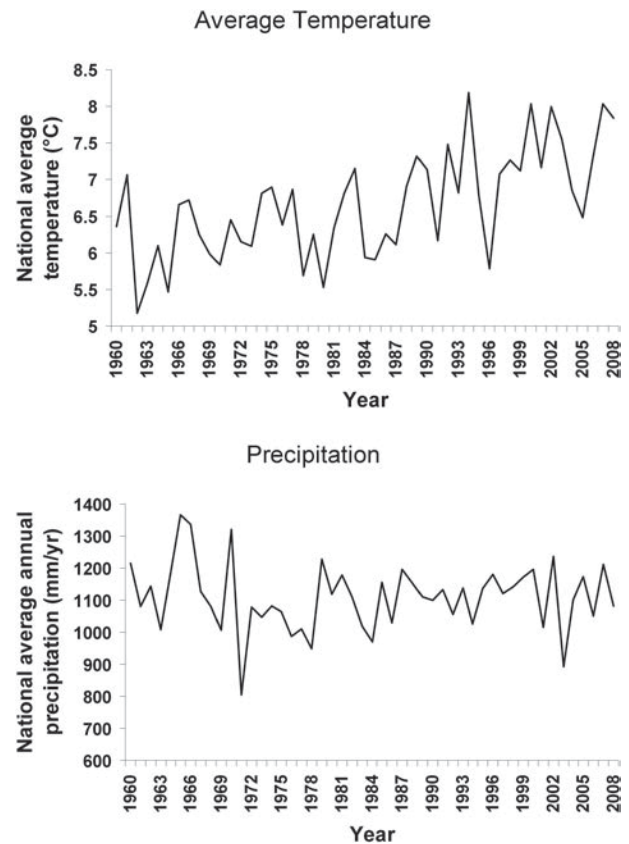


Figure 1. National forest climate trends over the Austrian forest estate (adapted from Eastaugh et al. 2010).

the potential shadowing effect of surrounding mountains and the radiation reflections due to snow pack.

The distributions of the mean trends of the climate on the 2224 sites represented in Figure 1 are approximately normal (Figure 2). Data points falling outside of the ± 1 SD from the mean national trend are geographically clustered, and substantial regional differences are apparent in both temperature and precipitation trends across the Austrian forest estate (Eastaugh et al. 2010). Some regions have warmed substantially more than others, while regional changes in precipitation may be either positive or negative. This allows us to define in this paper 'forest climate change regions', where regional forest growth may potentially be compared with the national mean. We do not suggest that the climate follows a linear development; this methodology is followed purely for the purpose of defining

geographic regions where we could perhaps expect to see more (or less) impact from a changing climate.

A Gaussian kernel smoothing procedure contained in the package 'spatstat' for *R* statistics (Baddeley and Turner 2005, Baddeley 2008) is used to develop relatively smooth (smoothing parameter $K = 0.5$) isolines of forest climate trends for both temperature and precipitation. Using the isolines that correspond to ± 1 SD of the unsmoothed data from the mean, coherent regions may be delineated that exhibit annual or seasonal climate change trends substantially different from the national mean. Figure 3 shows the combined annual and seasonal regions, and Table 1 gives the summary climate statistics (of the unsmoothed data) for each region.

While input data for process modeling should, wherever possible, be site specific, there is still often a need to

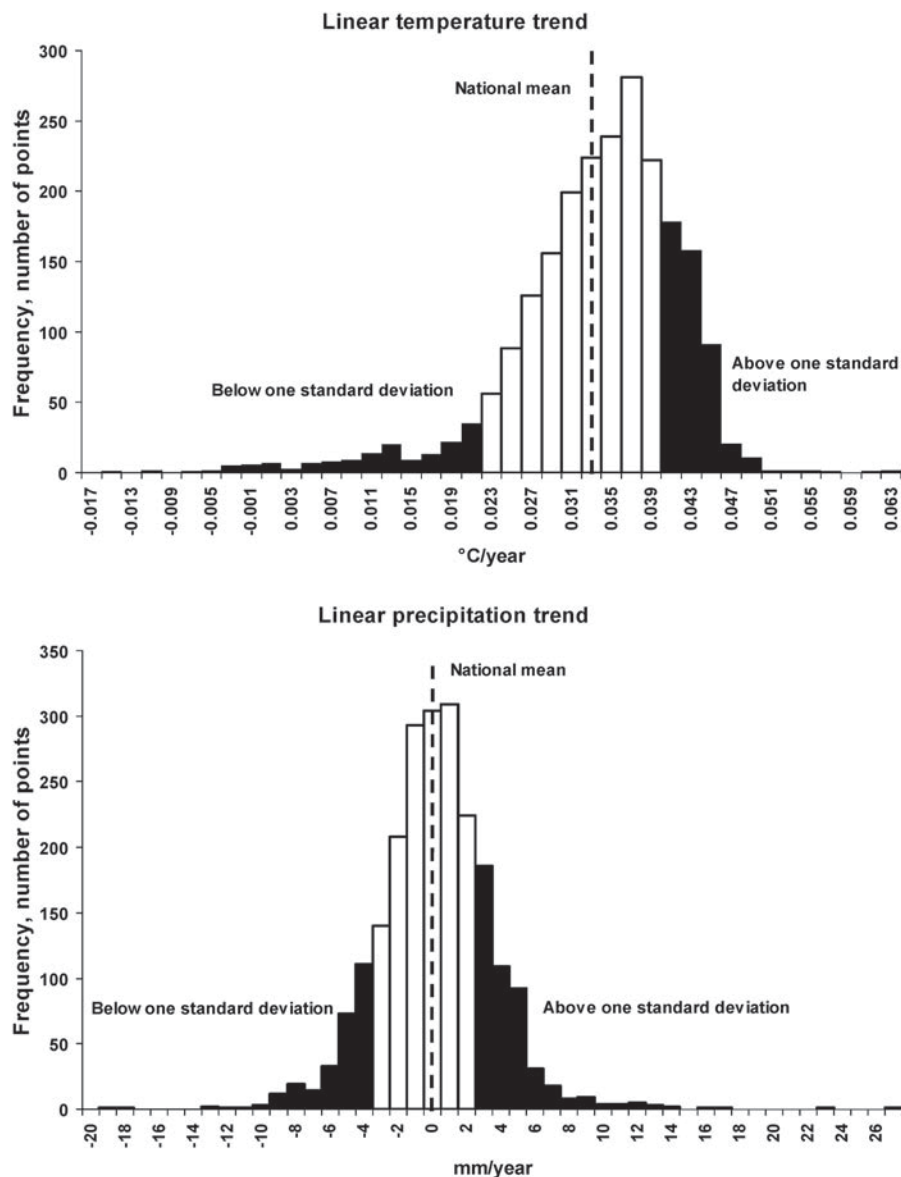


Figure 2. Distribution of linear forest climate trends. Shaded areas are those where the trend differs from the national mean trend by >1 SD.

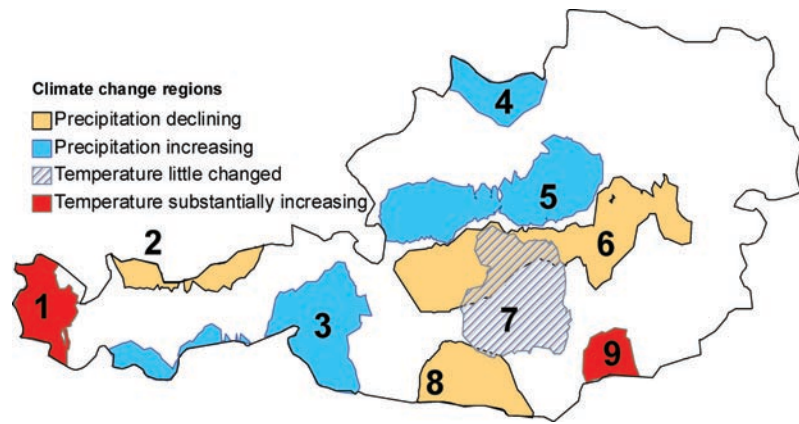


Figure 3. Climate change regions. Colored regions are those showing an average trend in average temperature or precipitation change that is outside ± 1 SD from the national mean trend; white areas are within ± 1 SD for both parameters. The overlap between regions 6 and 7 indicates both substantially less warming and reducing precipitation trends in this area.

Table 1. Summary statistics of forest climate change regions.

Region	Mean elevation (m)	NFI plots (n)/ Norway spruce plots (n)	Average annual temperature				Precipitation			
			Mean ($^{\circ}\text{C}$)	SD	Mean trend ($^{\circ}\text{C year}^{-1}$)	SD of trends	Mean (mm year $^{-1}$)	SD	Mean trend (mm year $^{-1}$)	SD of trends
National	917	2224/1188	6.65	1.86	0.033	0.0086	1109	300	-0.33	3.14
1	989	40/21	6.86	1.40	0.045	0.0074	1614	198	0.75	3.79
2	1209	33/17	5.37	1.03	0.023	0.0045	1341	114	-5.20	1.25
3	1492	83/54	4.35	1.44	0.028	0.0065	1072	215	4.44	2.04
4	728	51/32	6.93	0.96	0.032	0.0021	951	175	3.93	3.48
5	829	211/108	6.94	1.18	0.034	0.0061	1515	360	3.99	3.64
6	1150	298/198	5.42	1.30	0.029	0.0058	1276	186	-4.01	3.21
7	1289	206/141	4.98	1.25	0.016	0.0105	1132	202	-1.00	3.80
8	1069	112/61	6.14	1.76	0.036	0.0048	1125	70	-4.61	0.93
9	955	44/27	6.86	1.83	0.041	0.0020	1129	199	1.3	2.36

aggregate results to obtain meaningful outputs or to compare them with results from other methodologies. Climate regions are based on the full 2224 NFI points rather than just the 1188 spruce-dominated point in order to best represent the 'forest climate' of Austria. This gives a more accurate smoothing, less likely to be influenced by the presence of a few abnormal points. The climate data themselves are not used in this paper as a statistical parameter, but as a means of defining the regions and as an input to the modeling. Our delineation based on climate change trends gives regions that contain between 33 and 298 points (of which 17–198 are dominated by Norway spruce). Aggregating regions with similar trends gives grouping of warming regions (48 spruce plots), less warming (141), increasing precipitation (194) and decreasing precipitation (276). The procedures for defining the forest 'climate change regions' in this paper are somewhat subjective, but are repeatable and designed to produce regions of sufficient size that meaningful aggregation of plot results is possible. Such sub-national regions are a necessary

requisite for detailed studies of forests' responses to climate change (Andreassen et al. 2006).

To separate the impact of climate on forest growth from other impactors, we prepared a synthetic climate database made up of a repeat of the daily climate values for 1960 in all years from 1960 to 2008. The year 1960 does not appear to be an exceptional climate year in any way (Figure 4), and provides a supportable annual climate constant with which to compare the observed climate development.

Although alternative scenario designs are certainly feasible, other possibilities (such as a repetition of 7 years from 1960 to 1966, results not shown) do not show different conclusions. Creating a synthetic climate from mean daily temperatures from the entire time series would have resulted in a 'smoothed' series with less day-to-day variability, while using a detrended version of the total series would have retained the influence of extreme events such as the 2003 heatwave. Our intent here was to use a synthetic baseline that included the natural variability that one would expect, while excluding

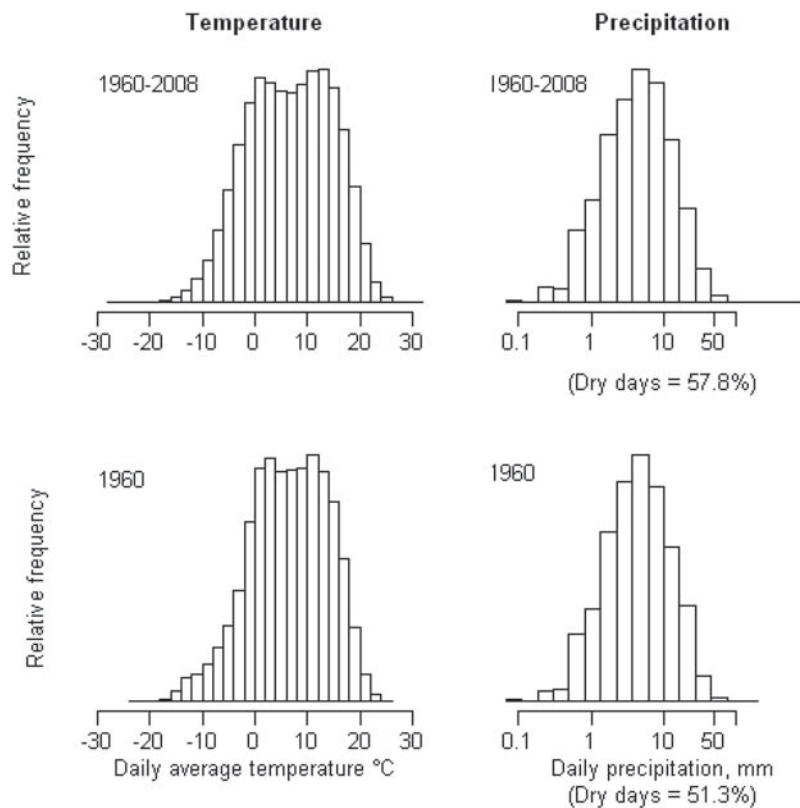


Figure 4. Comparison of 1960 climate with 1960–2008. The figures contain the interpolated daily weather parameters for all 2224 NFI plots. The relative distribution of days in each temperature or precipitation class in 1960 appears similar to the 1960–2008 distribution, in both the mean and the extreme.

the influences of climate change both in the trend and in the extremes.

Nitrogen

The UBA reports little change in NO_x and NH_3 emissions for the last 15 years (Anderl et al. 2009), which allows the assumption that deposition values have stayed relatively constant over that period. Hence, wet deposition from 1994 and dry deposition from 1998 can be summed and a constant total deposition from the mid-1990s onwards assumed for our modeling purposes.

The results of both UBA studies (Schneider 1998, Placer and Schneider 2001) were made available as raster maps covering the whole of Austria. Several processing steps were necessary to obtain the final map of total annual nitrogen deposition. To determine the annual dry deposition of N from NH_3 , NO_2 and HNO_3 , the annual deposition values of the different compounds were multiplied by the weight percentage of N of the respective molecules and summed using the ArcGIS 9.2 Raster calculator. As the resolutions of the wet and dry deposition maps were not identical (respectively 1000×1000 and 250×250 m), the dry deposition raster was resampled in ArcGIS to a one square kilometer resolution map by using the bilinear interpolation resampling technique. This enabled the

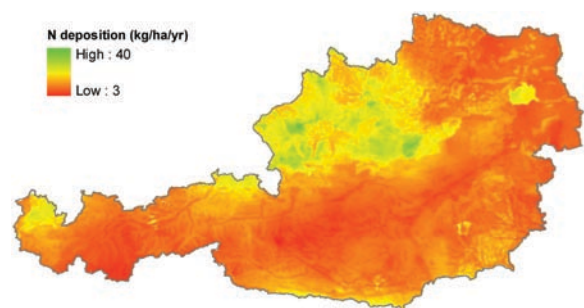


Figure 5. Gridded nitrogen deposition, resampled from Placer and Schneider (2001) and Schneider (1998).

determination of current wet and dry annual nitrogen deposition ($\text{kg N ha}^{-1} \text{ year}^{-1}$) (Figure 5).

The model also requires information on historical nitrogen deposition, which is difficult if not impossible to determine. However, since nitrogen deposition can be considered to be primarily a function of industrialization, we assume that it can be modeled as following the same pattern as the IPCC's IS92a curve for atmospheric CO_2 concentration (IPCC 1992) used in our simulations, starting from a pre-industrial deposition level of $1 \text{ kg N ha}^{-1} \text{ year}^{-1}$ (Holland et al. 1999) to the current levels shown in Figure 5.

Model

For this study we used the model BIOME-BGC Version 4.1.1 (Thornton et al. 2002) with the following extensions: the central European species-specific parameters of Pietsch et al. (2005), and the model self-initialization procedure with improved mortality assumptions of Pietsch and Hasenauer (2006). BIOME-BGC is a mechanistic model developed to simulate the ecosystem processes of a forest stand on a daily time step. The model integrates the main physical, biogeochemical and physiological processes, based on current understanding of key ecophysiological mechanisms. Storage and flux of water, carbon and nitrogen are tracked throughout various pools in the vegetation, litter and soil. The environmental driving forces for the ecological processes in the model are daily meteorological data (described above), site descriptive characteristics and the ecophysiological parameters describing the vegetation at a particular site.

BIOME-BGC allocates carbon and nitrogen ratios to new plant tissues in constant ratios particular to each vegetative pool. The C/N ratio of the total biomass changes with time, as leaves and fine roots enter litter pools and wood accumulates in stems and coarse roots. New growth in the model can only occur if sufficient mineral nitrogen is available to meet the defined C/N ratios, otherwise C assimilation is reduced. Biomass production starts as carbon enters the simulated ecosystem through plant CO₂ uptake via the stomata. Subsequent photosynthetic assimilation is calculated with the Farquhar photosynthesis routine (Farquhar et al. 1980, de Pury and Farquhar 1997), and is limited by temperature and nitrogen availability. Loss of assimilated carbon by autotrophic respiration (growth and maintenance respiration) reduces gross primary production to net primary production (NPP). Reduction of the biomass pools occurs through leaf senescence and litter fall and background mortality, transferring C and N to litter and coarse woody debris pools, or as biomass extraction from the system during thinning and harvest. Plant canopy leaf area index is a function of the carbon allocated to sun and shade leaves, and controls canopy radiation absorption, light transmission to the ground and precipitation interception and also adds litter input to the detrital pools. The model is also sensitive to feedback from mineralization processes. The amount of nitrogen for plant growth coming from the mineralization process is governed by the nitrogen demand of microorganisms (immobilization) and for plant growth. Plant nitrogen demand depends on NPP, whereas microbial demand depends on the amount of biomass available for decomposition (litter and coarse woody debris) and the temperature- and soil moisture-sensitive decomposition rates. Higher temperatures increase photosynthesis but maintenance respiration is also increased, limiting the positive effect of rising temperatures on assimilation. The model also focuses heavily on water input and cycling through the ecosystem. Precipitation is partially intercepted by

the canopy and the residual is input directly to the soil water pool. Depending on climatic conditions, canopy water either evaporates or is added to the soil water pool to represent canopy dripping. Evapotranspiration is calculated with the Penman–Monteith equation as a function of air temperature, air pressure, VPD, incident solar radiation and the transport resistance of water vapor and sensible heat. Precipitation input to the soil water pool can drain as outflow or be stored in the soil water pool, available for evaporative or transpirational loss from the system.

Stand age for each NFI plot was assumed to be the mean age of the trees recorded in the NFI data, weighted according to their proportion of the stand basal area. Geographic latitude and elevation were taken from the NFI data. Albedo values generally differ with the type of vegetation cover; for the Norway spruce forests of this study, an albedo of 0.2 was used. Soil texture and effective depth were interpolated from the Austrian National Forest Soil Survey (Englisch et al. 1992) by Petritsch and Hasenauer (2007) using the Kriging method. Cross-validation within that study produced a mean absolute error of 0.189 m for soil depth and a 12% mean error in the texture proportions. Two sets of ecophysiological parameters for spruce are used, for trees growing above or below elevations of 1000 m. A full description of the 39 species-specific parameters for each altitudinal zone can be found in Tables A6 and A7 of Pietsch et al. (2005). The model theory, its assumptions and methods of parameterization are more fully described by Thornton (1998), Thornton et al. (2002), White et al. (2000) and Pietsch and Hasenauer (2006).

Model application

BIOME-BGC is a fully prognostic model; hence no state variables of the modeled ecosystem need to be measured in the field or estimated to serve as input variables. A self-initialization of the model (the 'spin-up run') is implemented to achieve a dynamic equilibrium of all ecosystem pools, representing an aboriginal ecosystem. At the beginning of the spin-up, the system contains no soil organic matter, a minimal amount of carbon in the leaves (0.001 kg m⁻²) and a soil water saturation of 50%. Climatic inputs for the spin-up period are a repeating cycle of available daily data, in our case the 49 years from 1960 to 2008. Organic matter is accumulated during the ongoing simulation and the spin-up is finished when the running average of the soil carbon content (as the last pool to reach that state) does not change by >0.0005 kg C m⁻² between two successive simulation periods of the length of the weather record. The simulated time this process takes is of the order of 3000 and 60,000 years under different climatic conditions, at different sites and with different vegetation types (Pietsch and Hasenauer 2006).

Early versions of the BIOME-BGC model assumed that tree mortality rate during the spin-up was constant. Pietsch and

Hasenauer (2006) found that this could lead to an overestimation of the ecosystem carbon content by 400% or to imbalances in the soil, necromass and biomass pools. The mortality routine of Pietsch and Hasenauer (2006) assigns a dynamic elliptical mortality pattern to simulate increased mortality at the extreme earliest and latest growth stages. The length of the low and high elliptical mortality for this study was set to respectively 300 and 100 years, with a minimum and maximum annual mortality rate of 0.003 and 0.012%.

The spin-up is followed by simulations of the site history and establishment of the current stand. In central Europe, intensive forest management began several centuries ago, causing shifts in species distribution and degradation of soil nutrient conditions. To account for these changes in the ecosystem, it is necessary to simulate a certain number of successive rotations, assuming the clearcutting and replanting of the forest. With a clearcut, all the aboveground woody biomass is removed and the belowground biomass is transferred to the coarse woody debris compartment. Planting in the model is simulated by adding 0.01 kg m⁻² of carbon to the leaf pool and 0.025 kg m⁻² to the stem pool. Rotation length can be set by the user. Lacking detailed information on the explicit management history of our simulation sites, we use a consistent historical land use routine, assuming two rotations of Norway spruce on a rotation length of 120 years, before the establishment of the current stand.

Current management of the forest must also be considered, otherwise continuously fully stocked stands are assumed and simulated, a misrepresentation of managed forests. As the full management history of a plot is rarely available, thinning was determined according to the expert interview-based assumptions of Petritsch (2008), whereby stands are assumed to have been thinned by ~30% of stand volume at 40 years, followed by further minor removals each 30 years thereafter. 'Thinning' in the modeled sense also includes other possible removals from the biomass pools, not necessarily deliberate intervention for stand management purposes. Other methods of estimating historic management have been proposed (i.e., Eastaugh and Hasenauer 2010), but these are still in development and have not yet been adequately validated. The respective percentages of leaves and fine roots are left in the forest and are added to the litter pool, while the coarse roots are assigned to the coarse woody debris pool. A certain minimum degree of 'thinning' is required by the model to reflect the reduced natural mortality rates in managed forests (Pietsch and Hasenauer 2006).

The model is applied here with the generic assumptions described above, and is not especially calibrated for this study. Results are reported here in terms of aboveground woody biomass accumulation, being the sum of live-stem and dead-stem carbon, with an assumed carbon content in biomass of 49%.

Analysis and results

National Forest Inventory

At the national scale, clear increases in forest increment rates are apparent between the four inventories. The first inter-inventory period showed an increment of 5606 kg of aboveground woody biomass per hectare per year, the second 6300 and the third 6789. Although not a rigorous validation, the comparison of model outputs with NFI records shows that the model is consistent in both the magnitude of the increment nationally and in each aggregation of regions, and in the relative trends of the increment increases (Figure 6). Paired two-tailed 't'-tests show that the NFI increment results for each inter-measurement period are significant at $\alpha = 0.05$, $P < 0.0001$ for the national mean and the region without substantially different climate change trends to the national mean (region '0'), but only significant at $\alpha = 0.05$, $P < 0.01$ in the amalgamated 'wetting' regions and not significant in other amalgamated regions.

Climate impact

Modeling with BIOME-BGC shows a clear rising trend in aboveground woody biomass increment from 1960 to 2008. However, if the simulation is repeated with the climate input held annually stable with 1960 conditions, the acceleration in modeled growth increment is almost identical (Figure 7).

Both the real and synthetic climate-based simulations show a cyclic effect with a period of 10 years. This is probably an artifact due to our estimation of stand age from the first modern NFI period (1981–86), which gives tree age estimates in increments of 20 years, and the fact that our assumed prior management occurs at stand ages 40, 70, 100 or 130. All management interventions are thus assumed to occur in the early years of a decade. Calculating modeled productivity trends over short periods would have a high error, strongly influenced by the start and end times of the calculation. For this reason we present the productivity increase as a linear approximation of the 49-year trend, which appears to be supportable given the increment patterns apparent in Figure 7.

The similarity between simulated forest productivity with or without climate change suggests two possibilities: that extant climate change has had an imperceptible effect on Austrian forests and the rise in productivity is exclusively due to other factors, or that aggregating the productivity trends over the national scale is masking important regional differences. Separating trends into the regions delineated in Figure 4 shows that clear differences are apparent in modeled forest productivity trends at a sub-national scale, between regions that show different temperature and precipitation trends. This increase is represented by the upper extent of the columns in Figure 8.

All regions experience increasing modeled growth rates, but the rate of growth acceleration is not clearly correlated with trends in regional climate as other, non-climatic, factors also

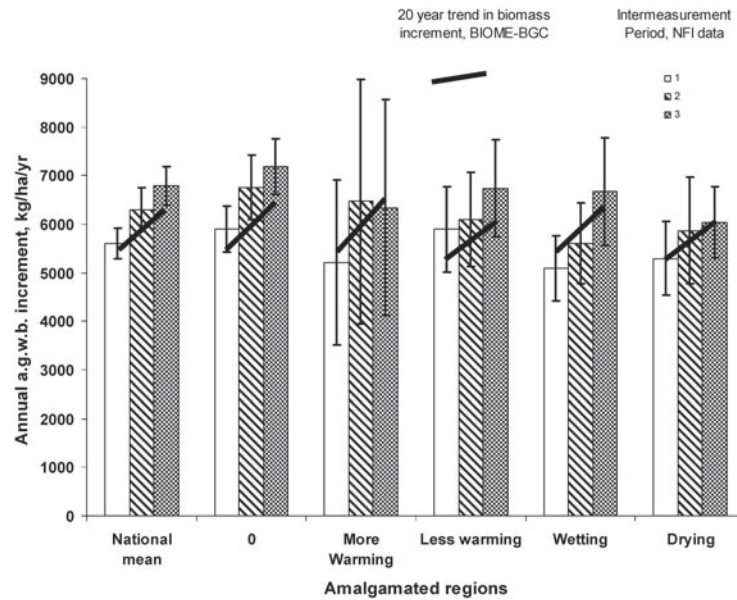


Figure 6. National Forest Inventory validation. Columns show the aboveground woody biomass (a.g.w.b.) increment for the three available intermeasurement periods from the Austrian rolling inventory, with 95% confidence limits. The four inventories were conducted from 1981 to 1985, 1986 to 1990, 1992 to 1996 and 2000 to 2002. Heavy diagonal lines show the linearized increment trends predicted by BIOME-BGC, scaled from 1981 to 2002.

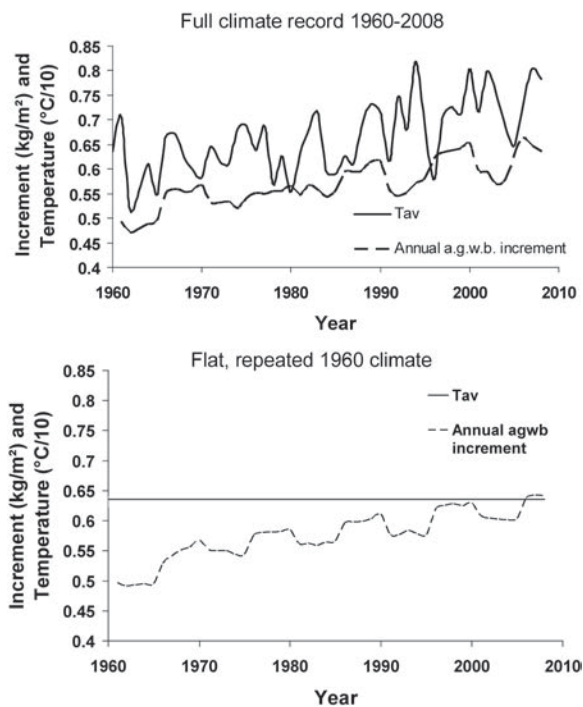


Figure 7. Growth increment development with or without climate change. The cyclic effect appears to be due to the management assumptions used in the simulation.

have a substantial impact. Comparison of the modeled rates of growth increase between the two simulation runs (with or without climate change) allows the impact of climate to be separated from other factors (such as CO_2 , nitrogen or stand age)

that were held consistent between the two runs. With the increment increases calculated both with and without climate change for each region, that part of the increase attributable to climate change can be determined and is represented in Figure 8 as the solid portions of the columns. The checked portions are therefore due to other factors. At the national scale the climatic effects accelerate increment by 0.45×10^{-3} kg of aboveground woody biomass per m^2 per year², compared with a non-climatic influence of 5.22×10^{-3} kg, which means that, nationally, climate change accounts for <8% of the modeled increase in forest growth. Regionally however, this may range from -30% to +34% of the total modeled increase.

Nitrogen impact

An examination of the non-climatic growth acceleration effect against the increase in nitrogen deposition since 1960 (Figure 9) produces results that correspond well with the published literature reviewed by de Vries et al. (2009), who suggested a mean response of around 25 kg of carbon/kg of added nitrogen (kg C/kg N). Note that the values in Figure 9 relate to the mean annual increase in nitrogen deposition rates and aboveground woody biomass increment, for a response of 44.0 kg biomass/kg N or, assuming a carbon content in biomass of 49%, 21.6 kg C/kg N.

Discussion

The increase in Norway spruce growth rates in Austria since the early 1980s shown in Figure 6 is substantial, and statistically

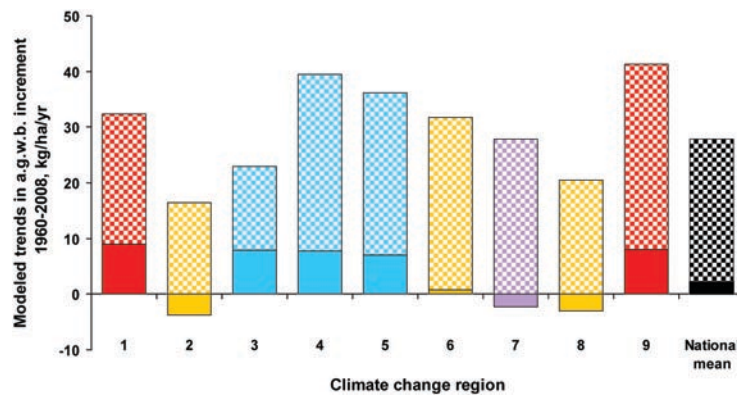


Figure 8. Separation of modeled climatic and non-climatic influences. The upper extents of the columns represent the mean annual increases in aboveground woody biomass increment rate per year from 1960 to 2008. The total height of each column is the modeled increase in increment rates under observed climate conditions. The solid portions of each column represent the influence of climate (the difference between the simulation results with or without climate change), while the checked portions of each column are the increases in increment rates that are common to both simulations and are thus driven by other impactors. Colors and numbering are consistent with Figure 3.

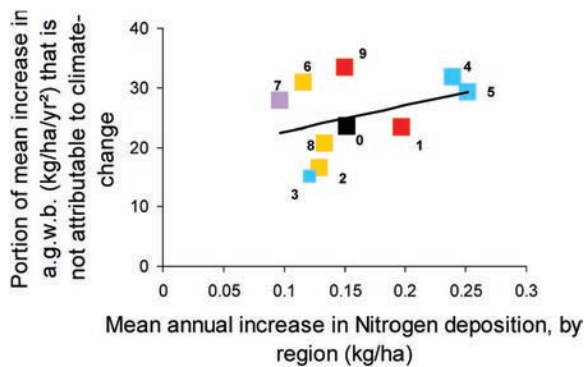


Figure 9. Correlation of the non-climatic portion of increasing increments in aboveground woody biomass (a.g.w.b.) with increasing nitrogen deposition from 1960 to 2008. The points represent each climate change region; colors and numbering are consistent with Figures 3 and 8. A least-squares regression suggests $y = 44.16x + 18.17$, $R^2 = 0.134$.

significant at the national scale. While this increase is apparent in all of our defined climate change regions, statistical significance is lost due to the lower number of data points. Providing a rigorous statistical analysis of the results finally presented in this paper is difficult (due to the multiple effects of model input uncertainty, model process uncertainty, NFI increment random error and the effect of defining regions through smoothed data), but the results suggest that regional climate influences may be detectable through future fieldwork, and may aid in the design of inventory data aggregation procedures and dendrological surveys to definitively confirm or otherwise the modeling results. While it may be possible mathematically to produce statistics regarding the strength of the model/NFI comparison or the significance of regional differences found in this study, it is difficult to see how these could be made meaningful given

the range of assumptions and random error likely to be found in both the model and the data.

Although Figure 7 shows that at a national level the impact of climate change on the growth of Norway spruce in Austria over the past half-century appears to be small, modeling suggests that this is due to a balancing effect of regionally positive and negative impacts rather than to a lack of ecosystem response. In all regions, however, the non-climatic positive influences on Norway spruce growth greatly outweigh the climatic effects. Laubhann et al.'s (2009) multivariate analysis found a non-significant influence of the warming climate on 152 Norway spruce plots across Europe, but suggested that this may have been due to temperature changes in their statistical model being reflected in the 'C/N ratio' variable rather than as a directly significant variable itself. Solberg et al. (2009) also find a positive influence of increasing temperature and reduced drought on spruce growth in Europe, but were hampered by uncertainty in the precipitation input to their statistical model and the positive correlation between warming temperatures and nitrogen deposition in central Europe. Our results for precipitation impacts may be similarly affected, with some of the highest nitrogen deposition rates in Austria occurring in regions that also show a substantial increase in precipitation (Figure 9).

Our comparison of forest productivity under both the real and the simulated 'no climate change' scenario in Figure 8 allows us to calculate a model-based estimate of the temperature changes at the regional scale: our 'warming' regions show an increasing temperature trend ~ 0.027 °C year⁻¹ greater than the 'less warming' region and the BIOME-BGC outputs suggest that increases in average temperature contribute an acceleration of increment rates of 11 kg of aboveground woody biomass ha⁻¹ year⁻². This translates to a warming influence on biomass increment of ~ 410 kg ha⁻¹ year⁻¹, or 6–8% per °C.

This is considerably less than Solberg et al.'s (2009) 2–4% per 0.1 °C, although Solberg et al. (2009) note the impact of multicollinearity between temperature increases and nitrogen deposition on their methodology and comment that their estimate 'seems high'.

Temperature regulates the speed of many physicochemical and physiological processes. A rising temperature acts to increase photosynthesis in various ways, e.g., by increasing the activity of the enzyme RubisCO, the kinetic constants for RubisCO carboxylation and oxygenation reactions (Woodrow and Berry 1988), and the leaf boundary layer and stomatal conductances (Jones 1992). On the other hand, maintenance respiration is also increased (Ryan 1991), limiting the positive effect of rising temperatures on assimilation. Changes in forest productivity due to precipitation trends could speculatively be attributed to changes in plant water stress levels, or less directly through effects on nitrogen mineralization. The regional concurrence of increasing precipitation with the greatest regional increase in nitrogen deposition, however, makes it difficult to draw firm conclusions regarding precipitation trend effects in this study.

Carbon assimilation can only take place when sufficient nitrogen is available in the system. Temperature and soil moisture positively influence mineralization (Lloyd and Taylor 1994, Thornton 1998) and thus the amount of nitrogen available for plant growth. The response of 44.0 kg extra aboveground woody biomass per year² per kilogram of extra nitrogen per year² found here (Figure 9) translates to ~22 kg of extra aboveground carbon per kilogram of extra nitrogen. Although the strength of the correlation is poor ($R^2 = 0.134$), this estimate compares well with de Vries et al.'s (2006) C/N ratio-based European estimates of 25 kg C/kg N and de Vries et al.'s (2008) 20–40 kg C/kg N obtained using a multivariate regression analysis. Solberg et al. (2009) and Laubhann et al. (2009) determined 19 and 21–26 kg C/kg N, respectively, from Europe-wide empirical modeling, while Wamelink et al. (2009) obtained an estimate of 20–30 kg C/kg N for Netherlands forests using a mechanistic model with a yearly time step. Our estimates are somewhat lower than Reay et al.'s (2008) 'expected lower limit' of 40 kg C/kg N for northern forests, Thomas et al.'s (2010) inventory/empirical estimate of 61 kg C/kg N in the eastern USA or Magnani et al.'s (2007, 2008) 175–225 kg C/kg N for northern hemisphere temperate and boreal forests. In addition, our model does not yet consider critical deposition levels/critical loads (UBA 1996) above which greater nitrogen deposition can lead to soil acidification, nutrient imbalances and eutrophication (Nilsson 1986). Overestimations of the positive effects of nitrogen deposition are therefore possible in some areas.

Nitrogen deposition, however, does not explain all of the non-climatic increase in growth. A further increase of around 18 kg of biomass year⁻² is unexplained by either climate

changes or increased nitrogen deposition. Speculatively, this could be attributed to forest age effects or (assumed spatially constant) atmospheric CO₂ increases, but to separate these other potential responses would require further specifically targeted studies.

Conclusions

At the national scale, the increase in Norway spruce productivity in Austria of >20% in the 15–20 years since the early 1980s is statistically significant. This increase, however, appears to be primarily due to increasing nitrogen deposition rather than climate change. Using the BIOME-BGC model as a diagnostic tool allowed us to compare increases in forest productivity under the observed changing climate of the past half-century with a hypothetical case where such change had not occurred, thus separating the effect of climate change from that of other impacting factors. The results show that forest responses are regionally predictable in sign, with warming regions or those with increasing precipitation being expected to show a greater acceleration in productivity than those in drying regions or regions with little warming, contingent on other influences.

Climate change is found to have negligible effect on modeled spruce productivity at the national scale, due in part to opposing effects at the regional level. All regions show accelerating productivity over the period, which suggests that influences other than climate are the major drivers of the effect. This effect is, however, difficult to demonstrate in field data, due to the high degree of random error in inventory increment data. We cannot conclusively attribute increased productivity to nitrogen deposition in this paper, but the non-climatic response found here is consistent with prior work on climate change and nitrogen deposition impacts on forest growth based on different methodologies, and support the thesis that increasing nitrogen deposition has been the major driver of observed increases in forest growth in central Europe.

Acknowledgments

Inventory data for this study were generously supplied by the Österreichische Waldinventur (ÖWI) department of the Bundesamt für Wald (BFW), Vienna. For provision of the nitrogen deposition data, we would like to thank the UBA. We are grateful to the International Union of Forest Research Organizations for the opportunity to present this work at the 24th IUFRO Conference for Specialists in Air Pollution and Climate Change Effects on Forest Ecosystems: Adaptation of Forest Ecosystems to Air Pollution and Climate Change, Antalya, Turkey, March 2010, and to the conference participants who gave much welcome feedback.

Funding

This research has been conducted partly within the frame of the Austrian Forest Research Initiative (AFFRI), which is funded by the Austrian Science Fund (FWF) with the reference number L539-N14, and the European Project ALP FFIRS (Alpine Forest Fire Warning System), which is funded by the European Regional Development Fund of the Alpine Space Program with the reference number 15-2-3-IT.

References

- Anderl, M., T. Köther, B. Muik, K. Pazdernik, S. Poupa and B. Schodl. 2009. Austria's annual air emission inventory 1990–2008. Umweltbundesamt GmbH, Vienna, 39 p.
- Andreassen, K., S. Solberg, O.E. Tveito and S.F. Lystad. 2006. Regional differences in climatic responses of Norway spruce (*Picea abies* L. Karst) growth in Norway. *For. Ecol. Manage.* 222:211–221.
- Baddeley, A. 2008. Analysing spatial point patterns in R. Commonwealth Scientific and Industrial Research Organisation, Sydney. <http://www.csiro.au/resources/Spatial-Point-Patterns-in-R.html>, accessed 21 January 2011.
- Baddeley, A. and R. Turner. 2005. Spatstat: an R package for analyzing spatial point patterns. *J. Stat. Softw.* 12:1–42.
- Boisvenue, C. and S.W. Running. 2006. Impacts of climate change on natural forest productivity—evidence since the middle of the 20th century. *Glob. Change Biol.* 12:862–882.
- Churkina, G., K. Trusilova, M. Vetter and F. Dentener. 2007. Contributions of nitrogen deposition and forest regrowth to terrestrial carbon uptake. *Carbon Balance Manage.* 2:5 doi:10.1186/1750-0680-2-5.
- de Pury, D.G.G. and G.D. Farquhar. 1997. Simple scaling of photosynthesis from leaves to canopies without the errors of big-leaf models. *Plant, Cell Environ.* 20:537–557.
- de Vries, W., G.J. Reinds, P. Gundersen and H. Sterba. 2006. The impact of nitrogen deposition on carbon sequestration in European forests and forest soils. *Glob. Change Biol.* 12:1151–1173.
- de Vries, W., S. Solberg, M. Dobbertin, H. Sterba, D. Laubhann, G.J. Reinds, G.J. Nabuurs, P. Gundersen and M.A. Sutton. 2008. Ecologically implausible carbon response? *Nature* 451:E1–E3.
- de Vries, W., S. Solberg, M. Dobbertin et al. 2009. The impact of nitrogen deposition on carbon sequestration by European forests and heathlands. *For. Ecol. Manage.* 258:1814–1823.
- Eastaugh, C.S. and H. Hasenauer. 2010. Incorporating management history into forest growth modeling. Paper presented at the COST FP0903 conference on 'Research, monitoring and modelling in the study of climate change and air pollution impacts on forest ecosystems', Rome, Italy, 5–7th October, 2010.
- Eastaugh, C.S., R. Petritsch and H. Hasenauer. 2010. Austrian forest estate climate development 1960–2008. *Austrian J. For. Sci.* 127: 133–146.
- Englisch, M., G. Karrer and F. Mutsch. 1992. Österreichische Waldboden Zustandsinventur. Teil 1: Methodische Grundlagen. *Mitteilunge. Forstlicher. Bundesversuchsanstalt. Wien* 168:5–22.
- European Commission 1994. Forest condition in Europe. Report EC-UN/ECE, Brussels, Geneva, 93 p.
- Farquhar, G., S. von Caemmerer and J. Berry. 1980. A biochemical model of photosynthesis CO₂ fixation in leaves of C₄ species. *Planta* 149:78–90.
- Gabler, K. and K. Schadauer. 2006. Methoden der Österreichischen Waldinventur 2000/02. *BFW Berichte* 135, 132 pp.
- Hasenauer, H., R.R. Nemani, K. Schadauer and S.W. Running. 1999. Forest growth response to changing climate between 1961 and 1990 in Austria. *For. Ecol. Manage.* 122:209–219.
- Hasenauer, H., K. Merganicova, R. Petritsch, S.A. Pietsch and P.E. Thornton. 2003. Validating daily climate interpolations over complex terrain in Austria. *Agric. For. Meteorol.* 119:87–107.
- Holland, E.A., F.J. Dentener, B.H. Braswell and J.M. Sulzman. 1999. Contemporary and pre-industrial global reactive nitrogen budgets. *Biogeochemistry* 46:7–43.
- IPCC 1992. Climate Change 1992: The Supplementary Report to the IPCC Scientific Assessment. Eds. J.T. Houghton, B.A. Callander and S.K. Varney. Cambridge University Press, Cambridge.
- Jones, H.G. 1992. Plants and microclimate. Cambridge University Press, Cambridge, 428 p.
- Karnosky, D.F. 2003. Impacts of elevated atmospheric CO₂ on forest trees and forest ecosystems: knowledge gaps. *Environ. Int.* 29: 161–169.
- Katzensteiner, K. and G. Glatzel. 1997. Causes of magnesium deficiency in forest ecosystems. In *Magnesium Deficiency in Forest Ecosystems*. Eds. R.F. Hüttl and W. Schaaf. Kluwer Academic Publisher, Dordrecht, pp 227–251.
- Kauppi, P.E., K. Mielikäinen and K. Kuusela. 1992. Biomass and carbon budgets of European forests, 1971 to 1990. *Science* 256:70–74.
- Keeling, C.D., T.P. Whorf, M. Wahlen and J. van der Plicht. 1995. Interannual extremes in the rate of rise of atmospheric carbon dioxide since 1980. *Nature* 375:666–670.
- Laubhann, D., H. Sterba, G.J. Reinds and W. de Vries. 2009. The impact of atmospheric deposition and climate on forest growth in European monitoring plots: an individual tree growth model. *For. Ecol. Manage.* 258:1751–1761.
- Lloyd, J. and J.A. Taylor. 1994. On the temperature dependence of soil respiration. *Funct. Ecol.* 8:315–323.
- Magnani, F., M. Mencuccini, M. Borghetti et al. 2007. The human footprint in the carbon cycle of temperate and boreal forests. *Nature* 447:848–850.
- Magnani, F., M. Mencuccini, M. Borghetti et al. 2008. Reply to de Vries et al. 2008, Ecologically implausible carbon response? *Nature* 451: E3–E4.
- McMahon, S.M., G.G. Parker and D.R. Miller. 2010. Evidence for a recent increase in forest growth. *Proc. Natl Acad. Sci.* 107:3611–3615.
- Myneni, R.R., C.D. Keeling, C.J. Tucker, G. Asrar and R.R. Nemani. 1997. Increased activity on northern vegetation inferred from satellite-based vegetation index, atmospheric carbon dioxide, and temperature data. *Nature* 386:698–702.
- Nilsson, J. 1986. Critical loads for sulphur and nitrogen. Nordic Council of Ministers. Copenhagen.
- Petritsch, R. 2008. Large scale mechanistic ecosystem modeling in Austria. Ph.D. thesis, University of Natural Resources and Applied Life Sciences, Vienna, 135 p.
- Petritsch, R. and H. Hasenauer. 2007. Interpolating input parameters for large scale ecosystem models. *Austrian J. For. Sci.* 124:135–151.
- Petritsch, R. and H. Hasenauer. 2009. Tägliche Wetterdaten im 1 km Raster von 1960 bis 2008 über Österreich. *Austrian J. For. Sci.* 126: 215–225.
- Pietsch, S.A. and H. Hasenauer. 2006. Evaluating the self-initialization procedure for large-scale ecosystem models. *Glob. Change Biol.* 12:1658–1669.
- Pietsch, S.A., H. Hasenauer and P.E. Thornton. 2005. BGC-model parameters for tree species growing in central European forests. *For. Ecol. Manage.* 211:264–295.
- Placer, K. and J. Schneider. 2001. Arbeit zur Kartierung der trockenen Deposition in Österreich. Federal Environment Agency, Austria.
- Reay, D.S., F. Dentener, P. Smith, J. Grace and R.A. Feely. 2008. Global nitrogen deposition and carbon sinks. *Nat. Geosci.* 1:430–437.

- Ryan, M.G. 1991. A simple method for estimating gross carbon budgets for vegetation in forest ecosystems. *Tree Physiol.* 9:255–266.
- Schadauer, K. 1996. Growth trends in Austria. *In* Growth Trends in Europe. Eds. H. Spiecker, K. Mielikäinen, M. Kohl and J.P. Skovsgaard. Springer, Berlin, pp 275–289.
- Schimel, D., J. Melillo, H. Tian et al. 2000. Contribution of increasing CO₂ and climate to carbon storage by ecosystems in the United States. *Science* 287:2004–2006.
- Schneider, J. 1998. Kartierung der nassen Deposition in Österreich. Austrian Federal Environment Agency, Vienna, 40 pp.
- Solberg, S., M. Dobbertin, G.J. Reinds, H. Lange, K. Andreassen, P.G. Fernandez, A. Hildingsson and W. deVries. 2009. Analyses of the impact of changes in atmospheric deposition and climate on forest growth in European monitoring plots: a stand growth approach. *For. Ecol. Manage.* 258:1735–1750.
- Spiecker, H. 1999. Overview of recent growth trends in European forests. *Water, Air Soil Pollut.* 116:33–46.
- Spiecker, H., K. Mielikäinen, M. Köhl and J.P. Skovsgaard. 1996. Growth trends in Europe. Springer, Berlin, 372 p.
- Thomas, R.Q., C.D. Canham, K.C. Weathers and C.L. Goodale. 2010. Increased tree carbon storage in response to nitrogen deposition in the US. *Nat. Geosci.* 3:13–17.
- Thornton, P.E. 1998. Description of a numerical simulation model for predicting the dynamics of energy, water carbon and nitrogen in a terrestrial ecosystem. Ph.D. thesis, University of Montana, Missoula.
- Thornton, P.E., S.W. Running and M.A. White. 1997. Generating surfaces of daily meteorological variables over large regions of complex terrain. *J. Hydrol.* 190:214–251.
- Thornton, P.E., H. Hasenauer and M.A. White. 2000. Simultaneous estimation of daily solar radiation and humidity from observed temperature and precipitation: an application over complex terrain in Austria. *Agric. For. Meteorol.* 104:255–271.
- Thornton, P.E., B.E. Law, H.L. Gholz et al. 2002. Modeling and measuring the effects of disturbance history and climate on carbon and water budgets in evergreen needle forests. *Agric. For. Meteorol.* 113:185–222.
- Umweltbundesamt 1996. Manual on methodologies and criteria for mapping critical loads/levels and geographical areas where they are exceeded. UN/ECE CLRTAP. UBA 71/96, Umweltbundesamt, Berlin.
- Van Deusen, P., P.R. Dell and C.E. Thomas. 1986. Volume growth estimation from permanent horizontal plots. *For. Sci.* 32:415–432.
- Wamelink, G.W.W., H.F. van Dobben, J.P. Mol-Dijkstra, E.P.A.G. Schouwenberg, J. Kros, W. de Vries and F. Berendse. 2009. Effect of nitrogen deposition reduction on biodiversity and carbon sequestration. *For. Ecol. Manage.* 258:1774–1779.
- White, M.A., P.E. Thornton, S.W. Running and R.R. Nemani. 2000. Parameterization and sensitivity analysis of the BIOME-BGC terrestrial ecosystem model: net primary production controls. *Earth Interact.* 4:1–85.
- Woodrow, I.E. and J.A. Berry. 1988. Enzymatic regulation of photosynthetic CO₂ fixation in C₃ plants. *Annu. Rev. Plant Physiol. Plant Mol. Biol.* 39:533–594.

BIOGEOCHEMICAL PROCESS MODELING OF FOREST FIRE IGNITION HAZARD

Eastaugh CS^{1*}, Hasenauer H¹

¹ *Institute of Silviculture*

Department of Forest and Soil Sciences

BOKU University of Natural Resources and Life Sciences Vienna

Peter Jordan Str. 82

A-1190 Wien

Ph. +43 1 7654 4050

* Corresponding author: chris.eastaugh@boku.ac.at

Submitted to Climatic Change 11/05/2012

ABSTRACT

While climatic conditions clearly have an impact on the growth of forest species, a changing climate may also affect disturbance regimes. This paper is concerned with the likelihood of forest fires in an Alpine Central European environment, traditionally not considered a fire-prone region but one where changing climatic conditions may promote such events in the future. Some parts of this region have experienced a 2.25°C rising trend in average temperatures over the past half-century, but unfortunately sufficiently reliable records of wildfire occurrence are not available for this length of time, making it difficult to definitively determine a link between climate change and fire. A further confounding factor is the influence of forest composition and fuel loading on fire ignition hazard, which is not considered by purely meteorological fire hazard indices. Both of these issues may be addressed through using biogeochemical forest growth models, which track the pools and fluxes of water, carbon and nitrogen through the ecosystem, and maintain information of several variables that may be used as proxies for fire hazard. The primary purpose of this study is to assess the usefulness of the ecophysiological model BIOME BGC's 'soil water' and 'labile litter carbon' variables in predicting fire hazard. We then provide a brief application case, examining historic fire ignition hazard trends over pre-defined regions of Austria from 1960 to 2008. The model variables are found to be superior to simple meteorological hazard indices, and suggest that particular Austrian regions have experienced a marked increase in wildfire hazard.

KEYWORDS

Wildfire, fire hazard, BIOME BGC, terpenes, fire index

1. INTRODUCTION

Climate change is expected to impact forests in a number of ways, both directly and indirectly. One of the most important indirect effects in many regions is the possibility of increasing wildfire risk (Brown et al 2004), and the introduction of fire as an important shaper of landscapes in areas where this has not been the case for centuries or millennia (Schumacher 2004). Fires are an integral part of many forest ecologies, and have always been fundamental in shaping forest structures and assemblages (Bond et al. 2005; Bowman 2005; Lynch et al. 2007). Fire regimes are strongly interlinked with climate changes (Whitlock et al. 2003; Meyer and Pierce, 2003; Taylor and Beaty 2005), and so it is not unreasonable to expect changes in the occurrence and severity of forest fires in many regions. Increased temperatures alone do not necessarily mean that more fires will occur; several other climatic and non-climatic factors are also involved such as ignition sources, fuel loads, vegetation characteristics, rainfall, humidity, wind, topography, landscape fragmentation and management policies (Flannigan et al. 2000). Taking these factors into account Flannigan et al. (2005) reviewed fire predictions for North America and suggest that overall increases in area burned may be in the order of 74-118% by the end of the 21st century. A further observed impact of recent environmental change is an increase in net primary production and forest growth in many areas (i.e. Phillips et al. 1998; Hasenauer et al. 1999; Nemani et al. 2003), which may lead to increased fire hazard due to changing fuel loads (Lenihan et al. 1998) and depleted soil moisture.

Several studies have been conducted in an attempt to assess possible future fire hazards under changed climatic conditions (i.e Pitman 2007; Malevskii-Malevich 2007; Good et al. 2008; Krawchuk et al. 2009). Well validated predictive tools for forest fire hazard would be useful for resource allocation (Cantwell 1974; McCarthy et al. 2003; Prestemon and Donovan 2008), emergency services budgeting (Thompson et al. 2012), infrastructure planning (Eastaugh and Molina 2011; 2012) and hazard warning systems (Valese et al. 2010). Such studies generally rely on defining some meteorological index of fire hazard, and calculating the development of that index under future climate scenarios. Inherent in this approach is the assumption that the relationship between the meteorological variables and fire hazard will remain constant, which may not be the case if the future climate, management activities or natural ecosystem development with aging alters forest conditions.

Several fire hazard indices have been developed over the past seventy years, beginning with the purely empirical meteorological indices of Ångström and Nesterov in the 1940s. Käse (1969) modified the Nesterov index to account for higher fire danger in spring, dependent on the budburst date of birch and robinia trees. Keetch and Byram (1968) developed an index of soil moisture deficit (KBDI) for use by fire agencies, on the principle that soil dryness is likely to be accompanied by fuel dryness. The more sophisticated Canadian Forest Fire Weather Index of Van Wagner (1987) expressly considers how weather conditions affect the moisture content of different fire fuel layers. The more easily ignited fine fuels lose moisture quickly under dry atmospheric conditions, while larger fuels dry only after extended periods. Tanskanen and Venäläinen (2008) have pointed out however that the accuracy of the indices can vary seasonally depending on the proportion of dead to live fine fuels on the forest floor. To some

extent this suggests that fire ignition hazard may potentially be reduced through appropriate management regimes, although this will require a sophisticated understanding of how ignition hazard relates to forest physiological processes.

Many of the various parameters implicated in forest fire ignition hazard are also important parameters in biogeochemical forest growth models. Keane (1996) took advantage of this in linking the FOREST-BGC model of (Running and Coughlan 1988) with the specifically fire-optimised gap model FIRESUM (Keane et al. 1989). More recently, Keane et al. (2011) uses the BIOME-BGC model (Thornton 1998) as an input into Fire-BGCv2, a highly sophisticated research tool linking biogeochemical modeling, forest succession models and fire spread behaviour. Management-sensitive parameters such as fuel volumes clearly have an impact on fire behaviour (Finney 2006), but the possible link between these parameters and the relative likelihood of fire ignition has not yet to our knowledge been explicitly modeled.

Biogeochemical models track the pools and fluxes of water, carbon and (often) nitrogen in an ecosystem, and allocate the carbon taken up by photosynthesis to various components of the system. With various degrees of complexity, the models include consideration of soil moisture and litter volumes and composition. Our contention is that these variables may prove to be reasonable indicators of forest fire ignition hazard, at least on a par with meteorological indices over short time frames. If this is the case, then it is likely that the model-derived indices would be superior over longer timescales, due to their incorporation of how forests change over time, particularly in a changing climate or under varying management regimes.

Although the focus of this work is on exploring the use of biogeochemical forest growth modeling in forest fire hazard assessments, we also provide a brief application case, examining the seasonal drivers and trends of fire hazard in Austria. Central European alpine regions are not typically considered high fire danger areas but there is mounting concern over the possibility of increased fire hazard in the near future (Conedera et al 2006; Gossow 2009; Wastl 2011). Fires are generally not large, but in rugged terrain they can be difficult to control and can have serious long term effects on the protection function of mountain forests (Brang et al 2006; Sass et al 2010; 2012a,b). Conedera (1996) reported an increase in forest fires in Switzerland from the 1960s and 1970s, and noted that this “could not be explained simply through the analysis of particular meteorological factors or the inclusion of the major anthropogenic causes”, while Zumbrunnen et al. (2009) have pointed to the importance of both meteorological and fuel load conditions to fire occurrence in Alpine areas. We choose the Austrian situation due to the availability of a quality-checked national fire database (Müller 2012; Eastaugh and Vacik in review), a validated climate interpolation (Thornton et al. 1997; Petritsch and Hasenauer 2007) and a previously parameterized biogeochemical model (Pietsch et al. 2005; Eastaugh et al. 2011).

The purpose of this study is to assess whether the inclusion of forest physiological properties can provide improved estimates of forest fire ignition hazards, compared to purely meteorological indices. We apply the species-specific version of BIOME-BGC (Pietsch et al. 2005) to 2014 sites of the Austrian

National Forest Inventory (Gabler and Schadauer 2006), and record daily values of simulated soil water content (*sw*), labile litter carbon (*llc*) and vapour pressure deficit (*vpd*) at each site from 1960 to 2008. Defining two indices as BGC-SW=*sw* and BGC-LV as *llc***vpd*, we assess their precision against recorded fire occurrence data from 1995 to 2008, and compare this with the precision of the Ångström, Nesterov and KBDI indices. For the application study the model outputs are geographically aggregated according to regions defined by Eastaugh et al. (2011), as those parts of Austria that have experienced climate change more than one standard deviation different to the national average. The output of the application study shows trends in the BGC-LV index from 1960 to 2008, and compares the BGC-SW extremes from 1991-2008 against a 1960-2008 baseline. The model and the index performance comparisons allow us to suggest explanations for the seasonal variation in forest fire hazard in Alpine areas. Specific outputs are:

- a) A comparative evaluation of the five indices at the national scale, for both summer and winter seasons, in terms of their ability to reflect overall fire ignition hazard and the occurrence of extreme hazard conditions,
- b) An analysis of overall trends in overall fire ignition hazard at the regional scale using the BGC-LV index, and
- c) An analysis of trends in extreme fire ignition hazard at the regional scale using the BGC-SW index.

2. TECHNICAL BACKGROUND

2.1 Meteorological indices

2.1.1 Ångström

Ångström (1942, cited by Ångström 1949) developed a simple instantaneous meteorological index relating fire danger to relative humidity (*Rh*) and temperature (*T*) (eq 1) from field experiments in Sweden. The Ångström index *AI* is calculated as:

$$AI = \frac{Rh}{20} + \frac{29 - T}{10} \quad \text{Equation 1}$$

The AI gives lower values when conditions are fire danger is higher. Fire is generally considered ‘very likely’ at values at values less than 2.0, and ‘unlikely’ at values over 4.0.

2.1.2 Nesterov

Nesterov (1949) constructed a cumulative index, where each day's calculated value is added to that from the previous day. Each daily increment is calculated as:

$$N_d = T_{\max} (T_{\max} - T_{dew}) \quad \text{Equation 2}$$

where T_{\max} and T_{dew} are the daily maximum and dew-point temperatures respectively. We estimate T_{dew} as being equal to the daily minimum temperature T_{\min} , an approximation that has been shown to be accurate except under arid conditions (Kimball et al. 1997). The summation continues until such time as some minimum amount of rainfall is experienced: in Austria 4mm is used (Arpaci 2010). The accumulated Nesterov index value NI then is:

$$NI = \sum_{i=1}^w N_{d_i} \quad \text{Equation 3}$$

Where W is the number of days since 4mm of rainfall was collected. The Nesterov index is currently used as an official indicator of fire hazard in Russia (McRae et al 2006) and in Austria (Arpaci 2010). The index is interpreted with the aid of the following threshold values:

Table 1 Risk classes of the Nesterov index.

<i>Index range</i>	<i>Class</i>	<i>Description</i>
< 300	1	no fire risk
301 - 1000	2	low fire risk
1001 - 4000	3	medium fire risk
4001 - 10 000	4	high fire risk
> 10000	5	very high fire risk

2.1.3 Keetch-Byram drought index

The Keetch-Byram drought index (KBDI; Keetch and Byram 1968, typographical errors corrected 1988) was specifically designed as a fire weather warning system. We use here the metric version presented by Crane (1982, cited by Alexander 1990).

$$dK = 10^{-3} \frac{(203.2 - KBDI_{t-1}^*) (0.968e^{(0.0875T_{\max} + 1.5552)} - 8.3)}{1 + 10.88e^{-0.001736R_{av}}} \quad \text{Equation 4}$$

where $KBDI_{t-1}^*$ = the previous day's moisture deficiency less the net rainfall
 R_{av} = local annual average precipitation
 dK = the daily addition to moisture deficiency.

The KBDI increases daily according to temperature and humidity, and decreases when rainfall P over consecutive days exceeds 5.1mm, by the depth of the rainfall less the 5.1mm buffer (net rainfall). After Janis et al. (2002):

$$\begin{aligned} KBDI_t &= KBDI_{t-1} + dK && \text{if } P_t = 0 \\ KBDI_t &= KBDI_{t-1} + dK && \text{if } P_t > 0 \text{ and } \Sigma P \leq 5.1 \text{mm} \\ KBDI_t &= KBDI_{t-1}^* + dK && \text{if } P_t > 0 \text{ and } \Sigma P > 5.1 \text{mm} \end{aligned}$$

The KBDI is intended as a direct indicator of soil water deficit. In its original form, it estimated the amount of net precipitation in points (1 point = 1/100th of an inch = 0.254mm) necessary to bring the soil to saturation. In the metric form the index is measured in millimeters, and ranges from zero (saturated soil) to a maximum of 203.2mm. Keetch and Byram (1960) divided the index into eight 'stages', but point out that the significance of each stage will depend on local climatological conditions. Geographical variations in KBDI across Austria were studied by Petritsch and Hasenauer (2012).

2.2 BIOME BGC

We use a version of the BIOME-BGC model modified and calibrated for central European conditions (Pietsch et al. 2005; Pietsch and Hasenauer 2006). Stages and fluxes of water, carbon and nitrogen are tracked throughout various pools in the vegetation, litter and soil on a daily timestep. Ecological processes in the model are driven by daily meteorological data, site characteristics and various ecophysiological parameters describing the vegetation at each site. The model is not specifically calibrated for this study, and is run in a 'standard trim', using the Central European species parameterisation of Pietsch et al. (2005) and other inputs and assumptions described by Eastaugh et al. (2011). The model has been comprehensively described elsewhere, so for reasons of space we refer the reader to Thornton et al. (2002) and the papers cited in this paragraph for more detailed technical descriptions of the model's operation. In brief, carbon is simulated as entering the ecosystem via photosynthesis, and lost through autotrophic respiration. The remaining net primary production is assigned to various vegetation pools as biomass. Biomass can be reduced through management activities (resulting in removal from the system or transfer to the detrital pools), through mortality or through leaf senescence and litterfall. Leaf area index (LAI) is an internally calculated variable and controls canopy radiation absorption, light transmission to the ground and precipitation interception. The litter input to the detrital pools also varies according to LAI. Atmospheric nitrogen is input to the soil via the stomatal uptake and detrital processes, and the model limits the amount of nitrogen available for plant growth depending on microbial demands in the soil, which in turn depend on the mass of litter and temperature and soil moisture sensitive decomposition rates.

The model includes four separate pools representing carbon in litter: labile carbon, two pools of cellulose carbon (depending on whether bound by lignins or unbound) and lignin carbon. Litterfall in coniferous forests is assumed to be constant for each day of the year (Pedersen and Bille-Hansen 1999), with the daily

rate reset each year depending the previous year's maximum LAI and a species-specific turnover rate. Breakdown of litter depends on the simulated action of soil microbes, which is highly temperature dependent. Labile carbon pools break down quickly (by definition), and as a result peak in the late winter/early spring season, as it has accumulated over the winter when conditions are not conducive to microbial degradation. After this time breakdown is swift in the warming soils of late spring and summer.

Our proposition in this work is that the mass of carbon in the labile litter carbon pool (*llc*) can be used as a proxy for the volume of highly flammable surface litter, which in coniferous forests contains high levels of volatile terpenoids. Although the model developers do not appear to have specifically considered the chemical compounds present in the labile litter pool, the rapid breakdown of terpenes by microbial action (Mikami 1988) suggests that their volume in the litter will be best matched by the rapidly decomposing labile carbon. Terpenes in litter have been shown to promote flammability (Ormeño et al 2009; Zhao et al. 2012), and thus the mass of labile carbon on the forest floor may be a useful input to a forest hazard index. Fine dead fuels dry quickly (Nelson 2001; Wotton 2009), and as a direct measure of the drying ability of the atmosphere we use the vapour pressure deficit (*vpd*). Our first model-derived index is thus:

$$\text{BGC-LV} = llc * vpd * 10^3 \quad \text{Equation 5}$$

Higher values indicate a greater mass of volatile litter and/or greater vapour pressure deficit, and thus higher fire ignition hazard.

Precipitation in BIOME-BGC may be intercepted by the canopy or entered into the soil water (*sw*) pool for either storage, deep drainage or overland flow. Soil water loss through evapotranspiration is calculated with the Penman–Monteith equation as a function of air temperature, air pressure, *vpd*, incident solar radiation and the transport resistance of water vapour and sensible heat. Evapotranspiration depends on both climatic and physiological characteristics of leaf area and species-specific parameters and thus is strongly linked to stand conditions.

Soil moisture can sometimes be a useful proxy for surface fuel moisture (Keetch and Byram 1968; Hatton et al 1988), so our second model-derived index is simply:

$$\text{BGC-SW} = sw$$

Higher values of the BGC-SW index indicate greater soil moisture content and thus lower fire ignition hazard.

3. DATA

3.1 Climate

Daily climate data is required to calculate fire index values and as drivers for the BIOME.BGC model. We interpolate daily climate to each NFI site through the DAYMET model of Thornton et al. (1997), as adjusted and validated by Hasenauer et al. (2003). DAYMET interpolations are generated based on the geographic position, elevation, slope, aspect and angle to the horizon and climate records from several hundred climate stations in Austria and surrounding countries. DAYMET directly interpolates precipitation and maximum and minimum temperature, and from this is possible to calculate mean daily temperature, growing season length, vapour pressure deficit, solar radiation and drought index. Solar radiation and water vapour pressure deficit values are derived from daily temperature and precipitation according to the methods of Thornton et al. (2000), validated for Austria by Hasenauer et al. (2003), and incorporate the potential shadowing effect of surrounding mountains and the radiation reflections due to snow pack. The DAYMET output thus provides all the necessary information to calculate daily values of the indices for each NFI point, and forms the climatic input for the BIOME BGC model.

Overall, Austrian forests have experienced an average warming of 1.5°C over the past fifty years, with no discernable trend in precipitation (Eastaugh et al. 2010). There is however marked sub-national variability, and Eastaugh et al. (2011) delineated nine ‘climate change regions’ where temperature or precipitation trends were more than one standard deviation outside the national average (figure 1).

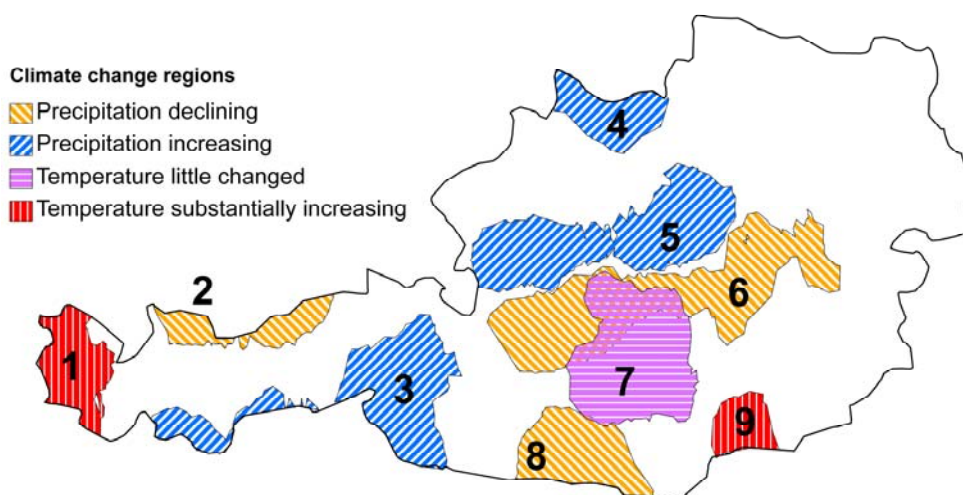


Figure 1 Climate change regions (Eastaugh et al. 2011)

3.2 Austrian fire database

As part of the ALP FFIRS project (Valese et al. 2010), a database of Austrian wildfires has been compiled based on historic documentary records (Vacik et al. 2011; Müller et al. 2012). The database has been assembled with information from a variety of sources that cover different time periods or geographical regions. The database contains records of 1035 forest fires between 1995 and 2008 and is used to assess the precision of each of the fire ignition hazard indices at the national scale, separately for summer and winter conditions. Data for periods prior to this is likely to be incomplete (Eastaugh and Vacik in review), so purely data-based analyses of long-term trends are impossible. Areas burnt are not recorded for all ignitions, those that are range from 1m² to 120ha. Numbers of ignitions per year range from seven in 1997 to 226 in 2007.

4. ANALYSIS METHODS

Daily values for all indices are calculated for each forest point, according to the equations below. The values are aggregated nationally, separately for the summer (May to November) and winter (December to April) periods. These cut-off dates were selected to be in line with work on Alpine forest fires from neighbouring Switzerland (Conedera et al. 2006) and north-eastern Italy (Valese 2009), which suggests that there may be two distinct fire seasons in alpine Central Europe. Trend comparisons aggregate values separately for each of the numbered regions in figure 1, and for the unnumbered '0' region. The methods are chosen specifically in order to assess the precision of the BIOME-BGC indices in both summer and winter conditions, and allow conclusions to be drawn as to why each index performs better or worse in each season.

4.1 Index comparison methods

4.1.1 Overall hazard

Fire indices should be expected to reflect the increase in fire ignition hazard as climatic (or other) conditions worsen. This is not necessarily a linear relationship, and various indices have different frequency occurrence distributions over a year or series of years. The shortcomings of using parametric methods of index performance comparison were pointed out by Eastaugh et al. (2012), who suggested a graphical percentile-based technique that we briefly reiterate here. The percentile of each index is calculated for each day in the period of interest, and the percentile values on days when a fire ignition is noted in the database are plotted in rank order (fig 2). The main characteristics of the resulting curve of points can be described by the intercept and slope of a robust regression line. A hypothetically 'perfect' fire index would have its highest values only on days

when a fire truly occurs, and thus would plot as a line with an intercept of 100 and a slope of 0, whereas an index of random numbers would approach an intercept of zero and a slope of 100 divided by the total number of fires. Indices are compared at the National scale separately for summer and winter.

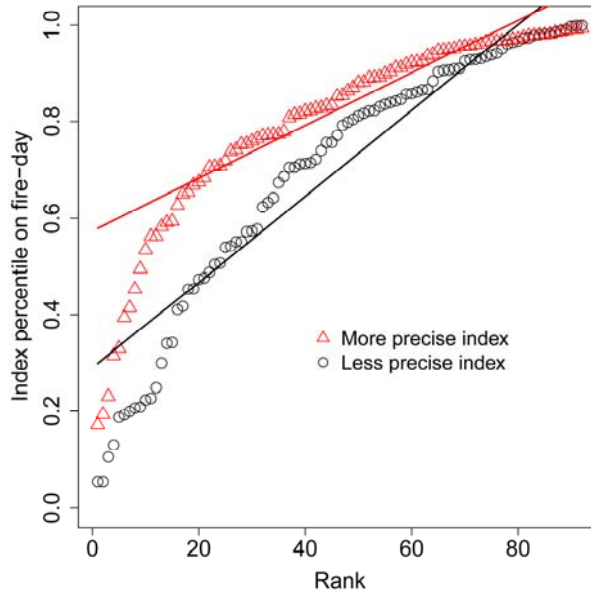


Figure 2 Example figure for index comparison method. For 100 fires, the percentile of the index on each fire day is plotted in rank order. The shape of the curve describes the precision of the index at any percentile, and may be summarized by the intercept and slope of a robust regression line (Eastaugh et al. 2012).

4.1.2 Extremes

For index comparison we define ‘extreme’ fire hazard in terms relative to each season, as that percentile of the index that on average would have a 50% chance of exceedence in each season (the 99.67th percentile in winter and the 99.77th in summer). The relative strength of each index at correctly determining extreme fire hazard is assessed by the number of fires that did occur at over this percentile value. In terms of figure 2, it would be seen as the number of fires above a horizontal line at that particular percentile value.

4.2 Trend comparisons

Having tested the usefulness of the BIOME-BGC-based indices, we apply them to each of the 9 climate change regions in Austria and the ‘0’ region that has exhibited change close to the national average (Eastaugh et al. 2011). This section of the work does not use the fire database, but tracks the progress of the indicators from 1960 to 2008. We compare the regions for their trends in both general fire hazard and for the occurrence of extremes.

4.2.1 Overall hazard

At the National scale and using all climate data from 1960 to 2008 we determine the percentile values of the Nesterov index that correspond to each of the risk classes in table 1. The BGC-LV index values at these percentiles are presented in a similar table. For each region in each season the trend of each BGC-LV class is estimated with a linear regression.

4.2.2 Extremes

Our earlier defined extreme percentiles proved to be too high for trend assessment, as in most regions this level was only exceeded in 2003. In order to make meaningful comparisons we chose a percentile of 99.07 for the summer, and 98.0 for the winter (on average, an expectation of 2 and 3 days per season respectively). For assessment of changes in extremes we determine the number of times per year that the chosen percentile of the BGC-SW index was exceeded in each region in the 1991 – 2008 period, and express it as a percentage of the 1960-1990 mean. As the increase is very high due to the extreme drought year of 2003, we also determine the average proportion of years that experienced more than 2 days of hazard above that percentile.

5. RESULTS

5.1 Fire seasonality

The seasonal distribution of forest fires in the Austrian database is shown to have two distinct peaks, in April and July (fig 3). Periods of high fire occurrence are from May to August in our defined ‘summer’ period, and March and April in ‘winter’.

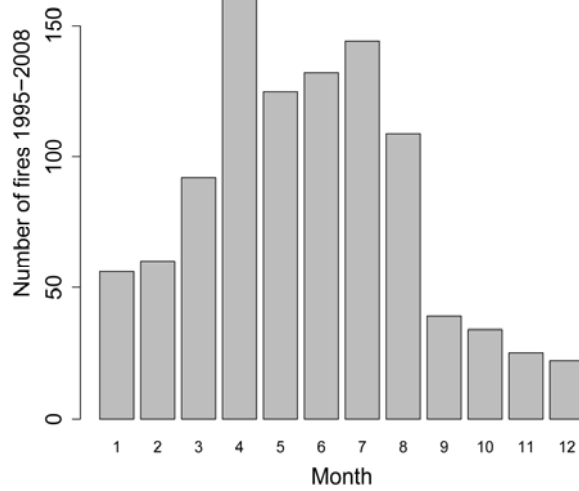


Figure 3 Seasonal distribution of forest fire records in the Austrian wildfire database throughout the year in the study period 1995 – 2008.

5.2 Index comparison

Histograms of the occurrence of daily values for each index are shown in figure 4, covering the period 1960 - 2008. The very low frequency of values in the most hazardous ranges (refer section 2.1) is clear, as are the substantially different distributions of the indices that necessitate the use of a non-parametric comparison method.

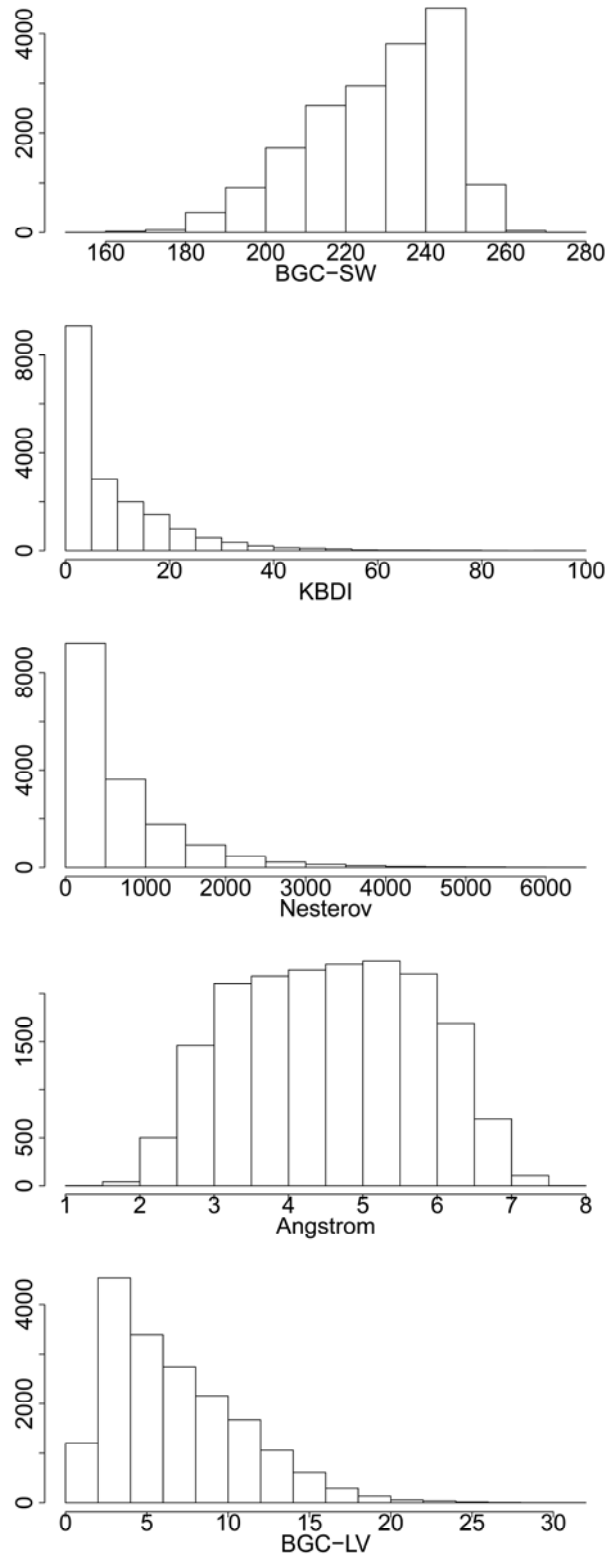


Figure 4 Frequency of occurrence histograms for the five indices, showing the distribution of daily values from 1960-2008. In the BGC-SW and Ångström indices higher values indicate lower fire hazard, in the others higher.

As an overall descriptor of the seasonal fire hazard, the BGC-derived LV index is superior in both seasons (table 2). BGC-SW performs poorly as an overall predictor of fires particularly in the winter, but is equal to the KBDI in more extreme conditions in winter and only slightly less precise at the given percentile

in summer. Both soil-based indices (BGC-SW and the KBDI) are particularly poor descriptors of overall hazard in the winter (fig 5, upper left panel) but perform well at extreme values in the summer (fig 5 lower right panel)

Table 2 Index performance. Best result in bold, worst in italic.

	BGC-SW	KBDI	Nesterov	Angström	BGC-LV
winter	0.032192	0.300434	0.454841	0.467464	0.527794
(150 days)	0.003801	0.002975	0.002544	0.002386	0.002079
	6	6	6	3	6
summer	0.269121	0.307885	0.335394	0.400872	0.462705
(215 days)	0.002146	0.002029	0.001881	0.001745	0.001484
	6	7	5	4	4

Based on the encouraging performance of the BGC based indices, trend analyses are performed using the BGC-LV index for an overall assessment of hazard, and BGC-SW for extremes.

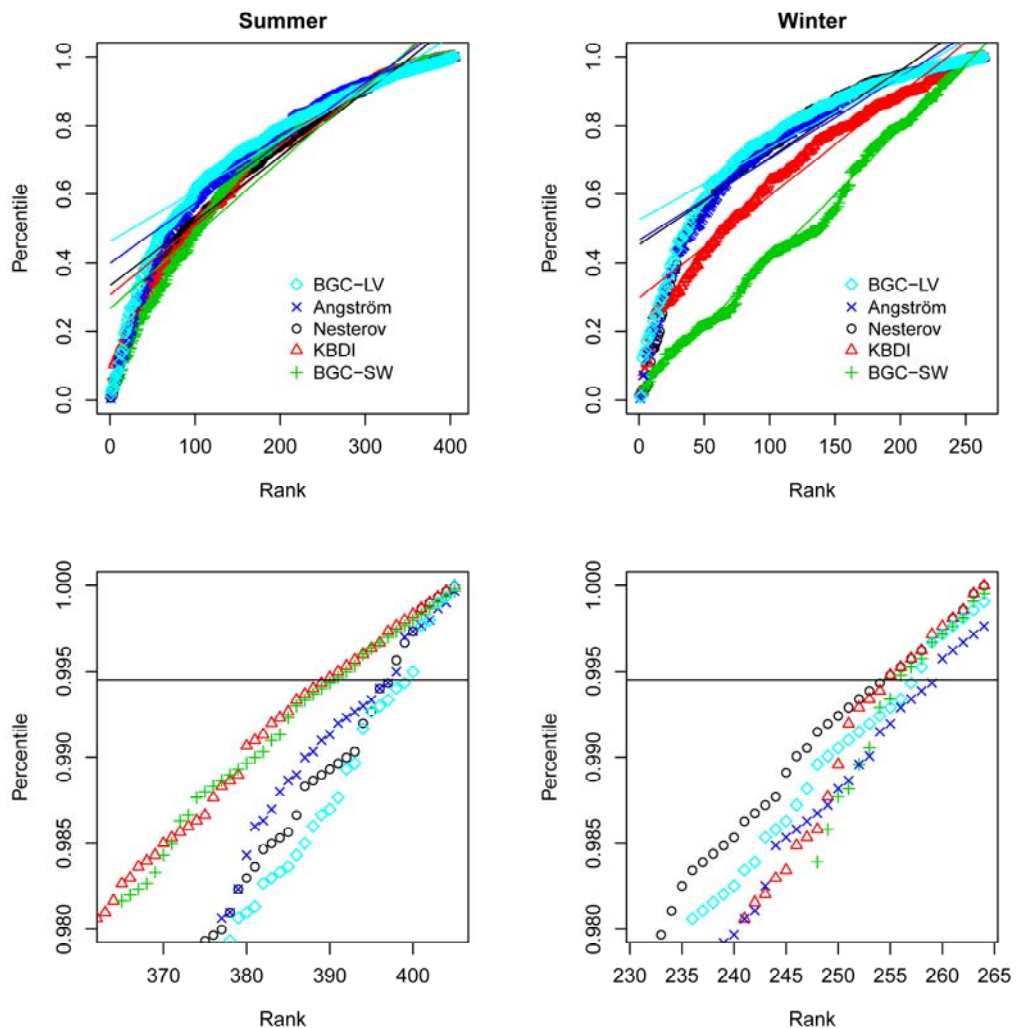


Figure 5 Ranked percentile curves of summer (left) and winter (right) fires. Lower panels are a closeup view of the extreme high values in the upper panels. The superiority of the soil-based indicators in extreme summer conditions is clear in the lower left panel, as is their comparatively poor overall performance in winter in the upper right. For clarity, the order of the indices in the legend matches the order of their ‘y’ intercepts in the upper panels.

5.3 Trends

Class limits for the BGC-LV index were determined as per table 3. The Nesterov index did not reach class 5 when averaged over the whole of Austria, so the BGC-LV value of 40 was chosen as a suitably rare event to define class 5 in BGC-LV.

Table 3 Class limits for the BGC-LV index.

<i>Nesterov lower bound</i>	<i>Percentile</i>	<i>Class</i>	<i>BGC-LV lower bound</i>	<i>BGC-LV upper bound</i>	<i>Description</i>
0		1	0	5.32	no fire risk
300	45.25	2	5.33	10.22	low fire risk
1000	79.95	3	10.23	20.57	medium fire risk
4000	99.49	4	20.58	39.99	high fire risk
10000	NA	5	40		very high fire risk

Figure 6 shows the nationally aggregated trends in each of the BGC-LV classes. Of here is the decline in the ‘no fire risk’ class, in both summer and winter. All individual regions show a decreasing trend of Class 1 and 2 days in summer (table 4), and an increase in Classes 3 and 4. In winter (table 5) Class 1 also reduces, but increases in Class 2 and 3.

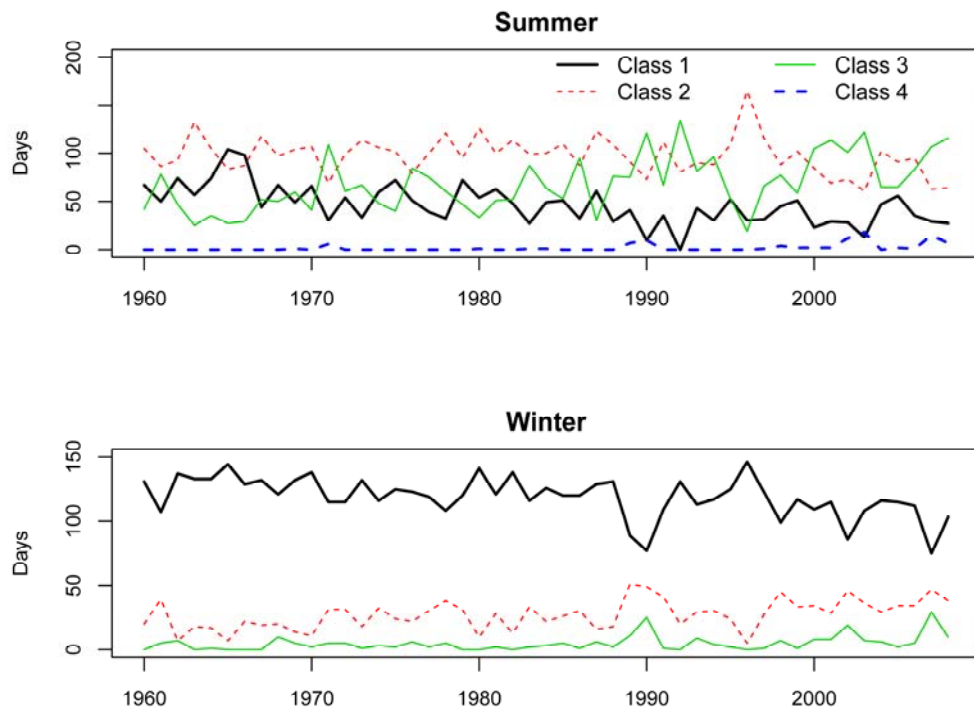


Figure 6 Trends in national average BGC-LV class occurrence. Nationally aggregated, class 5 does not occur in summer, and neither classes 4 nor 5 in winter.

Table 4 Trends in summer fire hazard in each climate change region. Trends stronger than the '0' region are shown in bold.

Region	Class 1		Class 2		Class 3		Class 4		Class 5	
	slope	sig ^a	slope	sig	slope	sig	slope	sig	slope	sig
0	-0.59112	***	-0.65908	**	0.799388	**	0.450816	***	0	ns
1	-0.06	ns	-0.18153	ns	0.17949	ns	0.062041	ns	0	ns
2	-0.86847	***	-0.47531	***	1.058367	***	0.285408	***	0	ns
3	-0.52102	***	-0.30745	*	0.506122	**	0.322347	***	0	ns
4	-0.68449	***	-0.48531	**	0.535714	**	0.631939	***	0.002143	ns
5	-0.71347	**	-0.10633	ns	0.703265	**	0.116531	**	0	ns
6	-0.91929	***	-0.26224	.	0.815306	***	0.366224	***	0	ns
7	-0.85214	***	-0.69684	***	0.692857	***	0.832857	***	0.023265	.
8	-0.66704	***	-0.68878	**	0.824592	**	0.529388	***	0.001837	ns
9	-0.49	**	-0.48541	*	0.678673	*	0.293163	**	0.003571	ns

^a Significance levels: p value 'ns' > .1 > '.' > .05 > '*' > .01 > '**' > .001 > '***'

Table 5 Trends in winter fire hazard in each climate change region. Trends stronger than the '0' region are shown in bold.

Region	Class 1		Class 2		Class 3		Class 4		Class 5	
	slope	sig ^a	slope	sig	slope	sig	slope	sig	slope	sig
0	-0.77439	***	0.460204	***	0.289592	**	0.024592	.	0	ns
1	-0.30755	*	0.222857	*	0.084694	.	0	ns	0	ns
2	-0.66551	***	0.529184	***	0.136327	**	0	ns	0	ns
3	-0.50439	**	0.314694	**	0.183367	*	0.006327	*	0	ns
4	-0.46112	**	0.253469	**	0.191429	**	0.016224	*	0	ns
5	-0.25867	**	0.194592	*	0.064082	.	0	ns	0	ns
6	-0.70286	***	0.510612	***	0.186327	**	0.005918	ns	0	ns
7	-1.1549	***	0.703673	***	0.380612	***	0.070612	*	0	ns
8	-0.82724	***	0.429286	***	0.388776	***	0.009184	ns	0	ns
9	-0.90153	***	0.461122	***	0.389796	**	0.050612	*	0	ns

^a Significance levels: p value 'ns' > .1 > '.' > .05 > '*' > .01 > '**' > .001 > '***'

Figure seven compares the occurrence of extreme values of the BGC-SW index in the 1991-2008 period with a 1960-1990 baseline, expressed as a percentage increase in yearly probability.

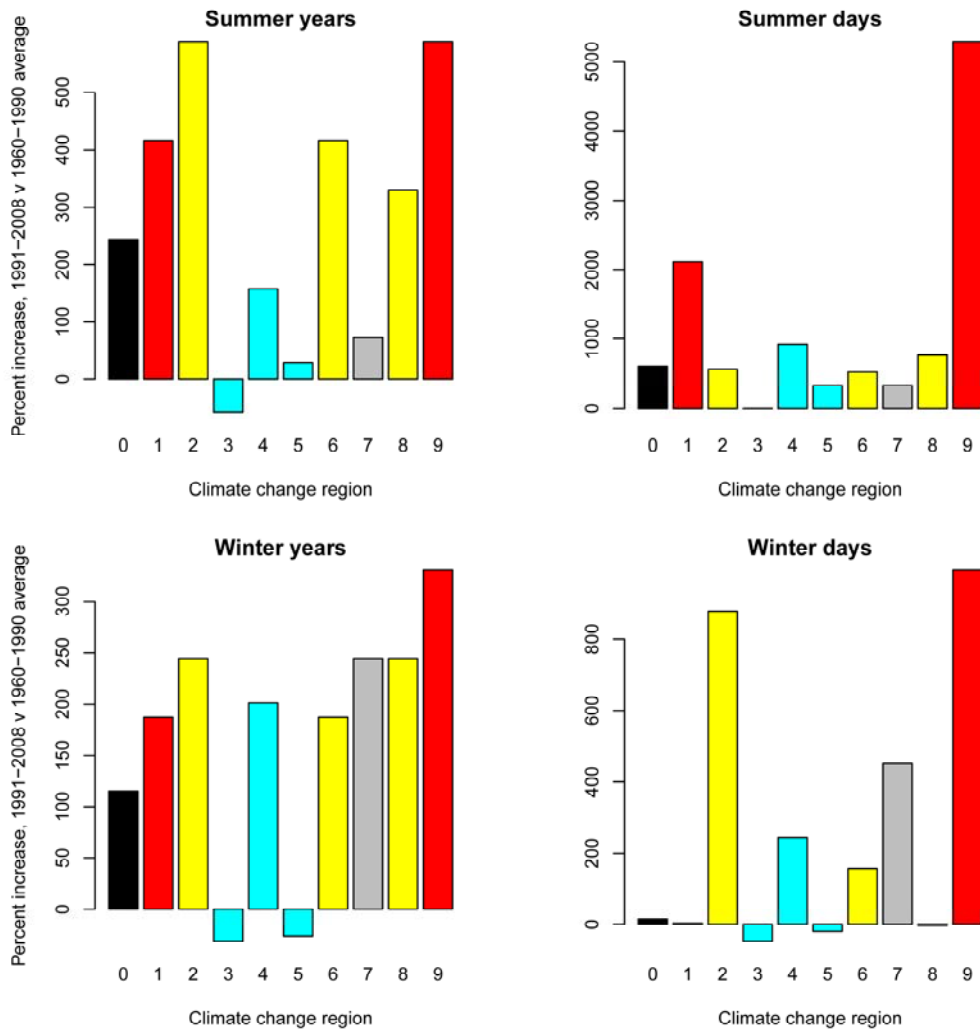


Figure 7 Left panels show the average proportion of years that experienced above average fire danger weather (more than x days above the $(1-x/\text{season length})$ percentile). Figure compares 1991-2008 period against a 1960-1990 baseline. $x=2$ in summer, $x=3$ in winter. Region numbers correspond to those in figure 1.

6. DISCUSSION

In principle, simulation models such as BIOME-BGC should be able to provide a more precise indication of fire ignition hazard than purely meteorological indices. Pausas and Paula (2012) have recently pointed out the strong links between forest productivity, fuel conditions and fire hazard. Biogeochemical process models that are optimized for the simulation of forest productivity can thus clearly have a role to play in forest fire science. The BIOME-BGC derived indices in this study are seen to perform well in comparison to the purely meteorological alternatives. The BGC-LV index is a more precise indicator of overall fire hazard in both summer and winter, and performs equally as well as the others in extreme winter conditions. Summer extremes however are best represented by the soil based indices, BGC-SW and the KBDI. Although table 2 suggests that these indices also perform well for winter extremes, the 99.67th percentile chosen for the comparison

proved to be too rare an event to make meaningful comparisons of trends. Reducing the threshold to a level where it was exceeded at least once in each region both before and after 1990 brought it down to 98% in the winter, which figure 5 (lower right panel) shows is well below the optimum. The winter results in figure 7 should thus be viewed with some caution. It is clear from figure 4 that the Nesterov index would be a better choice for winter assessments at this percentile. It is also possible that in some areas other meteorological indices may offer better performance than those presented here. As this study is primarily concerned with assessing the performance of the model based indices however, we leave that work to others (Arpaci et al. in prep). Extreme conditions in summer were assessed at the 99.07th percentile, at which level figure 5 shows the clear superiority of the soil-based indices (lower left panel). The overall strength of the BGC-LV index supports our proposition that volatile fine fuels may be represented by the BIOME-BGC model's labile litter carbon pool, and if modified by the drying power of the atmosphere it is a better overall indicator of fire hazard than the Nesterov index.

Conedera et al. (2006) noted the prevalence of winter fires in inner alpine valleys in Switzerland, and attributed this primarily to the higher levels of lightning activity in this period. Müller et al. (2012) however show that in Austria the winter fires are rarely lightning caused. Our work here does not deal with ignition causes, but we suggest that the high level of volatile fuels and commonly very high vapour pressure deficits will increase fire hazard regardless of the ignition source, as the forest floor becomes more susceptible to fires beginning. Winter fire risk overall is poorly represented by the soil based indices, strongly suggesting that short-term dryness and fuel availability are the key drivers of the hazard. In contrast, in summer the extreme risk days are better represented by soil moisture indices; while the overall summer hazard is better assessed with the BGC-LV index at extreme values the soil-based indices are superior, suggesting that long-term drought conditions become the key driver of the hazard in extreme summer conditions. This is consistent with the thesis that the availability of highly volatile fine fuels is decreased by microbial activity as summer progresses, and so coarser, slower drying fuels must be ignited for fire to occur.

The assessment of hazard trends in this work suggests that changes in extreme conditions in summer may be related closely to climate trends (fig 7), although the 'wetting' regions 4 and 5 still show an increase in hazard above the 1960-1990 baseline (albeit less than region 0). This can be explained by the acceleration in forest growth rates in Austria over recent decades (Hasenauer et al. 1999; Eastaugh et al. 2011). Forest growth trends in Austria in the last mentioned study were found to vary between regions, with warming and wetting regions experiencing greater growth increases, both in observed inventory data and in BIOME-BGC simulations. Faster growing forests must extract more water from the soil, and figure 5 shows the clear link between extreme soil dryness and extreme fire hazard. What is apparent is an increasing extreme summer fire hazard nationally, most clear in warming and drying regions. Only one region (3) has reducing risk, due to increasing precipitation. Other wetting regions (4,5) and the non-warming region (7) have less risk increase than the national average.

The difference between trends in overall hazard in tables 4 and 5 is less easy to interpret, and it may be that the BGC-LV index is weakened by its lack of

a cumulative fuel moisture proxy. The Nesterov, KBDI and BGC-SW indices all include consideration of weather conditions prior to the day of index calculation, and thus are sensitive to the drying of heavier fuels than the Angström or the BGC-LV. It seems likely that some combination of the BGC-LV and BGC-SW indices would be able to capture fire hazard under both short and long term drying conditions, but this would doubtless require region-specific parameterization and is well beyond the scope of this initial exploratory study. In an ideal world we would have sufficient data to match modeled hazard trends in each region against observed fire occurrence data, but as the length of reliable records is short (Valese et al. 2011; Eastaugh and Vacik in review), this is not possible.

Our work has focused on fire ignition hazard, rather than of fire extent and fire behaviour work of Pausas and Paula (2012) or Keane et al. (2011). To make the link between variables available in the BIOME-BGC modeling framework and fire ignition hazard we assume a direct relationship between the mass of labile carbon in the modelled litter pool and the flammability of fuels on the forest floor, due to their volatile terpene content. This is (at this stage) still a speculative hypothesis, but certainly not refuted by the results in this paper. Terpenes in general are still not a well understood aspect of forest physiology (Isidorov et al. 2010), and substantial experimental work would be needed to specifically mechanistically model flammable terpene levels in forest litter. It is important to note that the BIOME-BGC model in this study was not specifically calibrated for either soil water or litter levels, but was run under standard assumptions used previously for site-specific calibration (Pietsch et al. 2005) and national-scale forest productivity assessments (Eastaugh et al. 2011). Optimising the model specifically for fire hazard purposes would undoubtedly increase its precision. Nevertheless, this initial exploratory study shows the potential for biogeochemical modeling to add to understanding of how climate changes may impact fire hazards in forests, and opens a new and exciting direction of practical research.

7. CONCLUSION

Variables tracked in the BIOME-BGC model have proven to be able to track forest fire ignition hazard in Austria at precisions comparable to the currently used purely meteorological Nesterov index. In principle, the fact that BIOME-BGC variables are sensitive to both climatic and non-climatic influences suggests that it should be a better indicator of long-term hazard trends than solely climate-based indices. The hypothesis that BIOME-BGC's labile litter pool could be used as a proxy for the seasonal buildup of highly flammable fuels has proven reasonable, and in combination with vapour pressure deficit the results are an improvement on common existing risk indices. In extreme summer conditions BIOME-BGC's soil moisture variable closely matches the Keetch Byram index of soil drought, and has the advantage of being sensitive to changing vegetation demands on soil water. Applied to Austria over the past half-century the BIOME-BGC indices show a nationwide downward trend in days of no fire risk in both summer and winter, a reduction in days of low fire risk in summer, and an increase in extreme fire days in summer in most regions.

ACKNOWLEDGEMENTS

This work was jointly funded by the projects 'Comparing satellite versus ground driven carbon estimates for Austrian Forests' (MOTI), 'Alpine Forest Fire Warning System' (ALP FFIRS) and 'Austrian Forest Research Initiative' (AFFRI). We are grateful for the financial support provided by the Energy Fund of the Federal State of Austria (managed by Kommunalkredit Public Consulting GmbH under contract number K10AC1K00050), the European Regional Development fund of the Alpine Space Program (reference number 15-2-3-IT) and the Austrian Science Fund (reference number L539-N14).

REFERENCES

- Alexander ME (1990) Computer calculation of the Keetch-Byram drought index: Programmers beware! *Fire Management Notes* 51(4):23-25.
- Arpaci, A, Vacik H, Formayer H, Beck A (2010) A collection of possible Fire Weather Indices (FWI) for alpine landscapes, available at: http://www.alpffirs.eu/index.php?option=com_docman&task=doc_download&gid=240&Itemid=21&lang=en, Accessed April 20 2012.
- Arpaci A, Eastaugh CS, Vacik H (in prep) Selecting the best performing Fire Weather Indices for Austrian Ecozones.
- Bond WJ, Woodward FI, Midgley GF (2005) The global distribution of ecosystems in a world without fire. *New Phytologist* 165:525-538.
- Bowman DMJS (2005) Understanding a flammable planet - climate, fire and global vegetation patterns, *New Phytologist* 165(2):341-345.
- Brang P, Schönenberger W, Frehner M, Schwitter R, Thormann JJ, Wasser B (2006) Management of protection forests in the European Alps: An overview. *Forest Snow and Landscape Research*, 80, 23-44.
- Brown TJ, Hall BL, Westerling AL (2004) The impact of twenty-first century climate change on wildland fire danger in the western United States: An applications perspective. *Climatic Change* 62:365-388.
- Cantwell J (1974) Resource allocation for forest fire protection. *Irish Forestry* 31(1):46-54.
- Conedera M, Marxer P, Tinner W, Amman B, Hofmann C (1996) Fire Ecology and History Research in the Southern Part of Switzerland. *International Forest Fire News* 15:13-21.
- Conedera M, Cesti G, Pezzati GB, Zumbrunnen T, Spinedi F (2006) Lightning-induced fires in the Alpine region: An increasing problem. In: Viegas DX (ed) *Proceedings of the 5th International Conference on Forest Fire Research*, November 27-30 2006, Coimbra, Portugal, p.1-9.
- Crane WJB (1982) Computing grassland and forest fire behaviour, relative humidity and drought index by pocket calculator. *Australian Forestry* 45(2):89-97.
- Eastaugh CS, Petritsch R, Hasenauer H (2010) Climate characteristics across the Austrian forest estate from 1960 to 2008. *Austrian Journal of Forest Science* 127:133-146.
- Eastaugh CS, Molina DM (2011) Forest road networks: metrics for coverage, efficiency and convenience. *Australian Forestry* 74(1):54-61.
- Eastaugh CS, Pötzelsberger E, Hasenauer H (2011) Assessing the impacts of climate change and nitrogen deposition on Norway spruce (*Picea abies* L. Karst) growth in Austria with BIOME-BGC. *Tree Physiology* 31(3):262-274.
- Eastaugh CS, Arpaci A, Vacik H (2012) A cautionary note regarding comparisons of fire danger indices. *Natural Hazards and Earth System Sciences* 12 (in press) doi:10.5194/nhess-12-1-2012
- Eastaugh CS, Molina DM (2012) Forest road and fuelbreak siting with respect to reference fire intensities. *Forest Systems* 21(1):153-161.
- Eastaugh CS, Vacik H (submitted) Fire size/frequency distributions as a means of assessing wildfire database reliability. *PLoS ONE*.

- Finney MA (2006) An Overview of FlamMap Fire Modeling Capabilities. USDA Forest Service Proceedings RMPSP-412.
- Flannigan MD, Stocks BJ, Wotton BM (2000) Forest fires and climate change. *Science of the Total Environment* 262:221–230.
- Gabler K, Schadauer K (2006) Methoden der Österreichischen Waldinventur 2000/02. BFW Berichte 135, 132 pp.
- Good P, Moriondo M, Giannakopoulos C, Bindi M (2008) The meteorological conditions associated with extreme fire risk in Italy and Greece: relevance to climate model studies. *International Journal of Wildland Fire* 17(2) 155–165.
- Gossow H, Hafellner R, Arndt N (2008) More forest fires in the Austrian Alps – a real coming danger? pp 356-362 in: Borsdorf, A., Stötter, J., Veuillet, E., Managing Alpine Future - Proceedings of the Innsbruck Conference, October 2007, Verlag der Österr. Akademie der Wissenschaften, 446 p.
- Hasenauer H, Nemani RR, Schadauer K, Running SW. 1999. Forest growth response to changing climate between 1961 and 1990 in Austria. *Forest Ecology and Management* 122:209–219.
- Hasenauer H, Merganicova K, Petritsch R, Pietsch SA, Thornton PE. 2003. Validating daily climate interpolations over complex terrain in Austria. *Agricultural and Forest Meteorology* 119:87–107.
- Hatton TJ, Viney NR, Catchpole EA, DeMestre NJ (1988) The influence of soil moisture on Eucalyptus leaf litter moisture. *Forest Science* 34(2):292-301.
- Isidorov VA, Smolewska M, Purzyńska-Pugacewicz A, Tyszewicz Z (2010) Chemical composition of volatile and extractive components of pine and spruce leaf litter in the initial stages of decomposition. *Biogeosciences* 7:2785-2794.
- Janis MJ, Johnson MB, Forthun G (2002) Near-real time mapping of Keetch-Byram drought index in the south-eastern United States. *International Journal of Wildland Fire* 11:281-289.
- Kanerva S, Kitunen V, Lojonen J, Smolander A (2008) Phenolic compounds and terpenes in soil organic horizon layers under silver birch, Norway spruce and Scots pine. *Biology and Fertility of Soils* 44(4):547-556.
- Keane RE, Arno SF, Brown JK (1989) FIRESUM – An ecological process model for fire succession in Western conifer forests. USDA Forest Service, Intermountain Forest and Range Experimental Station, Ogden, Utah. Gen. Tech. Rep. INT-266, 76 pp.
- Keane RE, Ryan KC, Running SW (1996) Simulating the effects of fire on northern Rocky Mountain landscapes with the ecological process model FIRE-BGC. *Tree Physiology* 16:319-331.
- Keane RE, Loehman RA, Holsinger LM (2011) The FireBGCv2 landscape fire succession model: A research simulation platform for exploring fire and vegetation dynamics. USDA Forest Service, Rocky Mountain Research Station, Fort Collins, Colorado. Gen. Tech. Rep. RMRS-GTR-255, 137 pp.
- Keetch JJ, Byram GM (1968) A drought index for forest fire control. Research Paper SE-38, U.S. Department of Agriculture, Forest Service, Southeastern Forest Experiment Station, Asheville, North Carolina. 32 pp. (revised November 1988).
- Kimball JS, Running SW, Nemani R (1997) An improved method for estimating surface humidity from daily minimum temperature. *Agricultural and Forest Meteorology* 85(1-2):87-98.
- Krawchuk MA, Moritz MA, Parisien MA, Van Dorn J, Hayhoe K (2009) Global pyrogeography: the current and future distribution of wildfire. *PLoS ONE* 4(4): e5102.
- Käse H (1969) Ein Vorschlag für eine Methode zur Bestimmung und Vorhersage der

- Waldbrandgefährdung mit Hilfe komplexer Kennziffern. Akademie Verlag Berlin. 68 pp.
- Lenihan JM, Daly C, Bachelet D, Neilson RP (1998) Simulating Broad-Scale Fire Severity in a Dynamic Global Vegetation Model. *Northwest Science* 72:91-103.
- Lynch AH, Beringer J, Kershaw P, Marshall A, Mooney S, Tapper N, Turney C, Van Der Kaars S (2007) Using the Paleorecord to Evaluate Climate and Fire Interactions in Australia. *Annual Reviews of Earth and Planetary Sciences* 35:215-239.
- Malevskii-Malevich SP, Mol'kentin EK, Nadezhina ED, Semioshina AA, Sall IA, Khlebnikova EI, Shklyarevich OB (2007) Analysis of changes in fire-hazard conditions in the forests in Russia in the 20th and 21st centuries on the basis of climate modeling. *Russian Meteorology and Hydrology* 32(3):154-161.
- McCarthy GJ, Tolhurst KG, Wouters M (2003) Prediction of firefighting resources for suppression operations in Victoria's parks and forests. DSE Research Report No. 56, Department of Sustainability and Environment, Victoria, 31pp.
- McRae DJ, Conard SG, Ivanova GA, Sukhinin AI, Baker SP, Samsonov YN, Blanke TW, Ivanov VA, Ivanov AV, Churkina TV, Hao WM, Koutzenogi KP, Kovalev N (2006) Variability of fire behaviour, fire effects, and emissions in scotch pine forests of central Siberia. *Mitigation and Adaptation Strategies for Global Change* 11:45-74.
- Meyer GA, Pierce JL (2003) Climatic controls on fire-induced sediment pulses in Yellowstone National Park and central Idaho: a long-term perspective. *Forest Ecology and Management* 178:89-104.
- Mikami Y (1988) Microbial conversion of terpenoids. *Biotechnology & Genetic Engineering Reviews* 6:271-320.
- Müller M, Vacik H, Diendorfer G, Arpacı A, Formayer H, Gossow H (2012) Analysis of lightning induced forest fires in Austria. *Theoretical and Applied Climatology* (accepted).
- Nelson RM Jr (2001) Water relations of forest fuels. In 'Forest Fires: Behavior and Ecological Effects'. (Eds EA Johnson, K Miyanishi) pp. 79–149. (Academic Press: London, UK).
- Nemani R, Keeling CD, Hashimoto H, Jolly WM, Piper SC (2003) Climate-Driven Increases in Global Terrestrial Net Primary Production from 1982 to 1999. *Science* 300(5625):1560-1563.
- Nesterov VG (1949) Flammability of the forest and methods of its determination [In Russian: Горимость леса и методы ее определения]. USSR State Industry Press, Moscow, 76pp.
- Ormeño E, Céspedes B, Sánchez IA, Velasco-García A, Moreno JM, Fernandez C, Baldy V (2009) The relationship between terpenes and flammability of leaf litter. *Forest Ecology and Management* 257:471-482.
- Pausas JG, Paula S (2012) Fuel shapes the fire-climate relationship: evidence from Mediterranean ecosystems. *Global Ecology and Biogeography* (in press) DOI: 10.1111/j.1466-8238.2012.00769.x
- Pedersen LB, Bille-Hansen J (1999) A comparison of litterfall and element fluxes in even aged Norway spruce, sitka spruce and beech stands in Denmark. *Forest Ecology and Management* 114:55-70.
- Petritsch R, Hasenauer H (2007) Interpolating input parameters for large scale ecosystem models. *Austrian Journal of Forest Science* 124:135–151.
- Petritsch R, Hasenauer H (2012) Climate input parameters for real-time online risk assessment. *Natural Hazards* (in press) DOI 10.1007/s11069-011-9880-y.
- Pietsch SA, Hasenauer H, Thornton PE (2005) BGC-model parameters for tree species growing in central European forests. *Forest Ecology and Management* 211:264–295.

- Pietsch SA, Hasenauer H (2006) Evaluating the self-initialization procedure for large-scale ecosystem models. *Global Change Biology* 12:1658–1669.
- Pitman AJ, Narisma GT, McAneney J (2007) The impact of climate change on the risk of forest and grassland fires in Australia. *Climatic Change* 84:383–401.
- Phillips OL, Malhi Y, Higuchi N, Laurance WF, Nunez PV, Vasquez RM, Laurance SG, Ferreira LV, Stern M, Brown S, Grace J (1998) Changes in the carbon balance of tropical forests: evidence from long-term plots. *Science* 282(5388):439-442.
- Prestemon JP, Donovan GH (2008) Forecasting resource allocation decisions under climate uncertainty: Fire suppression with assessment of net benefits of research. *American Journal of Agricultural Economics* 90(4):1118-1129.
- Running SW, Coughlan JC (1988) A general model of forest ecosystem processes for regional applications. I. Hydrologic balance, canopy gas exchange and primary production processes. *Ecological Modelling* 42:125-154.
- Sass O, Heel M, Hoinkis R, Wetzel KF (2010) A six-year record of debris transport by avalanches on a wildfire slope (Arnspitze, Tyrol). *Zeitschrift für Geomorphologie* 54(2):181-193.
- Sass O, Haas F, Schimmer C, Heel M, Bremer M, Stöger F and Wetzel KF (2012a) Impact of forest fires on geomorphic processes in the Tyrolean Limestone Alps. *Geografiska Annaler* 94(1):117-133.
- Sass O, Heel M, Leistner I, Stöger F, Wetzel KF, Friedmann A (2012) Disturbance, geomorphic processes and recovery of wildfire slopes in North Tyrol. *Earth Surface Processes and Landforms* (in press).
- Schumacher S (2004) The role of large-scale disturbances and climate for the dynamics of the landscape in European Alps, PhD-thesis ETHZ no. 15573, Zurich, 141 pp.
- Tanskanen H, Venäläinen A (2008) The relationship between fire activity and fire weather indices at different stages of the growing season in Finland. *Boreal Environmental Research* 13:285-302.
- Taylor AH, Beaty RM (2005) Climatic influences on fire regimes in the northern Sierra Nevada mountains, Lake Tahoe Basin, Nevada, USA. *Journal of Biogeography* 32_425-438.
- Thornton PE (1998) Description of a numerical simulation model for predicting the dynamics of energy, water carbon and nitrogen in a terrestrial ecosystem. PhD thesis, University of Montana, Missoula, USA, pp. 280.
- Thompson MP, Calkin DE, Finney MA, Gebert KM, Hand MS (2012) A risk-based approach to wildland fire budgetary planning. *Forest Science* (in press).
- Thornton PE, Running SW, White MA. 1997. Generating surfaces of daily meteorological variables over large regions of complex terrain. *Journal of Hydrology* 190:214–251.
- Thornton PE, Hasenauer H, White MA. 2000. Simultaneous estimation of daily solar radiation and humidity from observed temperature and precipitation: an application over complex terrain in Austria. *Agricultural and Forest Meteorology* 104:255–271.
- Thornton PE, Law BE, Gholz HL, Clark KL, Falge E, Ellsworth DS, Goldstein AH, Monson RK, Hollinger D, Falk M, Chen J, Sparks JP (2002) Modeling and measuring the effects of disturbance history and climate on carbon and water budgets in evergreen needleleaf forests. *Agricultural and Forest Meteorology* 113:185-222.
- Vacik H, Arndt N, Arpaci A, Koch V, Müller M, Gossow H (2011) Characterisation of forest fires in Austria. *Austrian Journal of Forest Science* 128(1):1-31.

Valese E (2009) Wildland fires in the Alpine region of Italy: What's old, what's new? What's next? *International Forest Fire News* 38:97-101.

Valese E, Beck A, Comini B, Conedera M, Cvenkel H, Di Narda N, Ghiringhelli A, Japelj A, Lemessi A, Mangiavillano A, Pelfini F, Pelosini R, Ryser D, Vacik H, Wastl C (2010). The Alpine Forest Fire Warning System (ALP FFIRS) project. VI International Conference on Forest Fire Research D. X. Viegas (Ed.). Online at http://www.alpffirs.eu/index.php?option=com_docman&task=doc_download&gid=239&Itemid Accessed 14 April 2012.

Valese E, Conedera M, Vacik H, Japelj A, Beck A, Cocca G, Cvenkel H, Di Narda N, Ghiringhelli A, Lemessi A, Mangiavillano A, Pelfini F, Pelosini R, Ryser D, Wastl C (2011) Wildfires in the Alpine region: first results from the ALP FFIRS project. 5th International Wildland Fire Conference 9-13 May 2011, Sun City South Africa. Online at: http://www.wsl.ch/info/mitarbeitende/conedera/download/Valese_et_al_2011 Accessed 15 April 2012.

Van Wagner CE (1987) Development and structure of the Canadian Forest Fire Weather Index. Canadian Forest Service Forestry Technical Report 35.

Whitlock C, Shafer S, Marlon J (2003) The role of climate and vegetation change in shaping past and future fire regimes in the northwestern US and the implications for ecosystem management. *Forest Ecology and Management* 178:5-21.

Wotton BM (2009) Interpreting and using outputs from the Canadian Forest Fire Danger Rating System in research applications. *Environmental and Ecological Statistics* 16:107-131.

Zhao F-J, Shu, LF, Wang Q-H (2012) Terpenoid emissions from heated needles of *Pinus sylvestris* and their potential influences on forest fires. *Acta Ecologica Sinica* 32:33-37.

Zumbrunnen T, Burmann H, Conedera M, Bürgi M (2009) Linking Forest Fire Regimes and Climate—A Historical Analysis in a Dry Inner Alpine Valley. *Ecosystems* 12:73-86.

Ångström A (1942) The risks for forest fires and their relation to weather and climate [In Swedish: Riskerna för Skogsbrand och deras beroende av väder och klimat]. *Svenska skogårdsföreningens Tidskrift* 4, 18pp.

Ångström A (1949) Swedish Meteorological Research 1939–1948. *Tellus* 1(1):60-64.